

Author: George A. Gray
Senior Application Chemist
Eastern Applications Laboratory
Varian Associates
Springfield, New Jersey

Referee: Ian C. Smith
Research Officer
Division of Biological Sciences
National Research Council of Canada
Ottawa, Canada

INTRODUCTION

The last 20 years have seen a spectacular growth in the application of nuclear magnetic resonance in biochemistry. Most of the effort has been expended in high resolution nmr, and in that effort, proton magnetic resonance has dominated the scene. There are good reasons for the historical development of nmr in this way. Protons possess essentially 100% natural abundance, a strong magnetogyric ratio, and spin 1/2. These factors, plus the occurrence of hydrogen in most organic molecules, led investigators to concentrate on proton nmr. Since carbon, nitrogen, oxygen, and other heavier atoms contribute most to molecular binding and control the molecular properties, information gleaned from magnetic resonance studies of these should reflect more accurately the true molecular electronic structure than that obtained from peripheral protons. Recent advances in technique and instrumentation have stimulated a surge of interest and activity, particularly in ^{13}C nmr.

The early ^{13}C investigations of Lauterbur¹ and Holm² showed the promise of the determination of molecular structure. From 1957 until the mid

1960's, the main avenue of attack in overcoming the severe detection problems was the use of adiabatic rapid passage in dispersion-mode. The high scan rate allowed greater signal intensity, but at the price of linewidth on the order of one ppm. Large sample tubes were used, usually non-spinning, and at least 2 cc of liquid were normally required. In spite of these difficulties much work was accomplished detailing the relationship of the ^{13}C shift to molecular electronic structure. The primary contributors were small in number. Groups headed by Lauterbur, Stothers, Maciel, Savitsky, and Grant provided the bulk of reported work.³ Their efforts pointed out the great potential of ^{13}C nmr and helped contribute to and spur on the significant advances in instrumentation responsible for the growing contemporary interest.

The two major advances in technique responsible for the added sensitivity gained over that of rapid passage dispersion-mode techniques were proton decoupling and time-averaging. Proton decoupling collapses the multiplets arising from the often extensive ^{13}C - ^1H long and short range couplings and also gives nuclear Overhauser enhancement of up to a factor of three times the expected intensity. Time-averaging of scans at

slower rates allows more precise chemical shifts, permitting assignments and accurate spin coupling determinations. The advent of noise-decoupling, as developed by Ernst,⁴ enormously simplified the operation of decoupling and spectral interpretation.

Almost all of the work done in ^{13}C nmr until very recently has utilized the classical continuous-wave, slow-sweep method in which a weak perturbing rf field is used to induce radio-frequency transitions. True slow-passage requires a very low sweep rate to give accurate line shapes and intensities. Given true slow-passage, there are various methods available to enhance signal strength. The static magnetization may be increased by use of a large sample, large magnetic field, cooled sample (lattice), dynamic polarization, spin decoupling, and indirect detection (ENDOR and INDOR). Further signal strength may be gained by shortening the spin-lattice relaxation time (T_1) by the addition of paramagnetic species.

One very important and implicit drawback of slow-passage, continuous-wave experiments is the great amount of time spent on regions of the spectrum containing no information. If there are very few lines in a spectrum, this liability may be circumvented by using one or more phase-sensitive detectors tuned to frequencies at which these spectral features appear. As the complexity of the spectrum increases, this approach becomes impractical.

A technique that accomplishes essentially the same result as a large number of phase-sensitive detectors is Fourier transform (FT) spectroscopy. This method relies on the fact that the frequency response and the impulse response of a linear system form a Fourier transform pair. Ernst and Anderson⁵ have developed Fourier transform spectroscopy as applied to nuclear magnetic resonance. Very significant gains in sensitivity are realized without line shape distortion. Ernst and Anderson list the central features of the pulse technique as:

1. Spectra may be obtained in a much shorter time; the desired resolution varies as $1/T$ where T is the time spent accumulating a free-induction decay.
2. For spectra possessing much fine structure, FT offers much higher sensitivity than CW

experiments since all spins are excited simultaneously rather than sequentially.

3. Nuclear Overhauser effects may be investigated.

4. The total integral and higher moments of the spectrum are easily obtained.

5. The accurate frequency calibration is replaced with an easier-to-attain accurate time measurement.

The FT experiment consists of applying a series of short equidistant rf pulses to a spin system, detecting and coherently storing the responses in a time-averaging computer, and calculating the Fourier transform of the sum of responses by means of a computer (Figure 1). The rf pulses excite resonances within a bandwidth dependent on the duration of the rf pulse. If the pulse duration is short enough and the pulse power high, the entire spectrum can be excited uniformly. Through a careful analysis of signal-to-noise characteristics, Ernst and Anderson estimate a gain equal to the square root of the total available time to the time actually spent within a single line using slow-sweep techniques. The time actually saved in achieving a desired signal-to-noise ratio is approximately the ratio of the total sweep width to a characteristic linewidth. For nuclei such as ^{13}C , where shifts range over 7,500 Hz at 23,000 gG with linewidths often <1 Hz, this represents a considerable gain.⁶

FT nmr, by the very nature of its speed, forces attention on any time-dependent phenomenon. As opposed to time-averaging in CW nmr, where one particular line in a spectrum may be excited only once every several minutes or longer, each line in an FT experiment is excited at the repetition rate of the pulsing, perhaps as much as several times a second. If each pulse induces a maximum signal

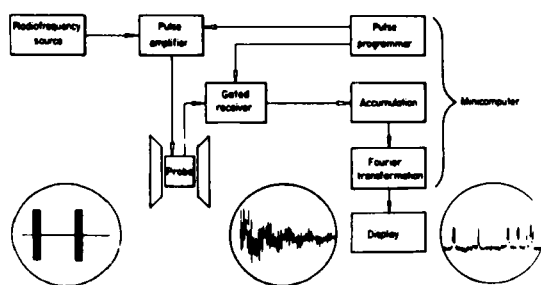


FIGURE 1. Schematic view of the fourier transform experiment. (With permission of Varian Associates.)

(90° pulse), then immediately after each pulse there is *no net magnetization* along the field direction. For maximum sensitivity per pulse it is desirable to have a return to full magnetization along the field axis before each exciting pulse. The recovery of this magnetization is exponential with time, having a time constant T_1 , and takes $5T_1$ to recover ~99% of the magnetization. It is clear then that the ability to gain sensitivity using time-averaging is restricted by T_1 . For accurate intensities in a spectrum possessing lines of varying T_1 , the line with the longest T_1 must be the controlling factor. Either a delay must be inserted between pulses or less than a 90° pulse used for sequential pulses. In practice there is a compromise between accurate intensities and speed of acquisition. The requirement for accurate intensities is much stricter in ^1H FT nmr since multiplets must be recognized to assign chemical shifts. This is not the case in ^{13}C FT nmr since ^1H decoupling results in one line per carbon. Thus, carbons with long T_1 's will normally not have sufficient time for relaxation to their normal equilibrium magnetization between exciting pulses and will appear to have diminished intensities relative to the carbons with shorter T_1 's in the final spectrum. In fact, the very difference in intensities serves as a diagnostic technique for molecular structure. To understand why, it is necessary to understand the ways in which nuclei undergo relaxation. There are four principal means: dipole-dipole, spin-rotation, chemical shift anisotropy, and scalar relaxation. Dipole-dipole relaxation occurs through a direct magnetic through-space interaction with surrounding fluctuating magnetic moments. In most organic molecules the protons serve as the dominant dipolar relaxers and control the ^{13}C T_1 by

$$\frac{1}{T_{1\text{DD}}} = \sum_{\text{all } ^1\text{H}} \frac{N_{\text{H}} \gamma_{\text{C}} \gamma_{\text{H}} \tau_{\text{C}}}{r_{\text{CH}}^6} \quad (1)$$

The r_{CH}^6 term gives dominant weight to directly attached protons, although for quaternary carbons nearby protons can serve for relaxation and usually do in large molecules. N_{H} is the number of each type of proton, γ the magnetogyric ratio, and τ_{C} the effective reorientation time of the ^{13}C - ^1H internuclear vector, which is in many cases on the order of the molecular tumbling time. It can be seen that small molecules with short τ_{C} will give longer $T_{1\text{DD}}$ and that large molecules with long τ_{C} will give a shorter $T_{1\text{DD}}$. The latter case is what,

in fact, makes ^{13}C nmr of biomolecules possible in view of their low molarity. It will be seen later how studies of T_1 using the dipole-dipole mechanism have aided in molecular structure determination via Equation 1.

Spin-rotation relaxation occurs when a molecular or fragment rotation is rapid enough so that the coupling of the rotational angular momentum and the nuclear moment can serve as an energy transfer mechanism. In practice this occurs only in small molecules and freely rotating methyl groups. It can then compete with any dipole-dipole relaxation present (recall that dipole-dipole relaxation becomes less efficient with short τ_{C}) and even dominate, especially for nonprotonated carbons. Freely rotating methyl groups will often give rise to smaller signals relative to protonated rigid ring or hindered methyls. This is a result of not only the longer T_1 (spin-rotation is still much less efficient than typical dipole-dipole relaxation), but also because the nuclear Overhauser enhancement is directly proportional to the importance of the dipole-dipole relaxation with the surrounding protons. Again, this can be useful in spectral interpretation. Measurement of Overhauser enhancement and T_1 can fix the relative importance of dipole-dipole and spin-rotational mechanisms, thereby giving useful structural information.

Chemical shift anisotropy in a tumbling molecule can present a fluctuating magnetic field that can relax a nucleus. It can be important for nonprotonated carbons at high magnetic fields, especially acetylinic carbons. The remaining scalar relaxation is only important for nonprotonated carbons bound to nuclei whose resonance frequency is very close to that of carbon. The only other case where scalar relaxation is important is for T_2 (spin-spin relaxation) when the carbon is spin coupled to a nucleus undergoing rapid quadrupolar relaxation (e.g., ^2H , ^{14}N , ^{35}Cl).

Although the normal ^{13}C experiment involves noise-modulated broadband proton decoupling giving single lines, it is often useful to use high-power, coherent, off-resonant, proton decoupling. In practice the noise modulation is removed and the ^1H frequency offset by ~1 kHz. The result is not a coupled spectrum with all the ^{13}C - ^1H splittings, but one in which the normal multiplets arising from one-bond couplings are observed; no long range ^{13}C - ^1H couplings are present; and the apparent one-bond coupling is

only a fraction of the true coupling (~ 20 Hz vs. 125 Hz). The decoupling still gives Overhauser enhancement while the splittings allow identification of the number of directly attached protons, a very powerful structural tool. Of course, a T_1 measurement also gives information concerning degree of protonation as seen above.

With this brief background, it is possible to discuss the exciting applications of ^{13}C nmr in biochemistry that have emerged in the last few years.

CARBOHYDRATES

The first concrete examples of how ^{13}C nmr could be of benefit in the realm of biochemistry were reported in 1966 by Buchanan, Ross, and Stothers.⁷ Their studies on 4-substituted cyclohexanols showed a strong stereospecificity in the C-1 ^{13}C shift depending on the axial or equatorial nature of the substituent OH group. Axially substituted C-1's were uniformly found up to 5 ppm upfield from the corresponding equatorially substituted C-1's. Three years later the same stereospecificity was noted in anomeric pyranose derivatives by Hall and Johnson,⁸ and Perlin and Casu.⁹ In examining mutarotated $\alpha:\beta$ anomeric mixtures, these investigators also noted that sensitivity to anomer identity extended over more than one bond to C-2 and C-3. Carbon identification was simplified by the fact that the anomeric carbons, having two oxygen substituents, had shifts of 91 to 105 ppm* while the ring carbons with only one oxygen substituent had shifts of 67 to 77 ppm. Normal hexose C-6 shifts were observed at ~ 62 ppm. The prediction of facile pyranose/furanose identification was made⁸ in view of the even greater C-1 shifts of the minor furanose component in D-ribose. Perlin and Casu⁹ uncovered additional structurally useful data in their examination of ^{13}C -enriched D-glucose. They found that in addition to the direct one-bond C-H coupling, the proton on C-1 is appreciably coupled (5 to 6 Hz) to ring carbon(s) *only* in the α anomer, i.e., the hydroxyl axial. Even the anomeric carbon $^1J_{\text{CH}}$ is anomer dependent: $^1J_{\text{CH}}^{\alpha} = 169$ Hz, $^1J_{\text{CH}}^{\beta} = 160$ Hz. The high ^{13}C enrichment allowed a similar stereospecificity to emerge for the one-bond couplings of the C-1 and

C-2 carbons: $^1J_{\text{CC}}^{\alpha} = 44.9$ Hz, $^1J_{\text{CC}}^{\beta} = 47.1$ Hz. No significant geminal CC couplings were observed.

In a detailed pair of investigations Dorman, Angyal, and Roberts¹⁰ and Dorman and Roberts¹¹ tackled the general problems of perhydroxy cyclohexanes¹⁰ (inositols) as model pyranose compounds, and then applied their results to pentose and hexose aldopyranoses.¹¹ The inositol chemical shifts were adequately predicted for various epimers by a set of substituent parameters applied to a reference shift given by either 74.0 ppm for an equatorially substituted carbon or 72.5 ppm for an axially substituted carbon. The orientation of the β , γ , and δ carbon hydroxy group dictates the addition of terms given by $\beta_e = -1.7 \pm 0.3$, $\beta_a = -0.6$, $\gamma_e = -2.8 \pm 0.3$, $\gamma_a = +2.3$, and $\delta_e = +0.7 \pm 0.5$ ppm. The large γ effects are a result of the significant 1,3-diaxial interactions that show up quite generally in ^{13}C shifts. Six O-methylated inositols were studied in sorting out the various inositol epimers. Applying these techniques to the sugars, Dorman and Roberts¹¹ examined gluco-, manno-, rhamno-, arabino-, allo-, xylo-, fuco-, and galactopyranoses in mutarotational equilibria, along with several O-methylated derivatives. Application of the inositol substituent effects to calculate shifts gave somewhat more scatter when applied to the sugars. Steric effects seemed to be the controlling factors in determining the differences between the sugars.

Perlin, Casu, and Koch¹² also examined the simple monosaccharides with the aim of explaining shifts in terms of charge densities, polarization, and steric effects. They studied glucose, galactose, mannose, allose, xylose, arabinose, lyxose, ribose, and their methyl glycopyranosides. They noted a general trend of chemical shift with computed charge density, which they used to suggest that C-2 and C-4, usually more shielded, possess greater electron density, possibly from interaction with the ring oxygen. Removal of a gauche O,O interaction is associated with carbon deshielding. Correlating total ^{13}C shielding with molecular energy, they argued that the anomeric effect does not arise through an inherent instability in the equatorial anomeric C-O bond, but through a sum of mutually canceling attractive and repulsive forces. An interesting inverse correlation was noted for ^1H and ^{13}C shieldings in several sugars.

*All shifts have been placed on the TMS ^{13}C scale using the following common references: dmsO +40.5, dioxane +67.4, benzene +128.5, and CS_2 + 192.8 ppm.

In a similar study using ^{13}C FT nmr, Breitmaier, Voelter, Jung, and Tänzer¹³ studied 20 methyl and aryl glycosides, primarily gluco-, galacto-, manno-, and arabinopyranosides, emphasizing the ability to make configurational and conformational assignments. In other publications the same group pointed out the utility of the upfield shift of axially oriented methoxy carbons for conformational analysis in solution¹⁴ and that the speed of ^{13}C FT nmr allows dynamic observation of the attainment of anomeric equilibrium.¹⁵ Coxon and Johnson¹⁶ exhaustively determined the nmr parameters of derivatives of ^{15}N -enriched 6-amino-6-deoxy-1,2:3,5-di-*O*-isopropylidene- α -D-glucopyranose. ^1H , ^{13}C , and ^{19}F resonance allowed determination of chemical shifts and magnitudes of ^1H - ^1H , ^1H - ^{15}N , ^1H - ^{19}F , ^{13}C - ^{15}N , and ^{15}N - ^{19}F couplings. The utility of ^{15}N magnetic resonance parameters in structural and conformational analysis of amino sugars and their derivatives was tested, and it was found that except for couplings over one bond, the ^{15}N coupling constants were small and that very good spectral resolution is mandatory for structural analysis. Their experiments illustrated the ability to differentiate proton resonances of *N*-acetyl groups from those of *O*-acetyl groups.

Carbon-13 nmr is especially suited to the study of polysaccharides. Doddrell and Allerhand¹⁷ have examined 3-*O*-(α -D-glucopyranosyl)-D-fructose (turanose) and found three species in equilibrium:

- 39% 3-*O*-(α -D-glucopyranosyl) - β -D-fructopyranose
- 41% 3-*O*-(α -D-glucopyranosyl)- α -D-fructofuranose
- 20% 3-*O*-(α -D-glucopyranosyl)- β -D-fructofuranose

No signals from the α -fructopyranose anomer were observed. Assignments were made on the basis of expected shifts and the anomers observed for D-fructose in the same study:

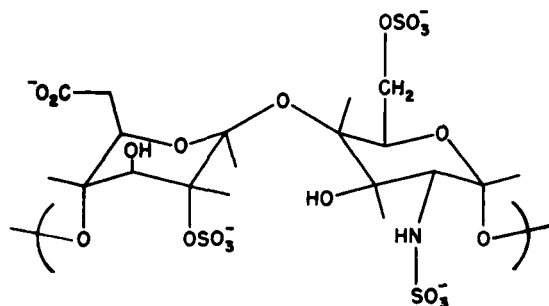
- 3% α -D-fructopyranose
- 57% β -D-fructopyranose
- 9% α -D-fructofuranose
- 31% β -D-fructofuranose

The data showed that the mutarotation of aqueous fructose is caused by a pyranose-furanose

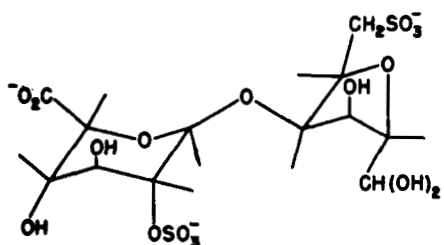
interconversion and not by α - β anomerization. In an accompanying investigation,¹⁸ the same authors considered a nonreducing tetrasaccharide, stachyose, as well as the trisaccharides, raffinose and melezitose, and sucrose, a disaccharide. On the basis of monosaccharide shifts and T_1 information, all the stachyose resonances were assigned. The latter technique was especially useful since there are two adjacent galactose units, one of them terminal. The terminal unit should have more freedom to rotate and thus a shorter reorientational correlation time. The data showed that one set of galactose protonated carbons had T_1 's of ~ 0.5 sec, while the other set had T_1 's significantly less than 0.5 sec. The former were then assigned to the more mobile terminal galactose subunit.

Yamoka et al.¹⁹ discussed the utility of the C-1's carbon shift for determining the type of glycosidic linkage in disaccharides. In three α -type linkages, kojibiose (1,2- α), nigerose (1,3- α), and maltose (1,4- α), the C-1' shifts were 96.7, 99.4, and 100.4 ppm, respectively, while in the β -types sophorose (1,2- β), laminarbiose (1,3- β), and cellibiose (1,4- β), the shifts were 104.6, 103.1, and 103.1 ppm.

Two recent investigations used ^{13}C nmr for gaining information regarding the biopolymer heparin.^{20,21} In a groundwork study Perlin et al.²⁰ examined methyl α - and β -D-idopyranosiduronic acids and found that, in solution, the α anomer adopts a conformation represented mainly by the C1(D) form, and the β anomer favors this conformation almost exclusively. They then extended their analysis to heparin,²¹ a molecular structure based on 12 carbons involved in an alternating sequence consisting of (1 \rightarrow 4) linked residues of α -L-idopyranosiduronic acid 2-sulfate and 2-deoxy-2-sulfamino- α -D-glucopyranosyl 6-sulfate.

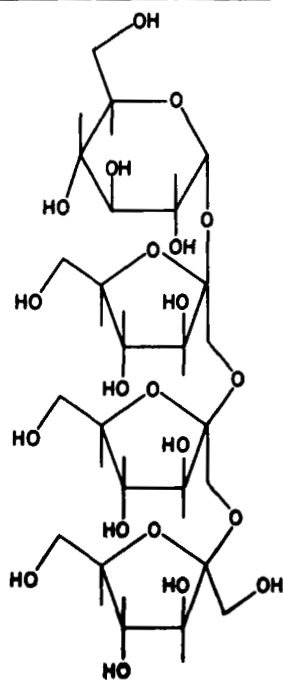


In comparing the shifts of heparin, methyl α -D-idopyranosiduronic acid, and the disaccharide,

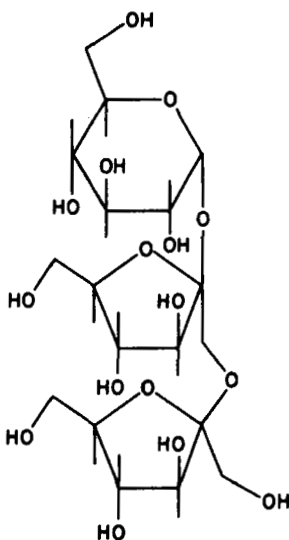


it was apparent that the conformation of the L-iduronic acid residues in heparin is close to that in the smaller molecules and accordingly may be depicted most satisfactorily by the $1C(L)$ conformation.

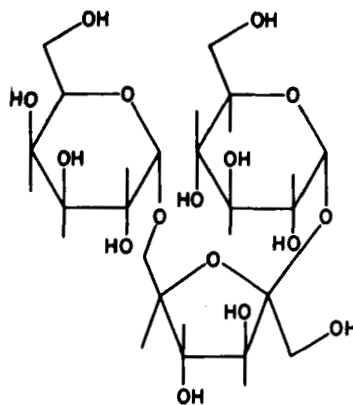
Very recently Binkley et al.²² reported ^{13}C nmr studies of nystose, 1-kestose, and planteose.



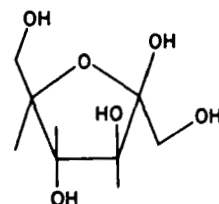
Nystose



1-Kestose



Planteose



β -D-Fructofuranose

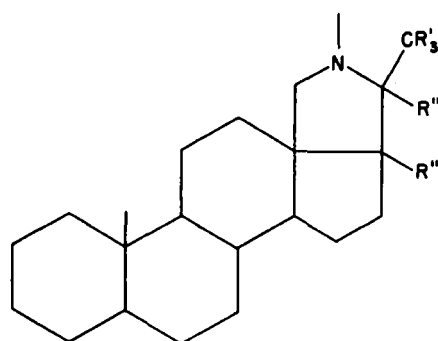
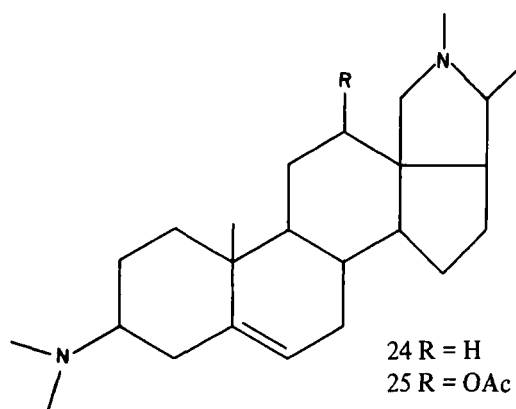
In their analysis they made extensive use of off-resonance decoupling for determination of degree of protonation, acetylation as a diagnostic test for hydroxylated carbons (large downfield shift), specific deuteration (useful for carbons α to carbonyls), and selective proton decoupling. Specific compounds studied (see Figures 2 to 6) were cholestane (1), cholestan-3-one (2), cholestan-3-ols (3,4), cholesterol (6), 7-dehydrocholesterol (7), ergosterol (8), cholesta-3,5-diene (9), cholesta-3,5-dien-7-one (10), cholest-5-en-7-on-3 β -yl acetate (11a), androstane-3,17-dione (12),

dehydroisoandrosterone (13), progesterone (14), 11 α -hydroxyprogesterone (15), 16-dehydropregesterone (16), androst-4-ene-3,17-dione (17), 19-norandrost-4-ene-3, 17-dione (18), 19-nortestosterone (19), testosterone (20), 7 α -methyltestosterone (21), 19-nor-7 α -methyltestosterone (22), and estrone (23). Systematic variation of structure and use of substituent effects from model compounds allowed shift assignment.

In other recent work Lukas et al.²⁴ have assigned shifts for a series of conessine derivatives (24 to 31) using ^{13}C nmr,

STERIODS

In an elegant and herculean task, Reich et al.²³ applied ^{13}C nmr (CW mode) to the study of a large number of sterols and steroidal hormones. This work laid the foundation for the systematic use of ^{13}C nmr in this vital area of biochemistry.

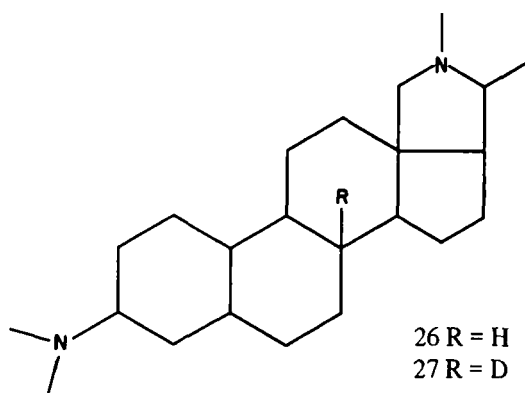


28 R''' = H, R' = H, R'' = H

29 R''' = D, R' = H, R'' = H

30 R''' = H, R' = H, R'' = D

31 R''' = H, R' = D, R'' = H



and in later studies from the same group the ^{13}C resonances in lanosterol (32) and dihydrolanosterol (33), their acetates and ketones, and the steroids 34 to 37 were assigned.²⁶

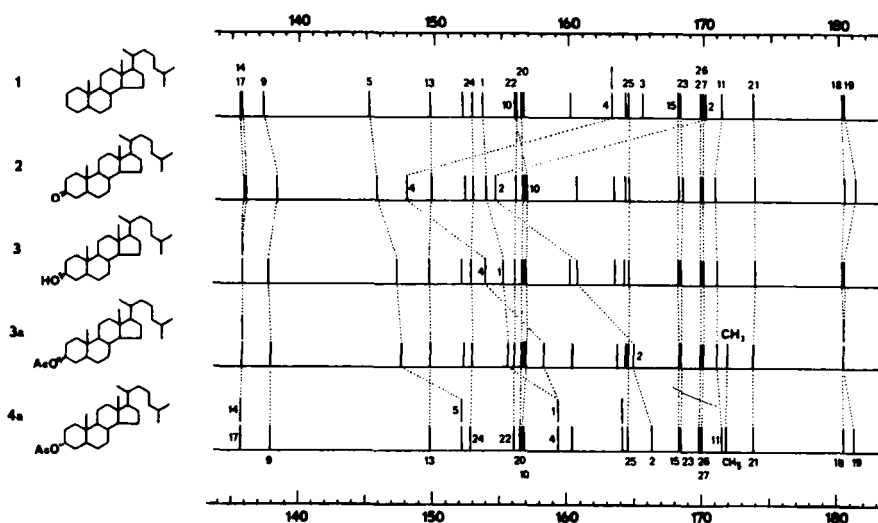


FIGURE 2. ^{13}C chemical shift correlation for cholestane (1), cholestan-3-one (2), cholestan-3 β -ol (3), cholestan-3 β -yl acetate (3a), and cholestan-3 α -yl acetate (4a) (in ppm upfield from $^{13}\text{CS}_2$). (From Reich, H. J., Jautelat, M., Messe, M. T., Weigert, F. J., and Roberts, J. D., Nuclear magnetic resonance spectroscopy. Carbon-13 spectra of steroids, *J. Am. Chem. Soc.*, 91, 7445, 1969. With permission of the American Chemical Society.)

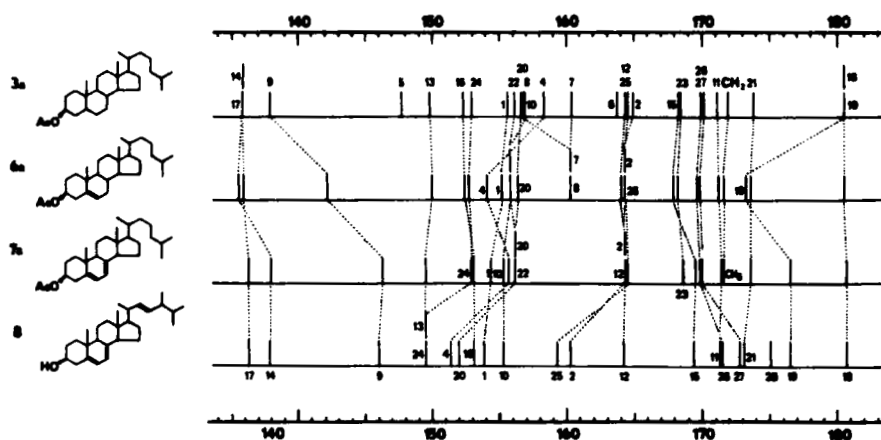


FIGURE 3. ^{13}C chemical shift correlation for cholestan-3 β -yl acetate (3a), cholesteryl acetate (6a), 7-dehydrocholesteryl acetate (7a), and ergosterol (8) (in ppm upfield from $^{13}\text{CS}_2$). (From Reich, H. J., Jautelat, M., Messe, M. T., Weigert, F. J., and Roberts, J. D., Nuclear magnetic resonance spectroscopy. Carbon-13 spectra of steroids, *J. Am. Chem. Soc.*, 91, 7445, 1969. With permission of the American Chemical Society.)

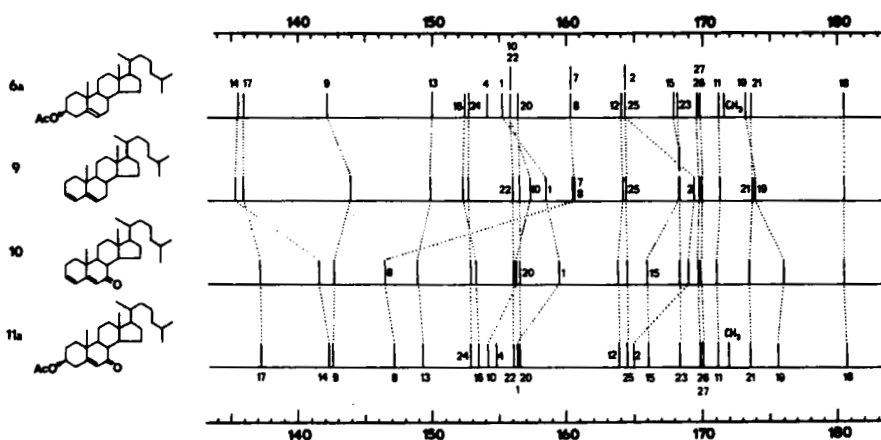


FIGURE 4. ^{13}C chemical shift correlation for cholesterol acetate (6a), cholesta-3,5-diene (9), cholesta-3,5-dien-7-one (10), cholest-5-en-7-on-3 β -yl acetate (11a) (in ppm from $^{13}\text{CS}_2$). (From Reich, H. J., Jautelat, M., Messe, M. T., Weigert, F. J., and Roberts, J. D., Nuclear magnetic resonance spectroscopy. Carbon-13 spectra of steroids, *J. Am. Chem. Soc.*, 91, 7445, 1969. With permission of the American Chemical Society.)

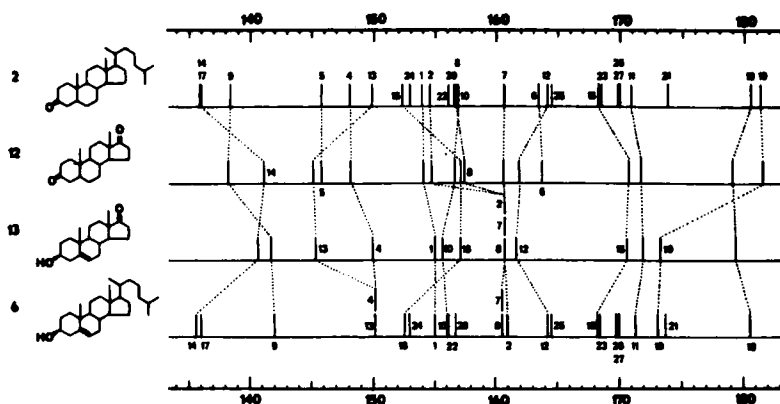


FIGURE 5. ^{13}C chemical shift correlation for cholestan-3-one (2), androstane-3, 17-dione (12), 5-dehydroisoandrosterone (13), and cholesterol (6) (in ppm upfield from $^{13}\text{CS}_2$). (From Reich, H. J., Jautelat, M., Messe, M. T., Weigert, F. J., and Roberts, J. D., Nuclear magnetic resonance spectroscopy. Carbon-13 spectra of steroids, *J. Am. Chem. Soc.*, 91, 7445, 1969. With permission of the American Chemical Society.)

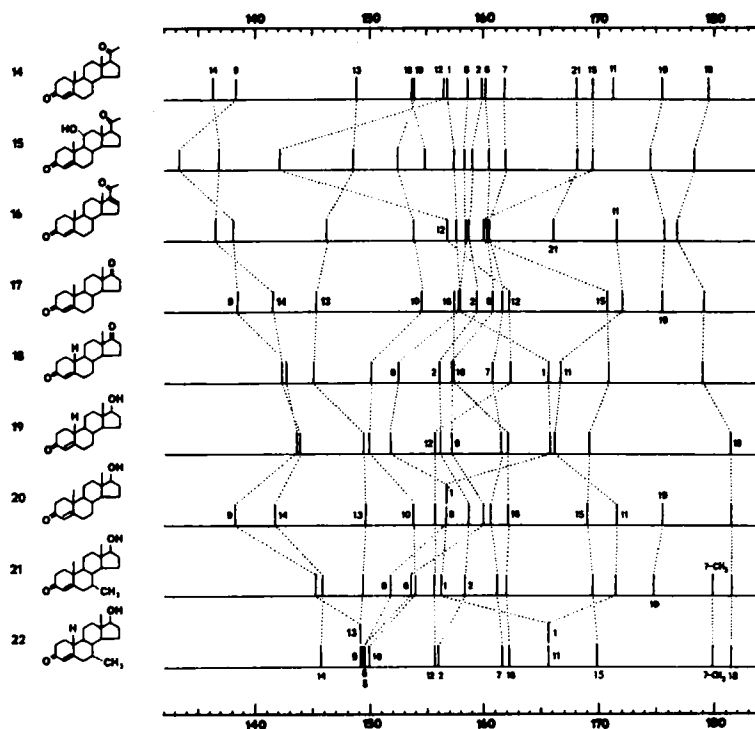
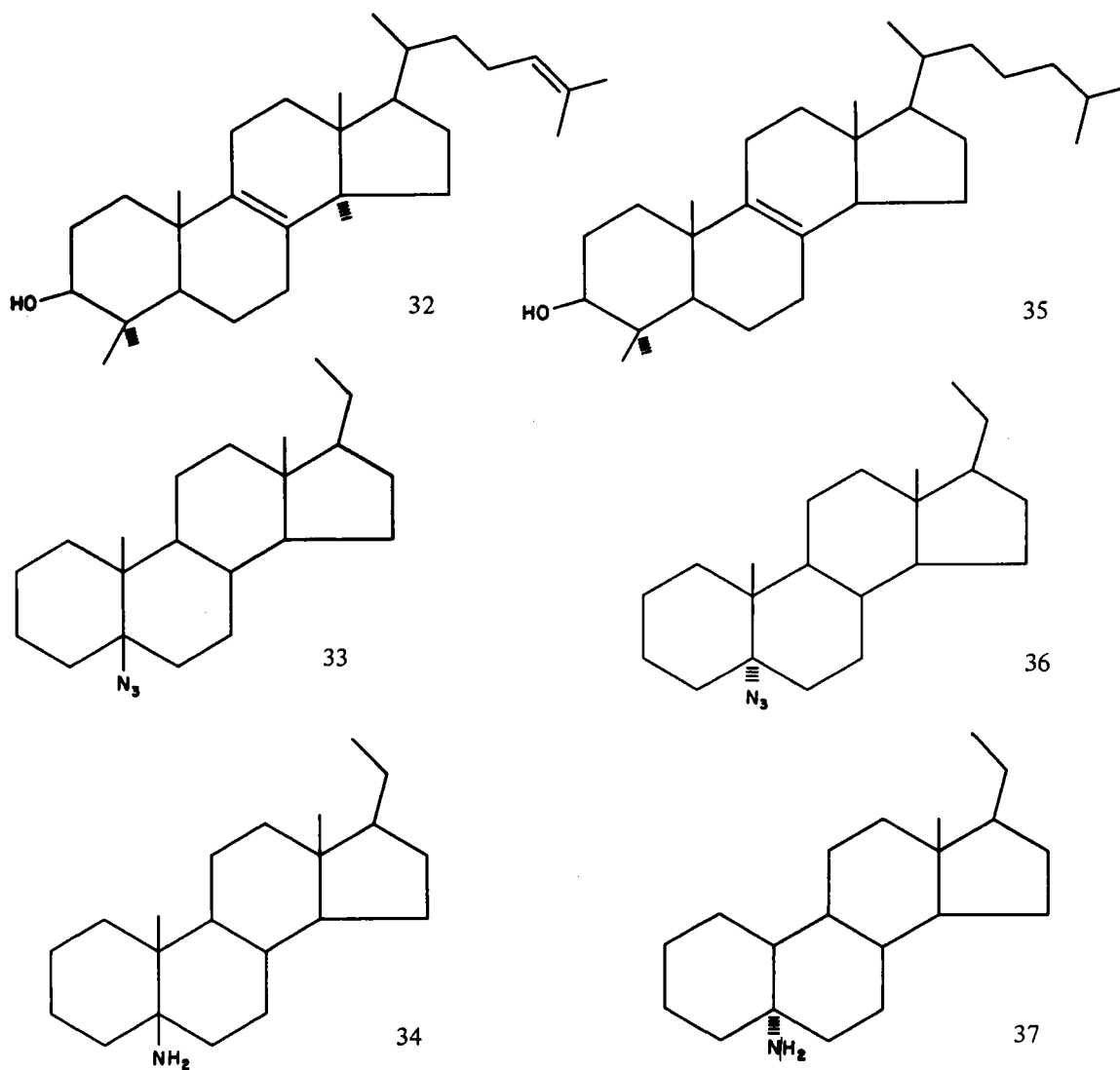


FIGURE 6. ^{13}C Chemical shift correlation for changes in structure for progesterones (14 to 17), androst-4-enedione (18 to 19), and testosterone (19 to 22) (in ppm upfield from $^{13}\text{CS}_2$). (From Reich, H. J., Jautelat, M., Messe, M. T., Weigert, F. J., and Roberts, J. D., Nuclear magnetic resonance spectroscopy. Carbon-13 spectra of steroids, *J. Am. Chem. Soc.*, 91, 7445, 1969. With permission of the American Chemical Society.)



As an example of natural product analysis using ^{13}C nmr, Balogh, Wilson, and Burlingame²⁷ analyzed steranes from oil shale (5- to 15-mg amounts) with Fourier transform techniques. The C_{27} and C_{28} isolates were conclusively identified as 5α-cholestane and 5α-ergostane from the close fit of their spectra (Figure 7). The sensitivity and "fingerprint" nature of the spectra were documented by exploring the sensitivity to structural change for several model compounds (Figure 8). As noticed in this study and explored in more detail by Gough, Guthrie, and Stothers,²⁸ in going from the 5α- to the 5β-steroid, the C-19 methyl carbon is heavily deshielded. This is the result of the general deshielding of antivicinally oriented carbons with respect to nuclei in a gauche vicinal orientation. Large effects on the shift of C-19 are

observed, i.e., 11 to 12 ppm (see 5α- vs. 5β-cholestane), as well as for C-9 (12 to 15 ppm), which also experiences gauche interactions with C-2 and C-4 in the 5β-systems. These two shifts provide straightforward diagnostics for the stereochemistry of the A/B junction, wherein it is not necessary to have both isomers to identify the stereochemistry of an unknown compound if substituent effects from neighboring groups are considered in predicting the C-19 and C-9 shifts for each isomer.

Another aid in spectral interpretation was reported by Lukacs et al.²⁹ where they used fluorine-substituted steroids for help in the assignment of parent compounds. The characteristic shifts upon fluorination and the several couplings available allowed facile identification among lines

close in chemical shift in compounds 38 to 43:

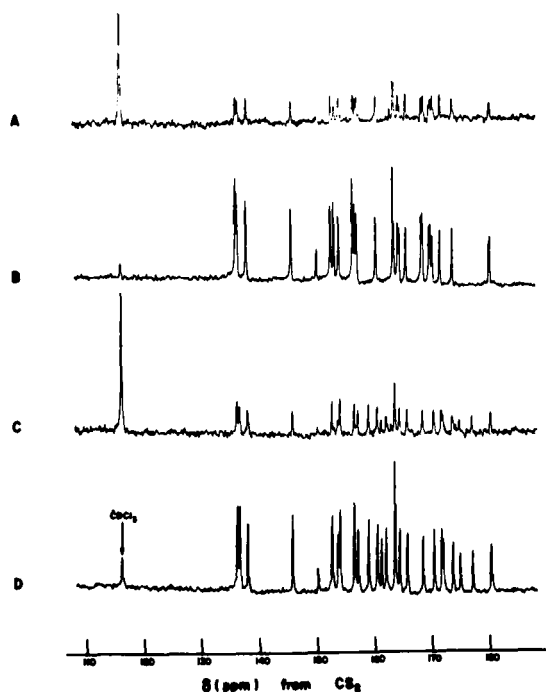
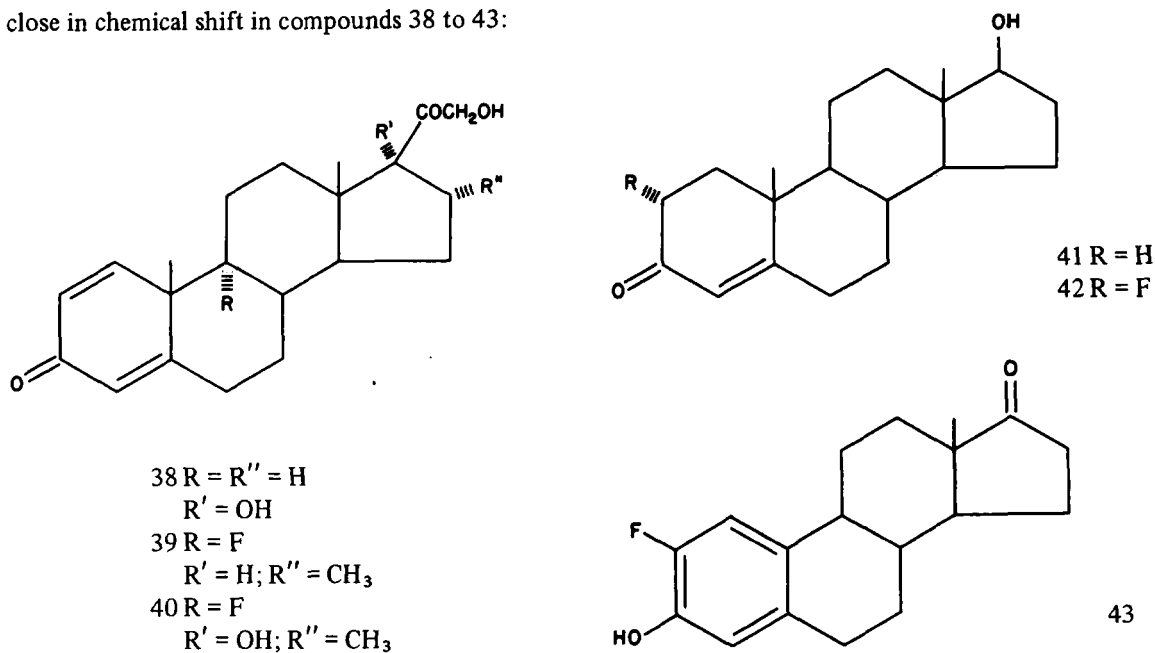


FIGURE 7. ^{13}C spectra of steranes. A, 12-mg sample of C_{27} sterane from Green River Shale. B, 5 α -cholestane. C, 8-mg sample of C_{28} Green River Shale sterane. D, 5 α -ergostane. (From Balogh, B., Wilson, D. M., and Burlingame, A. L., Carbon-13 NMR study of the stereochemistry of steranes from oil shale of the Green River Formation (Eocene), *Nature*, 233, 261, 1971. With permission.)

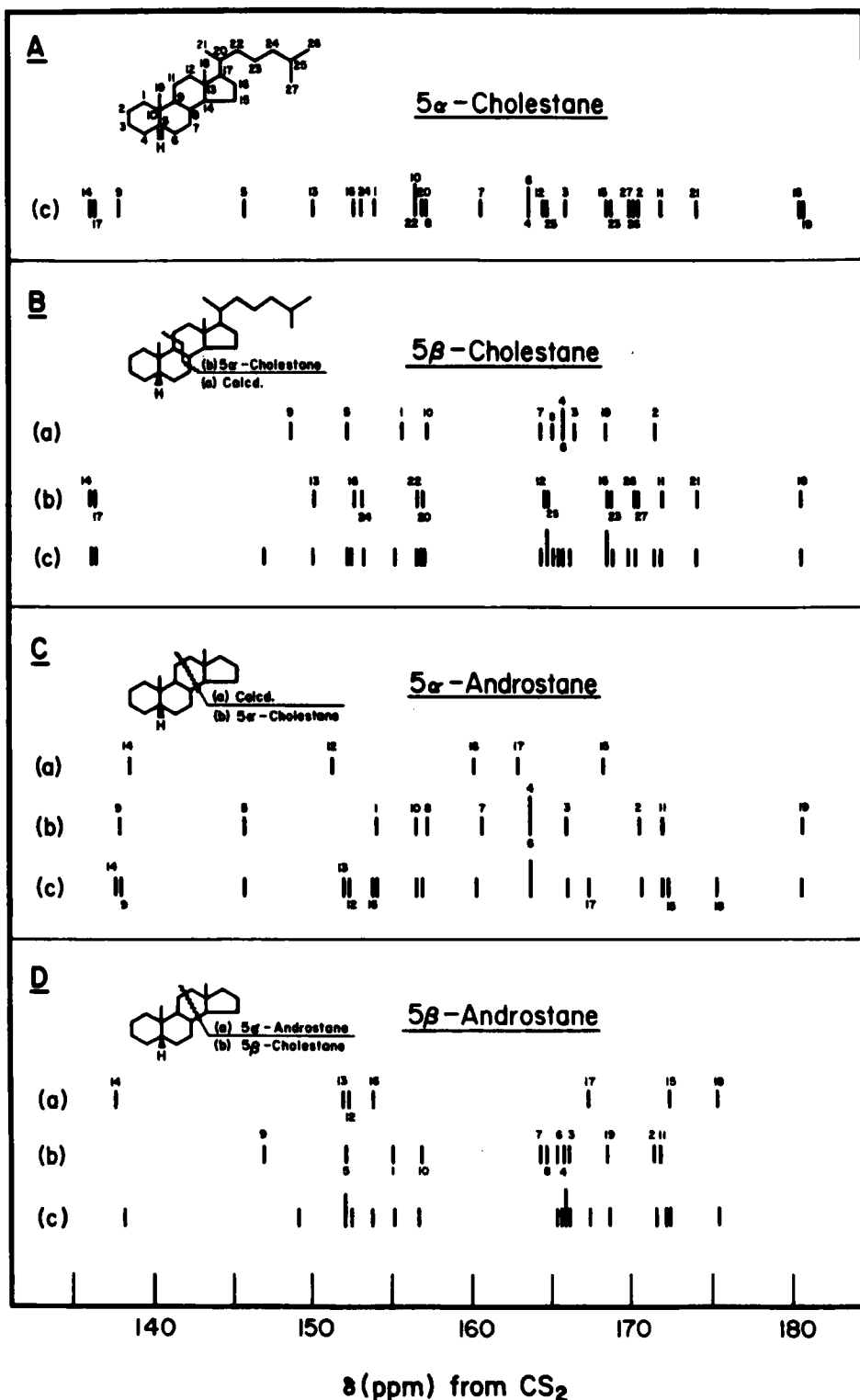
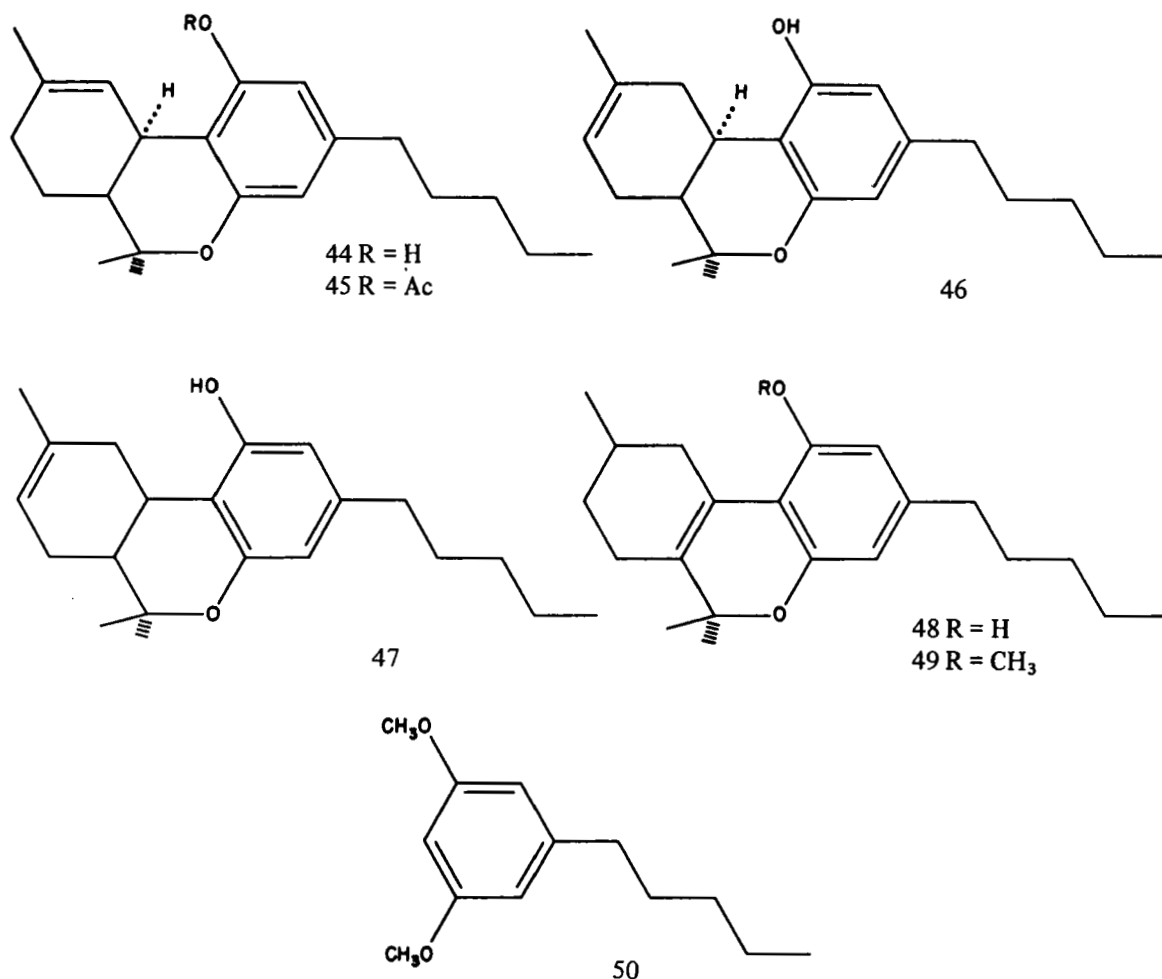


FIGURE 8. ^{13}C chemical shift correlation for 5 α -cholestane, 5 β -cholestane, 5 α -androstane, and 5 β -androstane: a, predicted using additive parameters; b, predicted using shifts from appropriate part of reference compound; c, experimental values. (From Balogh, B., Wilson, D. M., and Burlingame, A. L., Carbon-13 NMR study of the stereochemistry of steranes from oil shale of the Green River Formation (Eocene), *Nature*, 233, 261, 1971. With permission.)

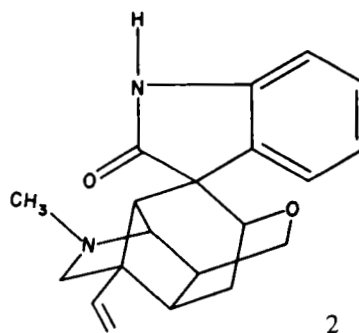
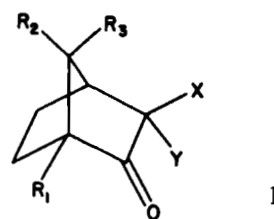
Of somewhat more topical interest, Wenkert et al.³⁰ have looked at the psychotomimetic tetra-

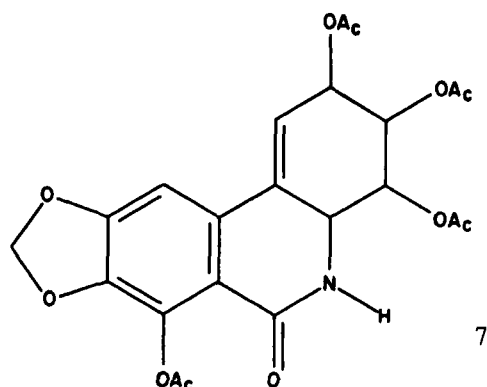
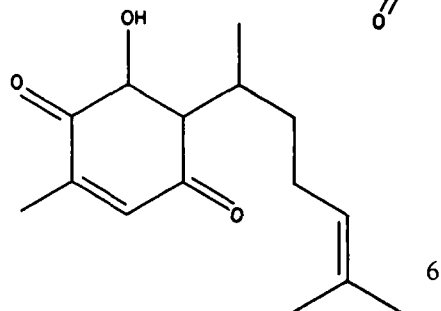
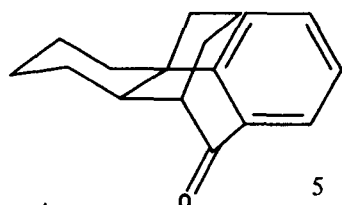
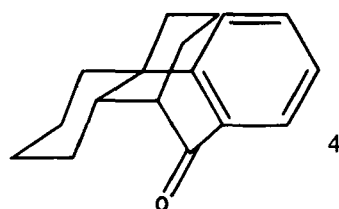
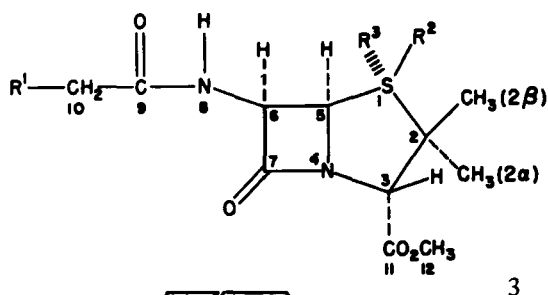
hydrocannabinol and isomers 44 to 49 and the model compound 50.



ALKALOIDS AND NATURAL PRODUCTS

There has been a flurry of exploration of the utility of ¹³C nmr for the natural product chemist or biochemist, particularly since so many biologically important compounds are of intermediate size and thus should provide well-resolved and potentially assignable carbon resonances. These first began to appear in 1969. Assignments for camphor (1) and related compounds,³¹ the alkaloid gelsemine (2),³² penicillin (3), and penicillin sulfoxide derivatives,³³ 10-oxo-des-*N*-morphinan (4), and 10-oxo-des-*N*-isomorphinan (5),³⁴ perezone (6) and derivatives,³⁵ and narciclasine tetraacetate (7)³⁶ have been accomplished.





The penicillin study nicely illustrated the value of off-resonance, coherent, proton decoupling for identification of carbons. In 3, for $R^1=H$, $R^2=O$ and $R^3=\text{lone pair}$, residual $^1J_{CH}$ couplings were calculated using the relation derived by Ernst.⁴

$$J_T \approx \frac{\Delta f \cdot J}{\gamma H_2 / 2\pi} \quad (2)$$

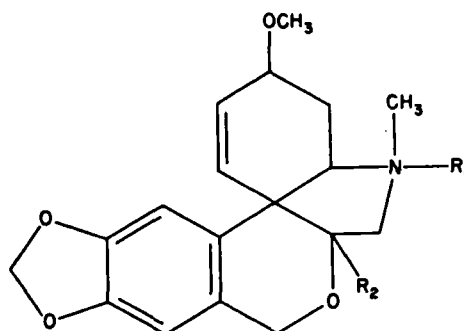
Proton shifts were known for this compound, and

$^1J_{CH}$ couplings were estimated from additivity relations. For a $\gamma H_2 / 2\pi$ decoupling field of 2100 Hz, the results below clearly show the sensitivity of the approach.

| Proton | $\delta \text{ } ^1H$ | $\delta \text{ } ^{13}C$ | $J_T \text{ (obs)}$ | $J_T \text{ (calc)}$ |
|-----------------------------|-----------------------|--------------------------|---------------------|----------------------|
| 3-H | 4.43 | 65.1 | 12.2 | 12.4 |
| 5-H | 5.44 | 75.5 | 22.7 | 21.3 |
| 6-H | 5.76 | 55.7 | 22.7 | 21.4 |
| 2 β -CH ₃ | 1.57 | 18.7 | 6.0 | 5.3 |
| 2 α -CH ₃ | 1.17 | 17.6 | 7.9 | 7.6 |
| C-10 | 1.92 | 22.1 | 3.8 | 3.5 |
| C-12 | 3.74 | 52.2 | 8.3 | 8.5 |

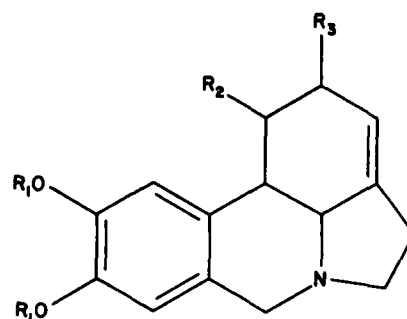
For those situations in which proton shifts are widely spread or even partially spread, this method offers a direct tie to the proton shifts and $^1J_{CH}$ and hence is of great aid in spectral analysis.

The *Amaryllidaceae* alkaloids 8 to 17, as well as nicotine (18) and quinine (19), have been examined by Crain, Wildman, and Roberts.^{3,7} Proton nmr analysis of these is quite complex, whereas the ^{13}C shifts are assignable.



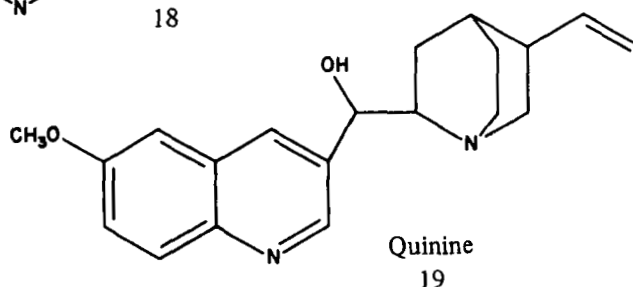
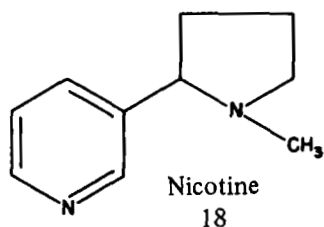
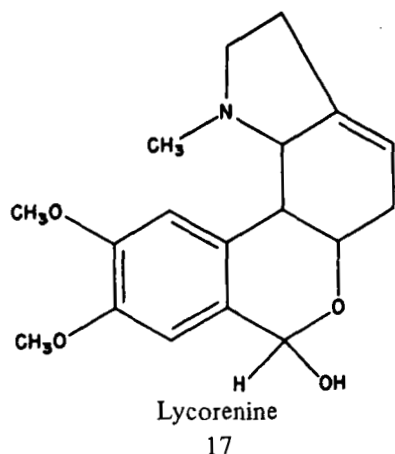
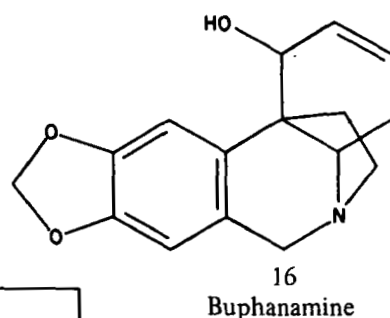
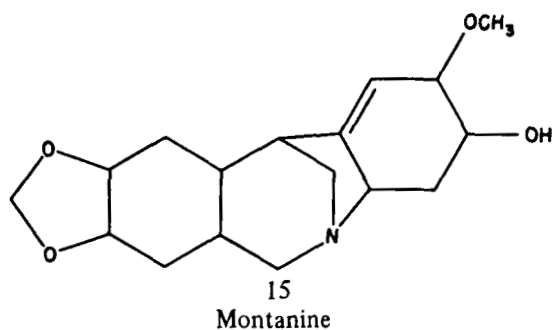
Tazettine (8)

- 8 No R_1 group; $R_2 = OH$
- 9 No R_1 group; $R_2 = H$
- 10 $R_1 = H$; $R_2 = OH$
- 11 $R_1 = CH_3$; $R_2 = OH$



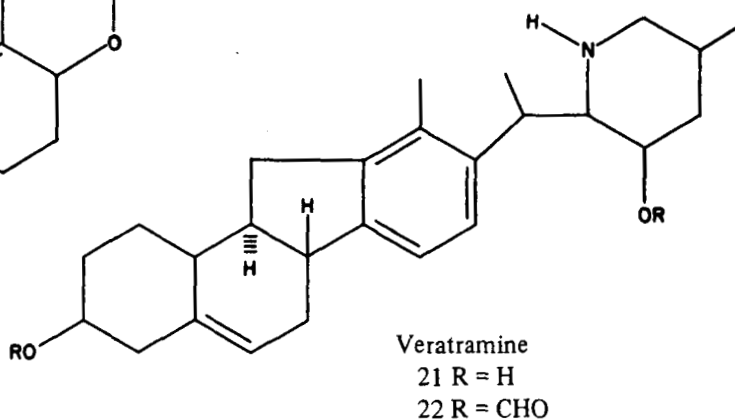
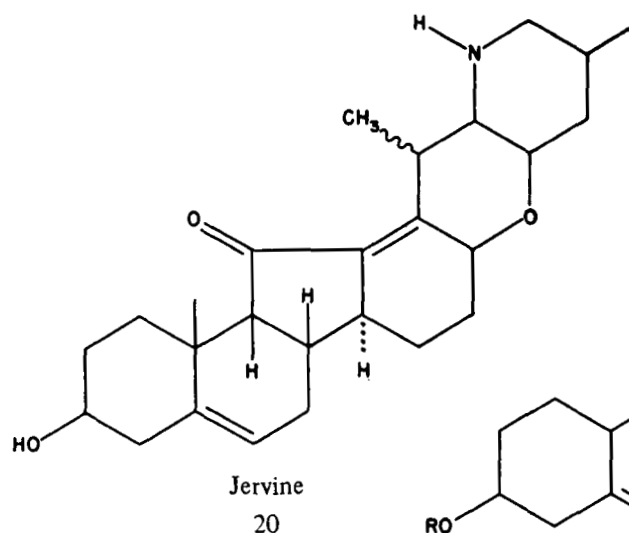
Galanthine (12)

- 12 $R_1 = CH_3$; $R_2 = OH$; $R_3 = OCH_3$
- 13 $R_1 = CH_2$; $R_2 = OAc$; $R_3 = H$
- 14 $R_1 = CH_2$; $R_2 = R_3 = OAc$

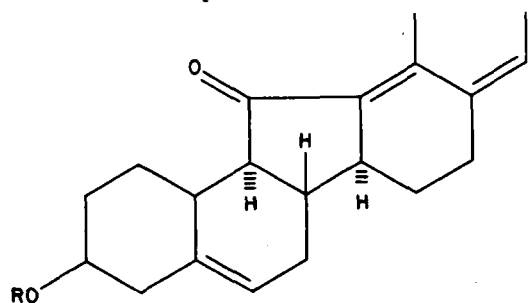


A particularly useful diagnostic technique was the observation that conversion of a nitrogen to its methyl iodide salt results in carbon shifts of 10 ppm downfield as opposed to the hydrochloride salts that give only small upfield shifts. As is obvious for 8 to 14 and many of the compounds

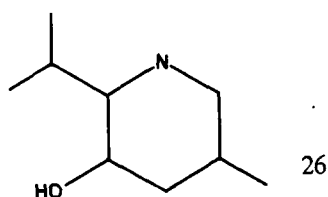
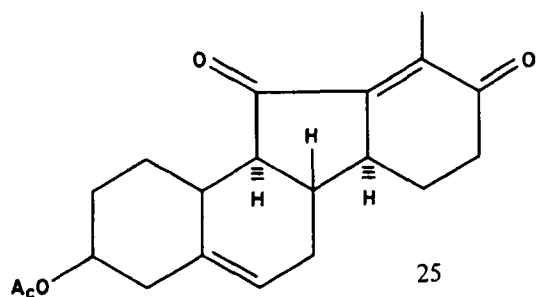
referred to above, use of suitable derivatives introducing specific interactions is a valuable assignment aid. So it was also in the case of jervine (20) and veratramine (21, 22) as studied by Sprague, Doddrell, and Roberts.³⁸



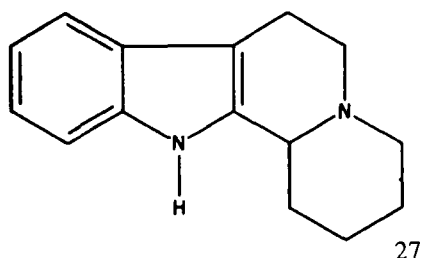
In their analysis Sprague et al.³⁸ depended heavily on the related compounds 23 to 26.



23 R = H
24 R = Ac

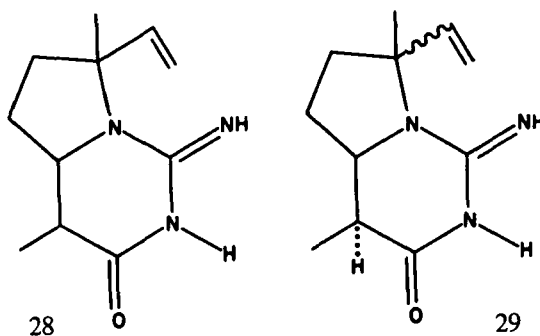


The parent compound for a class of alkaloids, 27, was the subject of a ^{13}C nmr study by Gribble et al.³⁹ Using FT techniques they were able to observe the effect of longer T_1 's for quaternary carbons in addition to potentially valuable general information concerning the *cis/trans* nature of the ring adjacent to the quinolizidine ring fusion in indole alkaloids.

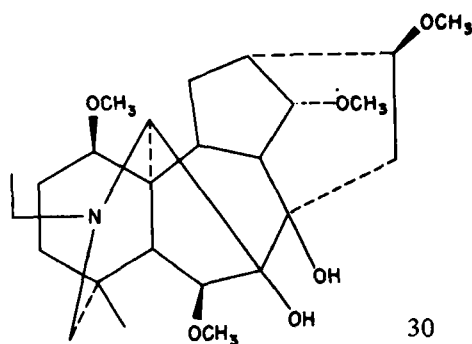


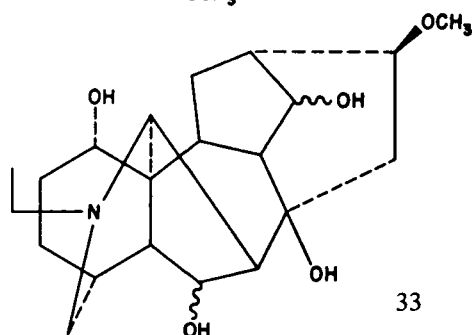
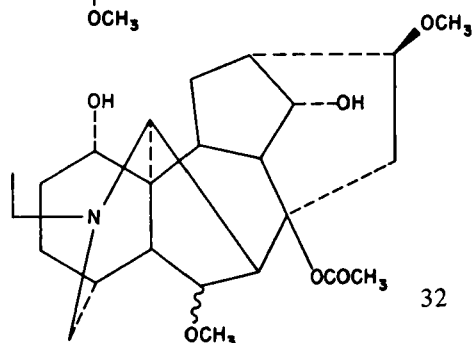
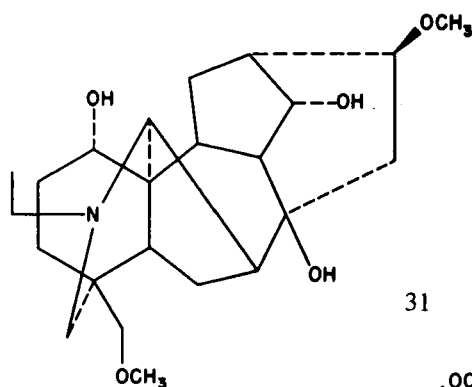
Rabaron et al.⁴⁰ provided a convincing example of the use of ^{13}C nmr for structure determination. The alkaloid arenaine was isolated

from the seeds of *Plantago arenaria* and has the composition $\text{C}_{11}\text{H}_{17}\text{ON}_3$. Other information suggested that arenaine possesses a structure similar to the guanidyl monoterpene, chaksine. The ^{13}C nmr data showed that the alkaloid has three nonprotonated carbons (carbonyl, guanidine, and an aminated tetrahedral site), three methines (one olefinic and an aminomethine), three methylenes (one olefinic and two saturated ones whose shifts suggested an $\text{R}_3\text{CCH}_2\text{CH}_2$ unit) and two methyl groups. Structure 28 is formulated from these facts and the consideration of observed shifts, while 29 details the stereochemistry using the stereochemical information present in the coupling between the methine hydrogens.

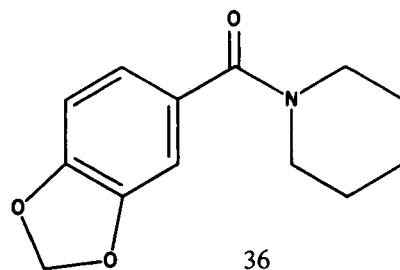
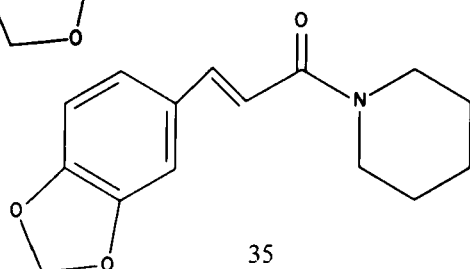
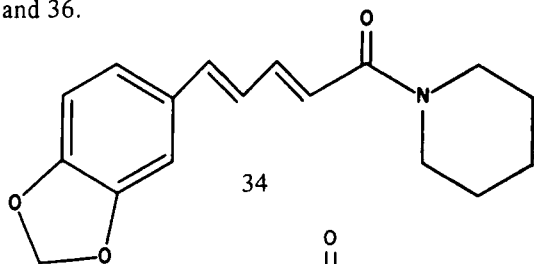


Jones and Benn⁴¹ employed ^{13}C nmr on a problem of similar nature in the identification of two new diterpenoid alkaloids from *Delphinium bicolor* nut; ^{13}C studies were of critical importance in determining the degree and locations of oxygen substitution in these molecules of composition $\text{C}_{25}\text{H}_{39}\text{NO}_6$ and $\text{C}_{22}\text{H}_{35}\text{NO}_5$. Prior work on *Delphinium* alkaloids, other physical data, and model compounds 30 (deoxylycotonine) and 31 (isolatizidine) provided enough evidence, along with the ^{13}C spectra of the two unknown alkaloids to assign 32 and 33 as the likely structures.



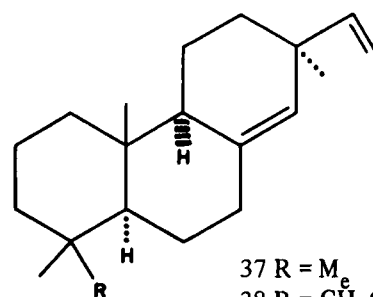


In cases where all the above techniques fail to distinguish carbons it may be useful to employ a paramagnetic shift agent as illustrated by Briggs et al.⁴² for borneol and Wenkert et al.⁴³ for the alkaloid piperine (34) and model compounds 35 and 36.



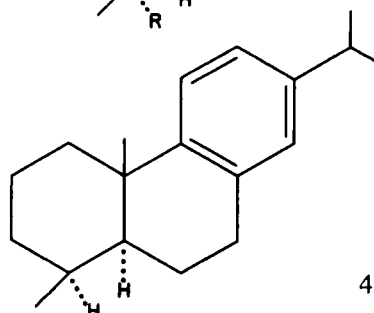
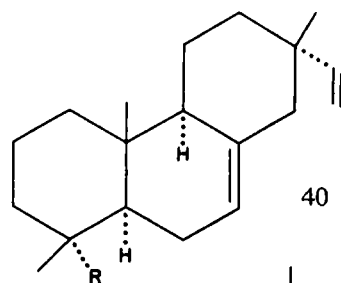
Standard techniques led to complete assignments for 35 and 36, but C-6 and the olefinic α and γ carbons and the olefinic β and δ carbon assignments were ambiguous. ^{13}C spectra of piperine- $\text{La}(\text{dpm})_3$ and $-\text{Eu}(\text{dpm})_3$ complexes led to individual assignments.

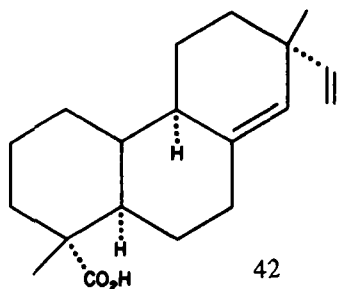
Pimaradiene derivatives 37 to 44 were studied by Wenkert and Buckwalter⁴⁴ as the first step in analysis of diterpenic compounds, with particular focus on determination of the C ring conformation. Again a paramagnetic shift agent was required to sort out several shifts. The ^{13}C shifts allowed the stereochemical orientation of the C ring to be unambiguously deduced.



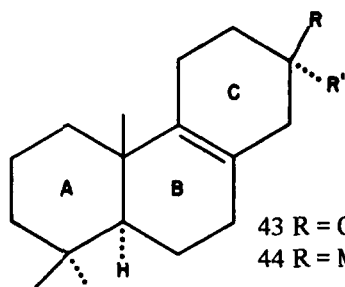
38 R = CH_2OH

39 R = CO_2H



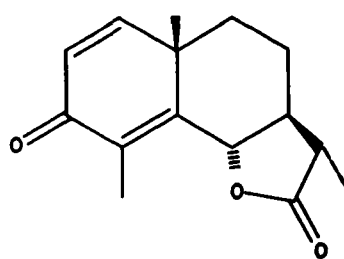


42

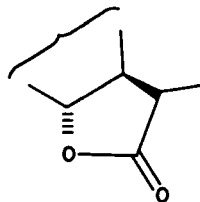


43 R = C₂H₅; R' = Me
44 R = Me; R' = C₂H₅

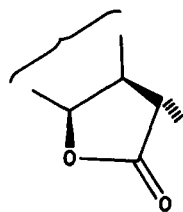
Pregosin, Randall, and McMurray⁴⁵ used ¹³C nmr to provide an elegant way of distinguishing and determining the various configurations of the lactone ring in santonin derivatives 45 to 48.



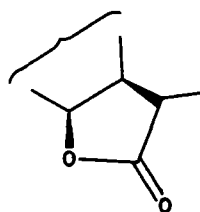
α-Santonin
45



β-Santonin
46



α-Episantonin
47



β-Episantonin
48

The oxygen-substituted carbon at the lactone ring junction has a shift dependent upon the orientation of the C-O bond, 76.5 ppm for 47 and 48, but 81 ppm for 45 and 46. The lactone methyl (and other nearby carbons) has a shift dependent on α- or β-identity, thereby completely determining the santonin conformation.

Other applications of ¹³C nmr include structural analysis of a metabolite from *Aspergillus*,

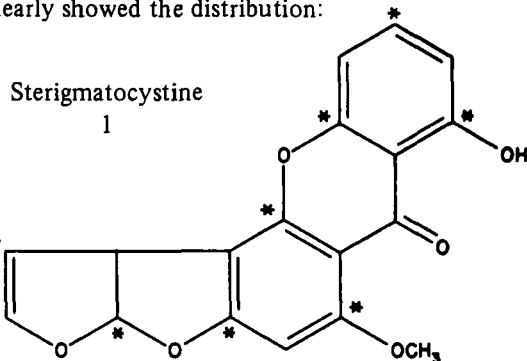
2-carboxymethyl -3-*N*-hexyl-maleic acid anhydride⁴⁶ and a new diterpenoid from the leaves of *Lencothoe grayana*.⁴⁷

Gansow, Beckenbaugh, and Sass⁴⁸ have surveyed a series of medically important benzocaine hydrochlorides as well as procaine amide and suggested that the interaction of the polar carbonyl group or the aromatic π system may be important in explaining drug potency in vivo by modifying the configuration of the anesthetic at the receptor site.

BIOSYNTHETIC STUDIES

The use of any material that differs appreciably in normal isotopic proportions as either a precursor in a chemical or biological sequence or a nutrient in a biological system allows the introduction of a safe, noninteracting label of non-destructive nature. ¹³C nmr studies of end products provide valuable information regarding the amounts and distribution of the enrichment, giving useful information about the reaction sequence or biochemical mechanism. Readily available labels are enriched ¹³C, ¹⁵N, and ²H. Each of these will cause distinctive changes in the observed ¹³C spectrum.

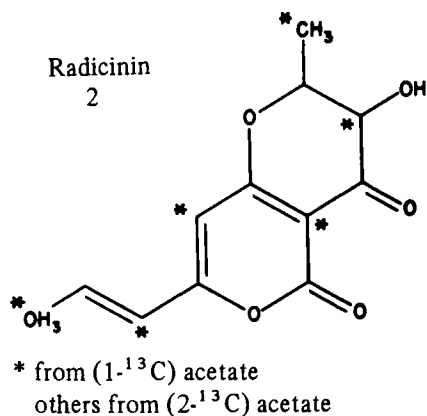
The first studies of this kind actually used ¹³C satellites in the proton nmr spectrum.⁴⁹ Tanabe et al.⁵⁰ reported the first ¹³C nmr spectra of a ¹³C-labeled metabolite, that of sterigmatocystin (1). Comparison of spectra of sterigmatocystin obtained from biosynthesis using the nutrient sodium (1-¹³C) acetate (56%) with spectra obtained using sodium (2-¹³C) acetate (61%) clearly showed the distribution:



Sterigmatocystine
1

* from (1-¹³C) acetate
others from (2-¹³C) acetate

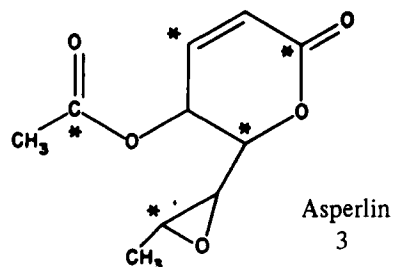
The results were consistent with previous biogenic hypotheses. A similar investigation on radicinin⁵¹ (2) by the same group led to the distribution



The results confirmed the polyacetate origin of radicinin with the expected alternating labeling. (Note that there is a nonalternating pair in the above sterigmatocystin pattern.)

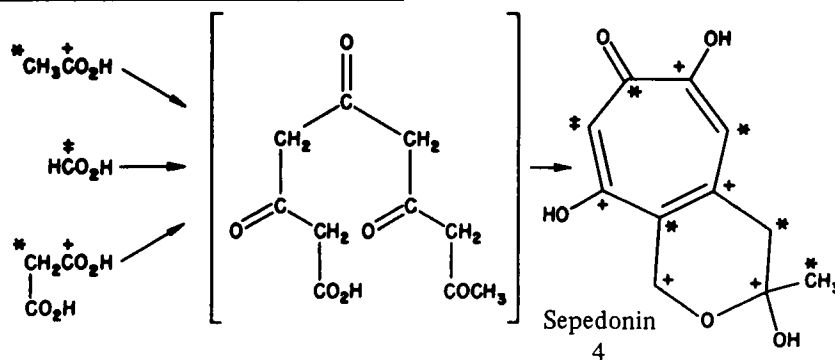
Off-resonance decoupling techniques proved very useful in a study by Tanabe et al.⁵² on the biosynthesis of asperlin (3) derived from sodium acetate-2-¹³C. The proton shifts were well spaced or could be made so by proper choice of solvent. For example, the two methyls appeared in the proton spectrum at $\delta = 1.31$ and $\delta = 2.10$. For a coherent off-resonance decoupling field of 2100 Hz strength, these methyls gave residual one-bond

splittings in the ¹³C spectrum of 10.0 and 13.5 Hz, allowing methyl assignments to be made. The observed (2-¹³C) acetate distribution in asperlin was found to be



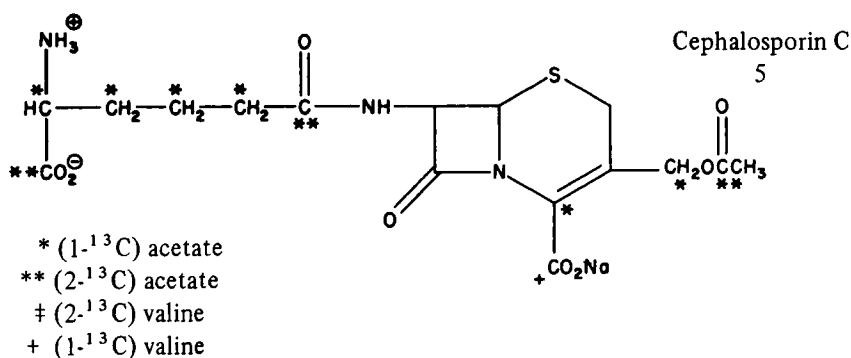
The labeling pattern supported the tetraacetate origin of the eight-carbon epoxy γ -lactone in the antibiotic.

McInnes et al.⁵³ used three different methods of enrichment (the two acetates and formate) in their study of the tropolone, sepedonin (4). Only one of the carbons was enhanced using the enriched formate in the nutrient, five from the (1-¹³C) acetate and five from the (2-¹³C) acetate. The results provide evidence that sepedonin is formed by insertion of the formate carbon between the third and fourth carbons of a ten-carbon polyketide chain derived from acetate.



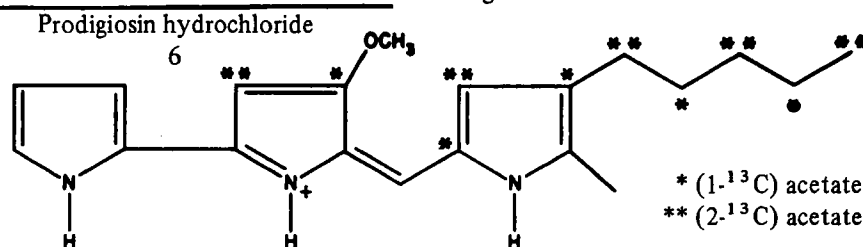
An investigation wherein not only the pattern but also the relative distribution of the ¹³C label

was determined was that of Neuss et al.^{54,55} for cephalosporin C (5).



Here the labeling in the trimethylene linkage amounted to roughly one half of the incorporation at the terminal amino acid methine carbon. This was interpreted as being consistent with cyclization of the tricarboxylic acids involved in the formation of α -aminoadipic acid via the Krebs cycle.

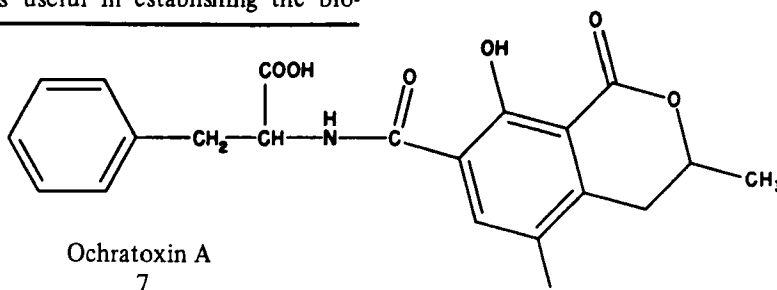
Off-resonance decoupling, progressive saturation, indor, single frequency proton decoupling, and coupled spectra were used by Cushley et al.^{5,6} in deciphering the biosynthetic pathway for prodigiosin (6). Figure 9 shows the spectra of the variously enriched derivatives. The labeling pattern is given below.



The methylamylpyrrole moiety (right-hand ring) is essentially constituted from an eight-carbon poly-acetate chain with the origin of the two remaining carbons yet to be determined. It is significant that no incorporation is found in the left-hand ring, indicating a possible novel route to this pyrrole ring.

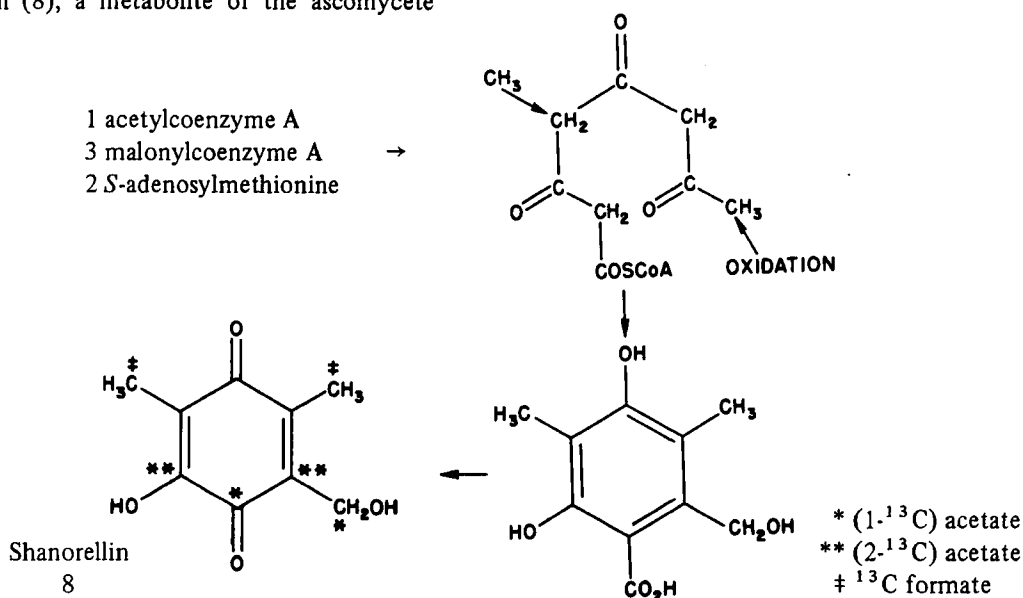
¹³C nmr was useful in establishing the bio-

synthetic carbonyl origin in ochratoxin A (7).^{5,7} Using ¹³C-formate as a nutrient, the lactone carbonyl resonance is not enhanced, pointing to the probability that the lactone carbonyl originally was a member of a polyketide chain and did not add through a subsequent step (as shown above for sepedonin).



Recently Wat et al.^{5,8} used 1- and 2-enriched ¹³C acetates along with ¹³C-formate in studying shanorellin (8), a metabolite of the ascomycete

Shanorella spirotricha. The biosynthetic scheme is proposed to be



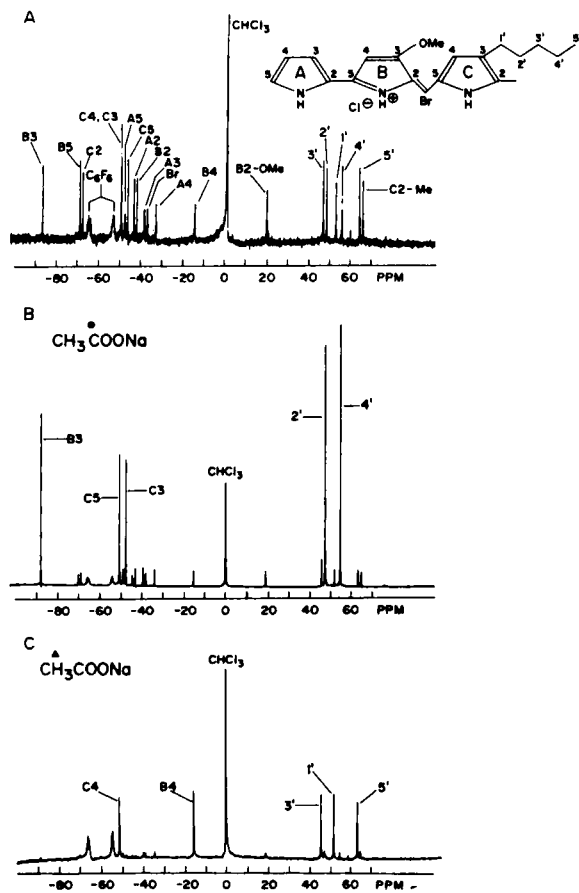
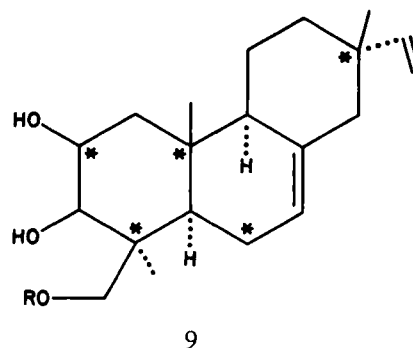


FIGURE 9. A, ^{13}C spectrum of 1 M prodigiosin hydrochloride in CHCl_3 ; B, ^{13}C spectrum of 0.5 M prodigiosin hydrochloride in CHCl_3 , biogenetically enriched with $1\text{-}^{13}\text{C}$ acetate; C, ^{13}C spectrum of 0.05 M prodigiosin hydrochloride in CHCl_3 , biogenetically enriched with $2\text{-}^{13}\text{C}$ acetate. (From Cushley, R. J., Anderson, D. R., Lipsky, S. R., Sykes, R. J., and Wasserman, H. H., Carbon-13 fourier transform nuclear magnetic resonance spectroscopy II. The pattern of biosynthetic incorporation of $(1\text{-}^{13}\text{C})$ - and $(2\text{-}^{13}\text{C})$ acetate into prodigiosin, *J. Am. Chem. Soc.*, 93, 6284, 1971. With permission of the American Chemical Society.)

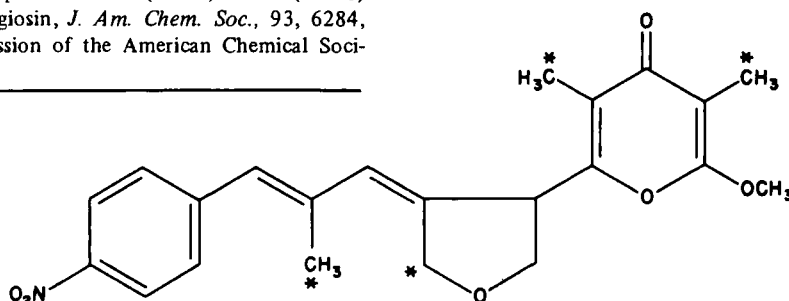
The results confirm that shanorellin is biosynthesized from four molecules of acetate with loss of one carboxyl group and addition of two methyl groups from a one-carbon donor. The labeling pattern is consistent with its formation via the acetate-polymalonate pathway although a malonate supplement was not specifically incorporated into the chain-extending units.

Polonsky et al.^{5,9} tested the biosynthesis of metabolites of the mushroom *Oospora Virescens*, the virescenosides (9). These are diterpenic glycosides and the first altrose derivatives found in nature. Addition of $(1\text{-}^{13}\text{C})$ - and $(2\text{-}^{13}\text{C})$ -acetates to culture media gave the enrichment pattern:



R = β -D-altropyranosyl
 * = $(1\text{-}^{13}\text{C})$ acetate
 others from $(2\text{-}^{13}\text{C})$ acetate

Sodium propionate- $3\text{-}^{13}\text{C}$ was used to test a biosynthetic hypothesis by Yamazaki et al.⁶⁰ for a nitro-containing metabolite of *Streptomyces luteoreticuli*, aureothin (10). The incorporation pattern was found to be

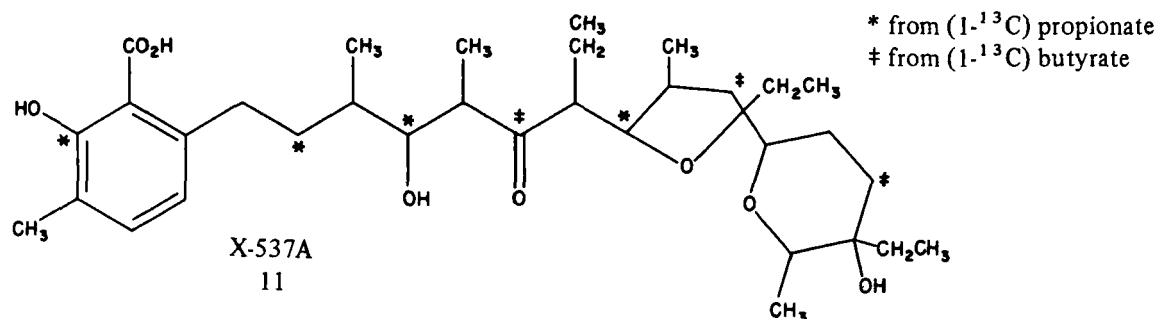


Aureothin
 10


and is consistent with the condensation of a *p*-amino (or *p*-nitro) benzoic acid with a poly-

ketide from propionate (with possible acetate) condensations.

production, but only the ^{13}C study enabled them to tell that *all three* C-ethyl groups were derived from butyrate

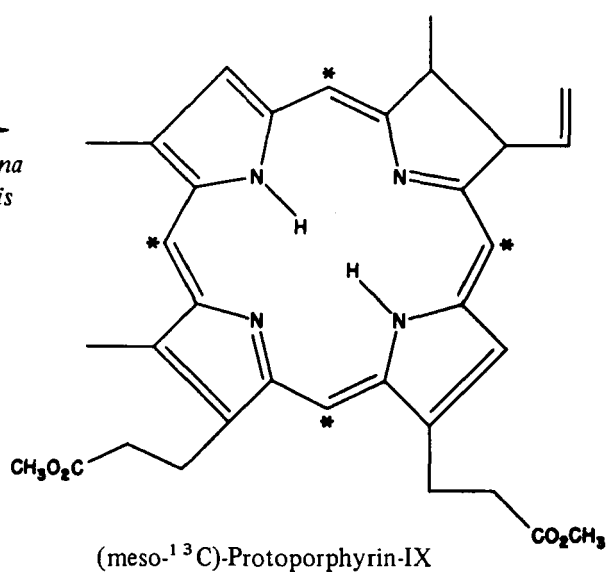


study of Battersby et al.⁶² This then served as a precursor for protoporphyrin-IX (13) via enzymatic reaction. The label resulted in equal enrichment of the four *meso* carbons of the porphyrin ring.



 $\text{PBG-}^{13}\text{C}$

 12

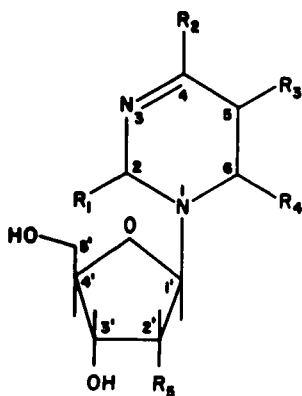


Finally, a comprehensive review (in French) of the use of ^{13}C satellites in proton spectra and ^{13}C nmr in biosynthetic problems has appeared very recently.⁶³

NUCLEOSIDES AND NUCLEOTIDES

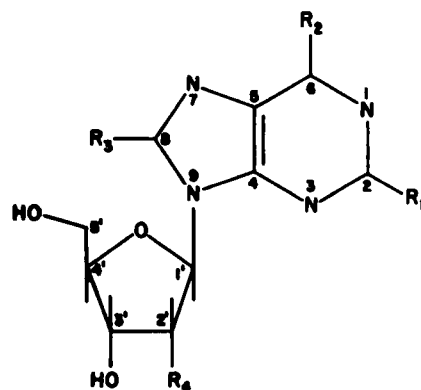
Nitrogen heterocycles have been intensively studied both from theoretical and experimental fronts. The published work to 1971 has been reviewed,⁶⁴ and several additional studies have been reported subsequently.⁶⁵⁻⁷² A thorough understanding of the range and factors involved in the nitrogen base shifts is essential for the extension to nucleosides and nucleotides, particularly for conformational analysis and tertiary structure determination in polynucleotides.

Jones et al.⁷³ conducted the first comprehensive survey of nucleoside chemical shifts. They examined uridine, thymidine, cytidine, deoxycytidine, adenosine, deoxyadenosine, guanosine, deoxyguanosine, inosine, deoxyinosine, and xanthosine. The shifts exhibited a 160 ppm/electron sensitivity to computed π -charge density, a value identical with that of Spiess and Schneider,⁷⁴ except that the quaternary C-4 and C-5 carbons of the purine nucleosides, while having the same sensitivity to charge, were offset in shift from the protonated carbons. The low shielding of the C-5 carbon was associated with a high positive charge density and the high electrophilic reactivity of this position. The same group subsequently⁷⁵ expanded this study to cover 29 nucleosides of the types:



Pyrimidine nucleosides

1

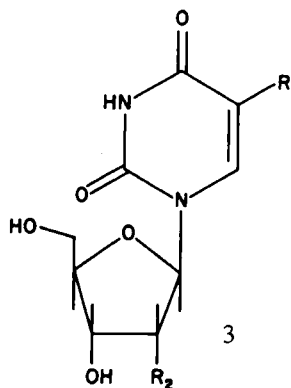


Purine nucleosides

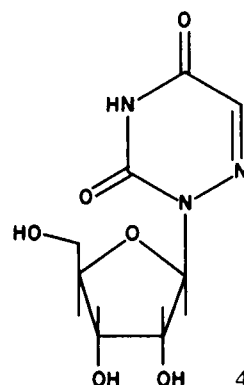
2

The spectra were clearly separated into ribose (39 to 91 ppm) and base (161 to 165 ppm) regions with only small effects on a given ribose spectrum with change of nitrogen base. Even going to *O*-glycosides only resulted in a downfield shift of 18 ppm for C-1 with respect to the corresponding *N*-glycoside, with the other ribose carbons being relatively unperturbed. The deoxyribosides did exhibit a 3 to 4 ppm upfield shift for C-1 compared to the oxyglycosides. Ribosides and deoxyribosides were easily distinguished by the higher C-2 shielding in the latter. Assignments for the purine and pyrimidine bases were grouped into classes of uridines, cytidines, purines, adenosines, and guanosines. The large variety in R_1 to R_4 and the expected substituent effects allowed individual carbon assignments. Attempts at correlation of ^{13}C shifts with theoretically calculated charge densities were of mixed success, but the shifts did seem to reflect the general nature of the nucleosides.

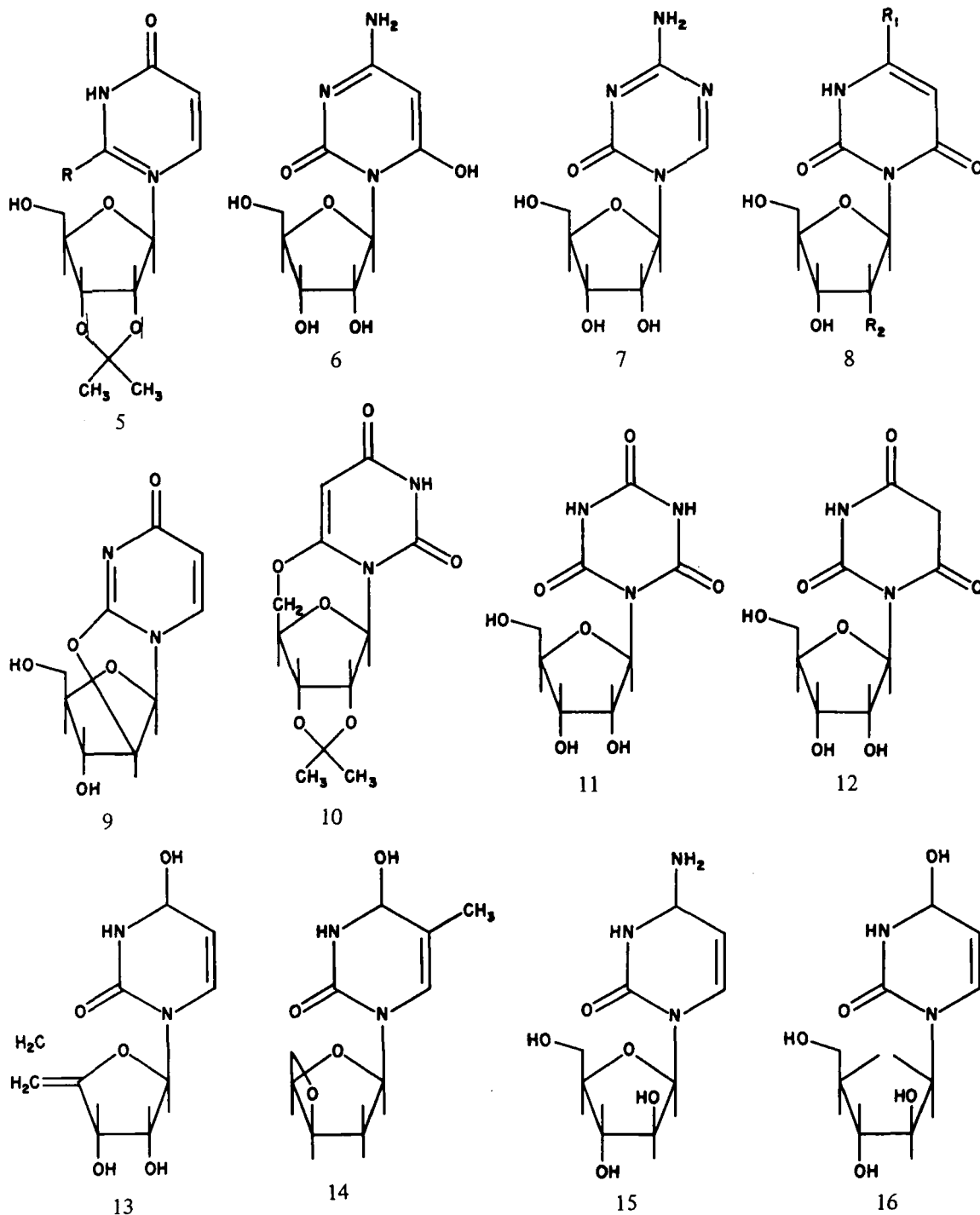
Extending these studies still further,⁷⁶ the same group considered 23 other pyrimidine nucleosides of the types 3 to 16.



3



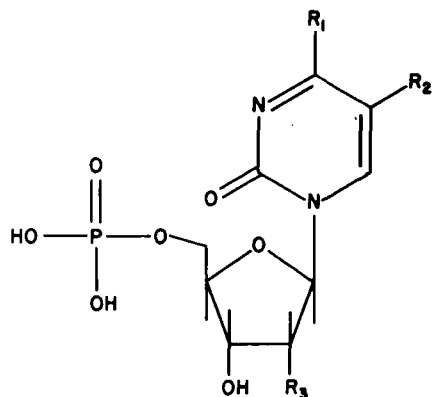
4



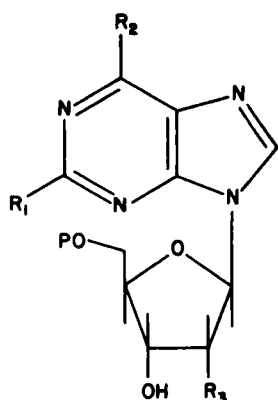
In these nucleosides the ribose shift order (in the direction of increased shielding) of C-1', C-4', C-3', C-2', and C-5', and the deoxyribose shift order of C-4', C-1', C-3', C-5', and C-2' were reported. The effect of an isopropylidene bridge in 10 induces a large 16 ppm downfield shift at C-5'. The cyclo-side 14 showed that geometry does play an

important role in determining the ribose shifts. C-5 and C-6 shifts show that 6 exists primarily in the diketo tautomer and, while 12 can exist in other tautomeric forms, the triketo form predominates.

The work of Dorman and Roberts⁷⁷ gave the corresponding nucleotide data. They examined compounds 17 to 26.



- 17 UMP $R_1 = R_3 = \text{OH}; R_2 = \text{H}$
 18 TMP $R_1 = \text{OH}; R_2 = \text{CH}_3; R_3 = \text{H}$
 19 CMP $R_1 = \text{NH}_2; R_2 = \text{H}; R_3 = \text{OH}$
 20 dCMP $R_1 = \text{NH}_2; R_2 = R_3 = \text{H}$

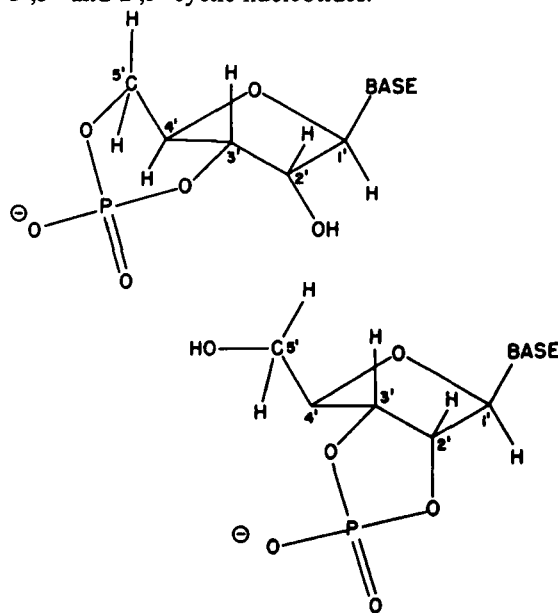


- 21 AMP $R_1 = \text{H}; R_2 = \text{NH}_2; R_3 = \text{OH}; P = \text{PO}_3\text{H}$
 22 dAMP $R_1 = R_3 = \text{H}; R_2 = \text{NH}_2; P = \text{PO}_3\text{H}$
 23 ATP $R_1 = \text{H}; R_2 = \text{NH}_2; R_3 = \text{OH}; P = \text{P}_3\text{O}_6\text{H}_4$
 24 GMP $R_1 = \text{NH}_2; R_2 = R_3 = \text{OH}; P = \text{PO}_3\text{H}$
 25 dGMP $R_1 = \text{NH}_2; R_2 = \text{OH}; R_3 = \text{H}; P = \text{PO}_3\text{H}$
 26 IMP $R_1 = \text{H}; R_2 = R_3 = \text{OH}; R = \text{PO}_3\text{H}$

The phosphorylated carbon was assigned from its higher shielding and ~ 4 Hz J_{POC} . Its shift was essentially constant except for ATP. The J_{POCC} coupling (~ 8 Hz) helped to assign C-4'. Other than in these changes, the nucleotides resemble the nucleosides. Dorman and Roberts⁷⁷ also carried out pH dependence studies on CMP and ATP. C-1 was the only ribose carbon to be affected while only C-5 was *unaffected* among the base carbons. Similar changes occurred in ATP; the carbons adjacent to the more weakly basic nitrogens were shifted upfield upon acidification while the reverse was true for those carbons attached to the more basic nitrogens. Various mixtures and concentrations of nucleotides gave no differences that could be traced to base stacking.

Mantsch and Smith⁷⁸ have recently corrected the above^{73,79} assignments of the 2' and 3' carbons of uridine through use of 2'-UMP, 3'-UMP, and 5'-UMP and the expected phosphorylation shifts. The higher resolution made practical through use of FT nmr allowed evaluation of long range ^{13}C - ^{31}P couplings to all but the 1' ribose carbons. The $^{13}\text{POC}^{13}\text{C}$ couplings were pointed out to be valuable for conformational analysis. They also examined the ^{13}C spectrum of a polynucleotide (poly U) of molecular weight 130,000 and related deviations from additivity to tertiary effects. C-2, C-4, C-6, C-4', and C-5' are affected in changing from 5'-UMP to the poly-uridine nucleotide. The large C-4' (1.44 ppm) shielding and C-5' (1.87 ppm) deshielding were related to an alteration in the position of the phosphate group relative to the ribose ring. The behavior of the $^3J_{\text{PC}}$ couplings suggested a similar pattern to ^1H - ^1H and ^1H - ^{31}P vicinal couplings, i.e., large (~ 10 Hz) couplings for *gauche* rotamers. Thus 5'-UMP has a preference for the 4'-*trans* rotamer, 2'-UMP the 1'-*trans* rotamer, and 3'-UMP somewhat less preference for the 4'-*trans* rotamer. In poly U the 5'-phosphate has a preference for the 4'-*trans* rotamer while the 3'-phosphate has preference for the 2'-*trans* rotamer.

Lapper, Mantsch, and Smith^{79,80} calibrated the angular dependence of $^3J_{\text{PC}}$ by considering 3',5'- and 2',3'-cyclic nucleotides.



In the six 3',5'-cyclic nucleotides they studied, the P-C_{2'}' couplings were 8.0 ± 0.3 Hz, an appropriate value to label as a *trans* coupling. The P-C_{4'}'

couplings were 4.6 ± 0.2 Hz but since the three-bond coupling can take place via two routes, they could only estimate the single *gauche* coupling to be ~ 2 Hz. The 3' couplings (4.2 ± 0.5 Hz) and 5' couplings (7.2 ± 0.2 Hz) were constant throughout the series for the bases uridine, cytidine, adenine, guanine, thymidine, and N^6 , $O^{2'}$ -dibutryl-adenosine. The $^3J_{PC}$ couplings were consistent with considerable conformational flexibility for the 2',3'-cyclic nucleotides. In this conformational equilibrium, the pyrimidine nucleotides tend toward the 3'-*endo* (2'-*exo*) conformers, whereas the purine nucleotides show no significant preferences for any of the principal conformers. Increasing temperature decreased any conformational preference.⁸¹

Lemieux et al.⁸² explored a similar vicinal correlation, but using $^3J_{CH}$ in C2-enriched (60% ^{13}C) uridine nucleotide and derivatives in which the dihedral angle was varied. A Karplus-like relationship was observed with $^3J_{CH}$ maximum (8 Hz) when in a *trans* (180°) orientation, zero at $\sim 90^\circ$, and 2 Hz for $\sim 50^\circ$ (*anti*).

In another recent application of ^{13}C nmr, Kreishman et al.⁸³ were able to pinpoint the glycosylation site in 1- β -D-ribofuranosyl-1,2,4-triazoles where classical UV spectra were useless because of weak absorption. Either C-3 or C-5 triazole substitution is possible but α - and β -substituent effects were only consistent with one set of isomer assignments. The success of the ^{13}C analysis should prompt future use for assignment of highly substituted heterocyclic ring compounds that exhibit very little UV absorption.

Using ^{13}C enrichment in the carboxamide group, Blumenstein and Raftery⁸⁴ examined the ^{13}C nmr titration curve of nicotinamide-adenine-dinucleotide. An apparent pK_a of 4 indicated that the carboxamide carbon has a chemical shift that is influenced by protonation of the adenine ring of the dinucleotide. No effect was noted on the carboxamide carbon shift upon ionization of the phosphate.

AMINO ACIDS, PEPTIDES, AND POLYPEPTIDES

The first systematic studies of amino acids were those from Sternlicht's group, beginning with indirect detection using indor⁸⁵ and later using FT direct detection on amino acids isolated from algae

fed on $^{13}CO_2$.^{86,87} Subsequently, the factors involving ^{13}C T_1 and T_2 relaxation times were critically examined in a study of protonated and deuterated amino acids bound to cation exchange resins.⁸⁸

Their indor study focused on the ^{13}C shifts of glycine, diglycine, triglycine, alanine, and alanyl-glycine as functions of pH. The pH studies showed that, for example, when a glycine loses a proton, the carbons shift downfield, more so when a $-NH_3^+$ proton is lost than when a $-COOH$ proton is lost.

Structurally, the ^{13}C shifts of the polypeptides were shown to have great potential. In diglycine, the α - and β -methylene resonances were symmetrically placed about the glycine resonance, the α unit being downfield. In triglycine the middle methylene had essentially the same shift as glycine, while the outer two methylenes had shifts similar to those in diglycine. Much effort was placed into arriving at a set of substituent effects for use in predicting shifts in other amino acids. A family of parameters was determined and subsequently revised following more data in a later publication.⁸⁷ Throughout these studies the shifts were analyzed in terms of charge density variations as controlling changes in the paramagnetic contribution to the chemical shift, σ_p . Apparently anomalous shifts were observed upon protonation or deprotonation, i.e., upfield carbonyl and α carbon values shift upon protonation, whereas a downfield shift might be expected from a simple attenuated inductive effect. These were explained by putting all changes in charge density on the peripheral protons and leaving the carbons relatively unchanged, or changed slightly, but in the opposite direction to that of the protons. Hence, the carbon electronic charge densities were interpreted as remaining constant or increasing upon protonation of nearby centers.

This reverse behavior on protonation was also noted in work by Hagen and Roberts⁸⁹ on aliphatic carboxylic acids and salts ranging from formic to valeric acids. For example, the effects of acid ionization on the butyric acid carbons are $\alpha = +4.7$ ppm, $\beta = +3.9$ ppm, $\gamma = +1.4$ ppm, and $\delta = +0.6$ ppm — all downfield shifts.

The amino acids obtained from algae^{86,87} were leucine, isoleucine, valine, alanine, threonine, glycine, lysine, arginine, serine, proline, glutamic acid, aspartic acid, methionine, histidine, phenyl-alanine, and tyrosine. The larger number of

compounds allowed the more refined array of chemical shift parameters given below:

| Substituent | Shift Parameter | | | |
|-------------------------------|-----------------|---------|----------|----------|
| | α | β | γ | δ |
| -CH ₃ | 9.1 | 9.4 | -2.5 | 0.3 |
| -OH | 48.5 | 10 | -5.7 | 0.5 |
| -NH ₂ | 29 | 11.4 | -4.6 | 0.6 |
| -NH ₃ ⁺ | 26 | 7.5 | -4.6 | |
| -COOH | 21.5 | 2 | -2.5 | 0.6 |
| -COO ⁻ | 24.5 | 3.5 | -2.5 | |

Some refinements for branching situations were also detailed. The parameters do give a good beginning for a predicted spectrum. The calculated shieldings should be close to those of carbons in a random-coil polypeptide. Differences between this and, for example, a helical form may then give important conformational information.

A technique which ultimately could have impact in the areas of biopolymers, catalysis, and biological membranes is that described by Sternlicht et al.,⁸⁸ wherein ¹³C nmr spectra of amino acids bound to cationic exchange resins were observed using FT techniques. The longer τ_c expected for bound species should allow much more facile observation of carbons with long solution T_1 's, particularly quaternary carbons in amino acids. This type of study provides a model for small side-chains on a biopolymer or a substrate in slow-exchange with a binding site on an enzyme.

Sternlicht et al.⁸⁸ examined glycine, alanine, glutamic acid, and histidine in solution and bound to 4 and 8% cross-linked resin. Chemical shifts were identical, within the sometimes large (2 to 500 Hz) linewidths in the free and bound species. For example, in cysteine bound to the 4% resin linewidths of 1.8, 9 and 14 Hz were observed for the carboxyl, α and β carbons. Proceeding to cystine, complete immobilization occurs on the resin since both -NH₃⁺ groups bind to the resin. Only a 20-Hz carboxyl resonance was observed. However, in solution essentially only α - and β -carbon signals were observed because of the long T_1 of the carboxyl carbon.

Large differences between T_1 and T_2 (measured from linewidths) were evident for those cases in which T_1 was measured. T_2 was considerably shorter than T_1 and changed appreciably with degree of cross-linking of the polymer while T_1 was relatively unaffected. While the gain in

intensity upon binding was large, it would be of little value in those cases where amino acids (or substrates in general) are quite soluble and not limited in quantity. However, for cases where little material is available or solubility very low, this technique could serve as a "chemical amplifier," especially for carbons with long solution T_1 's.

Since the bound species' T_2 's are usually very much shorter than the repetition rate of the sampling pulse, the linewidths are directly proportional to the number of protons attached to a carbon under observation. This serves to accomplish the same end as off-resonance proton decoupling techniques. The T_1 's, nuclear Overhauser effect enhancements, and T_2 's all point to very minimal, if any, contribution from ¹³C chemical shift anisotropies or resin dipolar interactions to the carbon relaxation times. Sternlicht et al.⁸⁸ postulated a model for the bound amino acids as anisotropic rotors on a resin backbone undergoing slow, "wobbling" motions. Slow anisotropic rotation with concomitant nonzero averaging of the ¹³C-¹H dipolar (through-space) magnetic interaction is necessary to explain the observation that ²H-bonded carbons had only a factor of 3 to 4 line-narrowing over their ¹H analogs, rather than the factor of 10 to 15 expected from the change from ¹H to ²H in the expression for the rapid rotational motion region,

$$X = {}^1\text{H}; S = \frac{1}{2}$$

$$\frac{1}{T_1} = \frac{1}{T_2} = \frac{4}{3} \gamma_C^2 \gamma_X^2 \hbar^2 S(S+1) r_{CX}^{-6} \tau_c \quad X = {}^2\text{H}; S = 1.$$

(3)

If rapid tumbling becomes anisotropic, the $\gamma_C^2 \gamma_X^2$ factor will still change by a factor of 10 to 15 for ¹H → ²H, but τ_c must be replaced by a complex function of correlation times. However, if the molecules are able to undergo anisotropic rotational reorientation at a rate slow compared with T_2 , the linewidth ratio reduces to a limit of 3.25. Since full Overhauser enhancements of 3 were observed for histidine carbons in the bound form, the carbon T_1 's must have been determined by a τ_c of less than 10⁻⁸ sec, since at longer times the maximum NOE drops to ~ 1.3 (i.e., for $\omega_C \tau_c > 1$). The dependence of T_2 on extent of cross-linking was suggested⁸⁸ as resulting from a wobbling motion of the resin lattice (slow motions and ordinary chemical exchange affect T_2 but not T_1). Thus the rapid internal motions dominate T_1 while the slow wobbling motion dominates T_2 . The rapid motions must be of the amino acids

since if segmented motion of the polymer were the source of the relaxation, the extent of cross-linking should affect T_1 , which it does not.

Peptides have been very popular recently as subjects for ^{13}C nmr investigation. Voelter et al.⁹⁰ have reported spectra and tabulated shifts for different types of substituted amino acids. Their studies included benzyloxycarbonyl-, tertbutyloxycarbony-, acetyl-, benzyloxy-, and tert-butyl derivatives of glycine, alanine, valine, leucine, isoleucine, serine, threonine, methionine, cysteine, cystine, ornithine, arginine, lysine, asparagine, aspartic acid, glutamic acid, glutamine, proline, phenylalanine, tyrosine, tryptophane, and histidine in D_2O or DMSO-d_6 . The shifts are reported with respect to $\text{TMS-}^{13}\text{C}$. They also reported shifts for the dipeptide carnosin (*c*-Ala-His) as well as various derivatives of Gly-Ala, Ala-Gly, Val-Val, Leu-Leu, Cys-Gly, and Asp-Cys-Gly. Freedman et al.⁹¹ also have determined ^{13}C shifts of small peptides, for some as a function of pH. Figure 10 shows spectra of the methyl ester of phenylalanine, histidine, His-Gly, and His-Phe, and Figure 11 gives a diagrammatic presentation of shift data for small peptides. The carboxyl resonance in phenylalanine methyl ester is virtually unaffected between pH 1 and 4, but does change at high pH. Both in histidine and the methyl ester of phenylalanine, the quaternary carbons show a shift sensitivity to pH reflecting the titration of the imidazole ($\text{pK} \sim 6.5$) and amino-terminal groups ($\text{pK} 9.5$), respectively.

A thorough pH dependence study was carried out by Gurd et al.⁹² on the tripeptides Leu-Ser-Glu and Ser-Glu-Gly, as well as the pentapeptide Val-Leu-Ser-Glu-Gly, a peptide comprising the first five residues of sperm whale myoglobin. As groundwork they also determined the ^{13}C shifts of valine, leucine in anionic dipolar and cationic form, serine, glutamic acid, and glycine, agreeing to within 0.4 ppm of the relevant results by Horsley and Sternlicht.⁸⁷ Figure 12 shows the pH dependences for these peptides. The largest changes are seen with titration of the α -amino group, monitored most readily by the carbonyl carbon of the amino-terminal residue. Side-chain carboxyl behavior is more drastic than that of the C-terminal carboxyl — pointing out a possible structural tool for carboxyl identification.

Christl and Roberts⁹³ later reported a comprehensive study of ^{13}C peptide shifts as a function of pH, preparing their peptides in

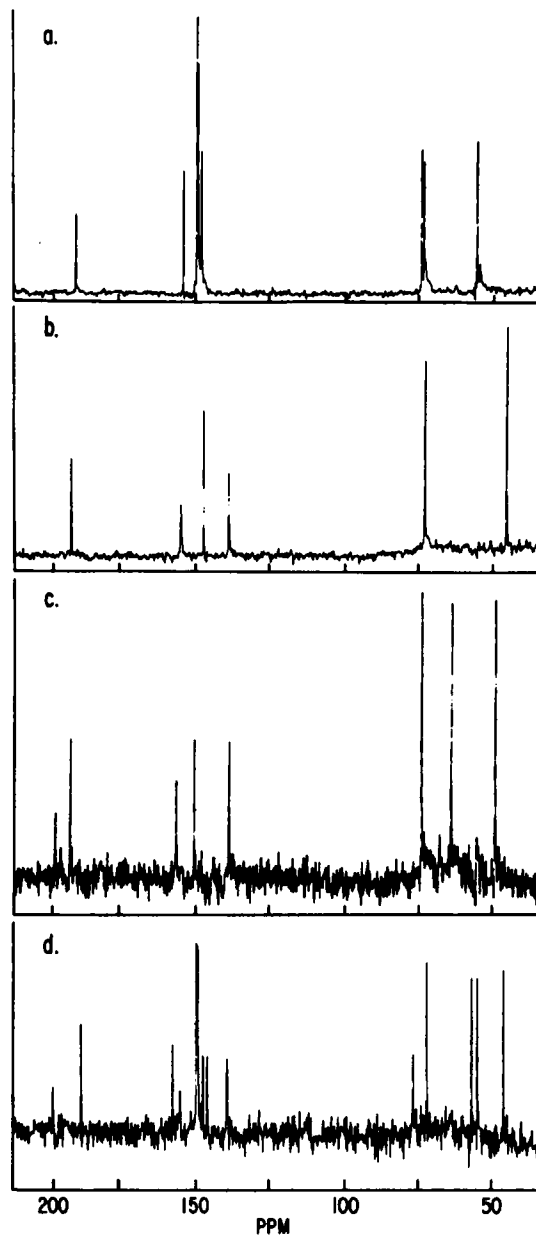


FIGURE 10. ^{13}C spectra: a, phenylalanine methyl ester, pH 1.86; b, histidine, pH 1.14; c, histidylglycine, pH 3.51; and d, histidylphenylalanine, pH 3.33 (in ppm downfield from external $^{13}\text{CH}_3\text{I}$). (From Freedman, M. H., Cohen, J. S., and Chaiken, I. M., Carbon-13 fourier transform nuclear magnetic resonance studies of peptides, *Biochem. Biophys. Res. Commun.*, 42, 1148, 1971. With permission.)

anionic, zwitterionic, and cationic forms. In studying the 16 dipeptides, 9 tripeptides, tetraglycine, and pentaglycine, they were able to classify the chemical shifts systematically with respect to the free amino acids. For example, glycine was examined as a subunit in 13 different

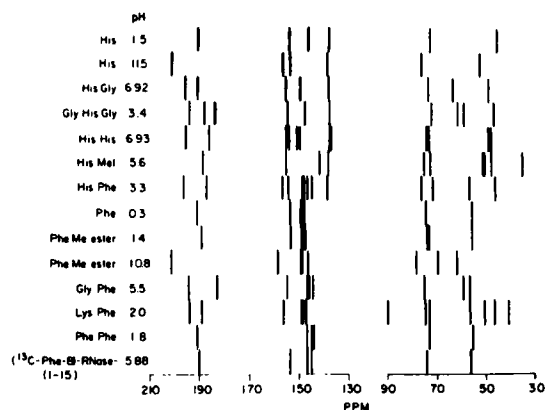


FIGURE 11. ^{13}C chemical shift correlation of amino acids and peptides (in ppm downfield from external $^{13}\text{CH}_3\text{I}$). (From Freedman, M. H., Cohen, J. S., and Chaiken, I. M., Carbon-13 fourier transform nuclear magnetic resonance studies of peptides, *Biochem. Biophys. Res. Commun.*, 42, 1148, 1971. With permission.)

peptides, in the three ionic forms, and as an N-terminal, C-terminal, and nonterminal unit. These peptides showed that the chemical shifts of

a glycine unit are, without exception, affected only by its position in the peptide, and not by the nature of the amino acids to which it is linked by means of peptide bonds. For example, C-terminal glycine at low pH (1.4 to 1.6) has α carbon and carbonyl resonances:

| | $\delta_{\text{C=O}}$ | $\delta_{\alpha\text{C}}$ |
|----------------|-----------------------|---------------------------|
| (Gly-) Gly | 174.2 | 42.6 |
| (Leu-) Gly | 174.3 | 42.7 |
| (Lys-) Gly | 174.5 | 42.7 |
| (Gly-Gly-) Gly | 174.5 | 42.6 |
| (Ala-Gly-) Gly | 174.7 | 42.7 |
| (Leu-Gly-) Gly | 174.7 | 42.6 |
| (Gly-Leu-) Gly | 174.6 | 42.6 |
| (Met-Phe-) Gly | 174.2 | 42.8 |

As is obvious, the nature of the neighboring amino acid is usually unimportant in determining the α and carbonyl carbon shifts. This fact should inject a note of caution in the use of ^{13}C shifts as sequence unravelers. There is sensitivity in the glycine shifts, but mostly in regard to position. This is documented by a summary of representative values from Table I of Christl and Roberts' work.

| Glycine type | Cation | | Zwitterion | | Anion | | Neighbor types used |
|--------------|-----------------------|-------------------|-----------------------|-------------------|-----------------------|-------------------|-------------------------|
| | $\delta_{\text{C=O}}$ | δ_{α} | $\delta_{\text{C=O}}$ | δ_{α} | $\delta_{\text{C=O}}$ | δ_{α} | |
| N-Terminal | 168.9 | 42.3 | 168.1 | 42.2 | 176 | 45.1 | Gly, Leu, Phe |
| C-Terminal | 174.5 | 42.4 | 177.5 | 44.7 | 177.6 | 45.1 | Gly, Leu, Lys, Ala, Met |
| Nonterminal | 172.5 | 43.8 | 172.3 | 43.9 | 173.1 | 43.8 | Gly, Ala, Leu |

The same kind of overall sensitivity to position, but not neighbor identity (except for proline), was shown for leucine, phenylalanine, alanine, and methionine. Other less generally treated amino acids included lysine, proline, valine, tyrosine, and arginine, although they appeared as neighbor amino acids frequently.

The pH dependence has several common

features. Carboxylate protonation induces increased shielding of the peptide carbons. Protonating a zwitterionic C-terminal peptide results in a -3 ppm carboxylate shift, -2.5 ppm α carbon shift, -1.2 ppm for the β carbon, and -0.3 ppm for the γ carbon. Detailed effects have been summarized by Christl and Roberts⁹³ and reproduced below.

^{13}C Chemical Shift Changes for: Amino Acid \rightarrow Peptide, Anion \rightarrow Zwitterion, and Cation \rightarrow Zwitterion

| Type ^a | $\Delta\delta_{\text{C=O}}$ | $\Delta\delta_{\alpha}$ ^b | $\Delta\delta_{\beta}$ | $\Delta\delta_{\gamma}$ |
|---------------------------------|-----------------------------|--------------------------------------|------------------------|-------------------------|
| aa \rightarrow N-terminal aa | -5.4 | -1.2 (-0.7) | 0.2 | -0.4 |
| aa \rightarrow C-terminal aa | 3.5 | 1.0 (2.0) | 1.2 | 0.4 |
| aa \rightarrow nonterminal aa | -1.5 | -0.6 (1.1) | 0.0 | 0.0 |
| titration of N-terminal | 6.9 | 1.0 (2.6) | 3.1 | 0.6 |
| titration of C-terminal | -3.0 | -2.6 (-2.2) | -1.2 | -0.3 |

^a aa = amino acid

^b glycine values only, in parenthesis

RIGHTS LINK
Copyright Clearance Center

While the cations were studied at pH 9.5, titration shifts continued up to pH 12.6 for lysyl glycine. Thus the N-terminal titration shifts should be considered as lower limits.

Unseen in earlier investigations, the effects of *cis/trans* isomerism about the amide bond in proline were recently observed by Thomas and Williams.^{94*} They examined aqueous solutions of glycyl-, alanyl-, and valyl-proline, using *N*-acetylproline as a reference compound. In each case there was a ~60:40 *trans:cis* mixture. Apparently the bulk of the side-chain in the amino acid preceding proline has negligible effects on the *cis/trans* ratio and the proline shifts. The α -carbon was fairly insensitive to isomer while the β and γ carbons gave ~2 ppm sensitivities to isomer, although different in direction. These differences will definitely be useful in conformational analysis of complex peptides including proline or other cyclic imino acids.

The dramatic effects of cystine-bond formation have been documented by Jung et al.⁹⁵ in considering glutathione (Glu-Cys-Gly) and its oxidized form containing an S-S bond. The resonance of the sulfur-bound carbon is shifted +13 ppm in the transition $-\text{CH}_2\text{SH}$ to $-\text{CH}_2\text{SSCH}_2-$ while the carbon two bonds away shifts -3 ppm. The distinctive value of 41.6 ppm for the carbons in the $-\text{CH}_2\text{SSCH}_2-$ group provides a diagnostic test for the cystine bond.

Several recent pieces of work have dealt with cyclic polypeptides or analogs.⁹⁶⁻¹⁰¹ An early polypeptide spectrum, CW mode, was published by Gibbons et al.⁹⁶ on cyclic decapeptide gramicidin S-A (Figure 13), an antibiotic. The spectra (Figure 14) allowed all carbons to be seen, although some ambiguities in the assignments exist. The symmetry is unequivocally C_2 from the spectrum, the five pairs of residues only yielding five carbonyl, five C_α , and five C_β chemical shifts. The two methyl carbons in valine are magnetically equivalent yet give different lines. This implies that the valine side-chain has different average rotational conformations in valine as an amino acid, in a peptide, and in gramicidin.

Macrocyclic ion complexes such as valinomycin and nonactin were the subject of a pair of recent investigations.^{97,98} Ohnishi et al.⁹⁷ reported the ^{13}C spectra of free and potassium-bound valinomycin (Figure 15). The resonances of the

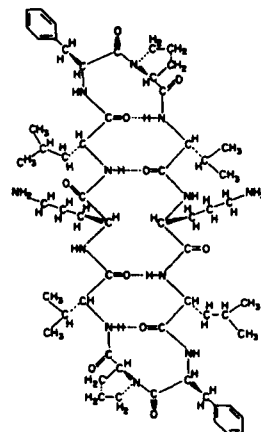
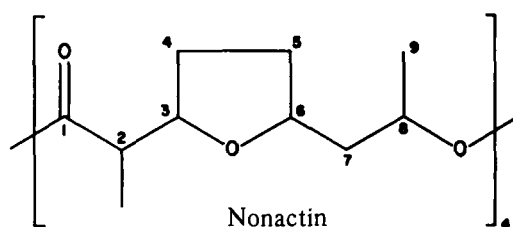


FIGURE 13. Gramicidin S-A, cyclo (-Phe-Pro-Val-Orn-Leu-)₂. (From Gibbons, W. A., Sogn, J. A., Stern, A., Craig, L. C., and Johnson, L. F., ^{13}C nuclear magnetic resonance spectrum of gramicidin S-A, a deca peptide antibiotic, *Nature*, 227, 840, 1970. With permission.)

two carbonyls directly coordinating the cation experience a downfield shift relative to the uncomplexed peptide. Comparison of free and complexed nonactin, a synthetic polyether, and the large complexation shifts of carbons farther away suggested the conformational rearrangements of the molecule as a whole can compete with direct interactions between carbons and the cation in determining the ^{13}C chemical shift differences between free and complexed species.

Pretsch, Vasák, and Simon⁹⁸ considered the antibiotic nonactin in greater detail, involving complexed ions Na^+ , K^+ , Rb^+ , Cs^+ , NH_4^+ , and Ba^{2+} to



explore the effect of atomic size of the bound ion. They studied free nonactin shifts as functions of solvents and found only minor variation. Significant variation with metal ion was noted only for carbons 3 and 8. Significantly, carbon 3 is several bonds away from the metal, and the sensitivity may possibly be due to overall conformational rearrangement. Comparison of the shifts showed no significant differences for NH_4^+ , and hence it is

*See also References 99, 166, 167, 168, and 170.

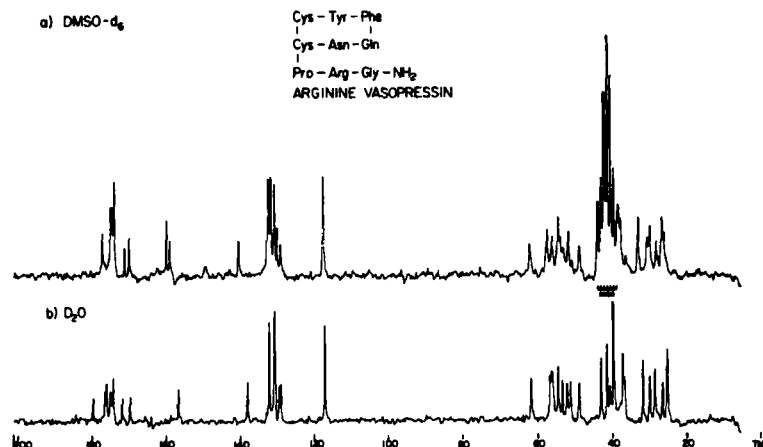


FIGURE 18. ^{13}C spectrum of arginine vasopressin. (From Smith, I. C. P., private communication. With permission.)

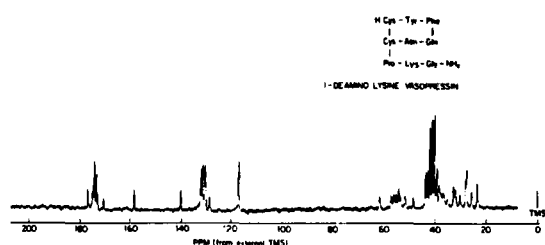


FIGURE 19. ^{13}C spectrum of one-deamino lysine vasopressin. (From Smith, I. C. P., private communication. With permission.)

glutamic acid). The carbon shows a 3.0 ppm upfield shift, the ester carbon 2.7 ppm upfield, the amide carbon 2.0 ppm downfield, the β carbon 1.2 ppm downfield, and the benzyl carbon 1.7 ppm downfield shifts upon undergoing the helix to random coil transition. A similar investigation on poly (*N*- δ -carbobenzoxy-L-ornithine) was reported by Boccalon et al.¹⁰³ again using trifluoroacetic acid as agent for the coil formation. The helix to coil transition has its most dramatic effects on the α carbon (~ 3 ppm upfield), the ornithine carbonyl (> 2 ppm upfield) and the γ CH_2 (~ 1 ppm upfield). However, while the β CH_2 gradually goes downfield by ~ 1 ppm (after the transition point), the carbon atoms of the urethane group, the carbobenzoxy carbons, show a gradual decrease in shielding well before coil formation, continuing through and after the transition to a final downfield shift of ~ 2 ppm. While no detailed conformational conclusions were made concerning either of the helix-coil transitions mentioned above, the sensitivity shown in the shifts bodes well for future analysis.

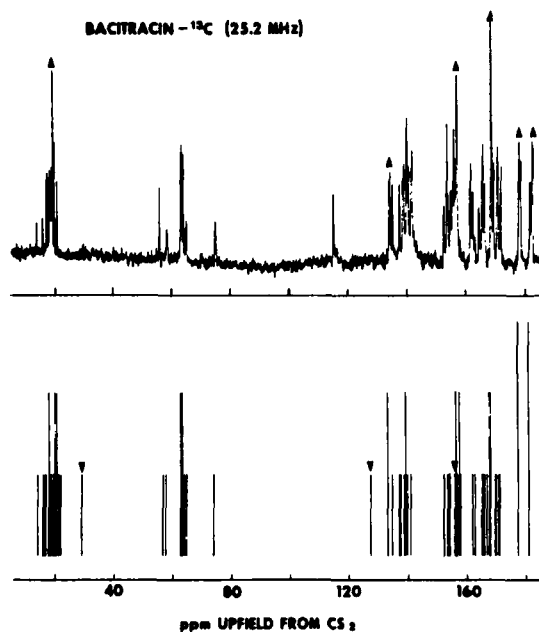


FIGURE 20. ^{13}C spectrum of 0.07 *M* bacitracin at pH 3.6. The upward darts refer to the ring resonances of 2-methyl thiazole while the downward darts refer to isoleucyl carbons. (From Lyerla, J. R., Jr. and Freedman, M. H., Spectral assignment and conformational analysis of cyclic peptides by carbon-13 nuclear magnetic resonance, *J. Biol. Chem.*, 8183, 1972. With permission.)

Lyerla, Barber, and Freedman¹⁰⁴ also examined the helix-coil transition in poly-L-glutamic acid, but in aqueous solution and on a function of pH. They observe a strong upfield shift for the peptide carbonyl group on going to high pH, the reverse of the behavior observed for glutamic acid alone. The α carbon in the polymer also experiences a strong 2 ppm upfield shift on

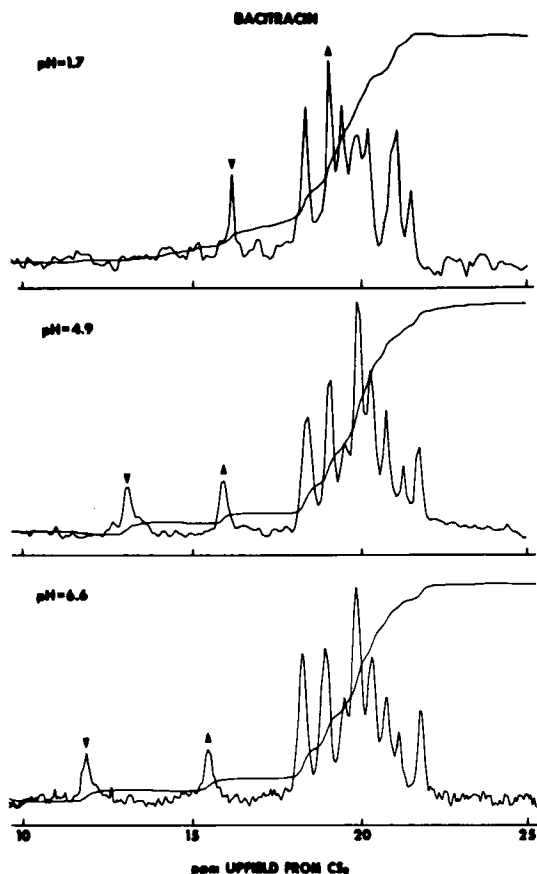
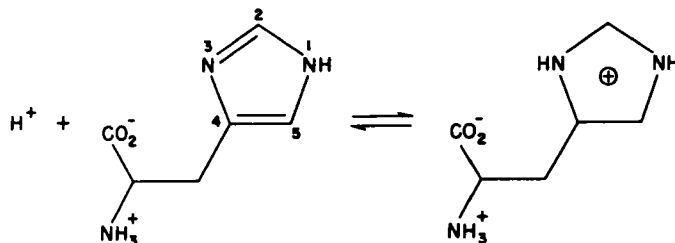


FIGURE 21. Carbonyl region of bacitracin as a function of pH. (From Lyster, J. R., Jr. and Freedman, M. H., Spectral assignment and conformational analysis of cyclic peptides by carbon-13 nuclear magnetic resonance, *J. Biol. Chem.*, 8183, 1972. With permission.)

deprotonation while the β , γ , and side-chain carboxyl all experience the typical downfield shifts normally experienced by amino acids. The possibility that the downfield shift of the carbonyl group at low pH was due to hydrogen bonding was mentioned.

Reynolds et al.¹⁰⁵ have recently attempted to determine the protonation behavior of histidine. The imidazole side-chain has a pK of 6.0, and protonation involves transition from a neutral species to a cation. The neutral ring can exist in either the 1-H tautomer (as shown below) or the 3-H tautomer.



Theoretical calculations on imidazole and histidine permitted prediction of ^{13}C shifts upon protonation. The imidazole shifts were accurately predicted assuming rapid 1 to 3 proton averaging. The imidazole shifts for the 1-H tautomer are very similar to those for histidine, but only for the 1-H histidine case. The calculated shifts for the 1-H tautomer of histidine were also in much better agreement with the experiment than the calculated shifts for the 3-H tautomer. To provide additional evidence ^{13}C shift pH titration was performed for 1-methyl and 3-methylhistidines. The 1-methyl titration curves were identical in sign and magnitude to those of histidine while the 3-methyl curves were inconsistent with those of histidine. This pH titration behavior was advocated for use in determination of tautomeric forms for histidines in polypeptides and proteins. Reynolds et al.¹⁰⁵ used this diagnostic for tautomeric analysis in *N*-acetylhistidine, histidine methyl ester, histidylglycine, glycyhistidylglycine, and bacitracin in which histidine is residue 10. All were consistent with the 1-H tautomer.

PROTEINS

What until recently was virtually unimaginable is now happening frequently, that is, the observation of ^{13}C nmr spectra of biopolymers such as large polypeptides or enzymes. Only with much patience is this possible in cw mode. Lauterbur¹⁰⁶ has reported perhaps the only published cw spectrum of a protein, that of hens' egg white lysozyme, molecular weight 14,300. This required 6,260 scans of 50 sec each for 87 hr. Use of FT techniques allows this time to be dropped by a factor of 10 to 100. This is illustrated in the report of Allerhand, Cochran, and Doddrell¹⁰⁷ for ribonuclease A. This protein contains 575 carbons distributed among 124 amino acid residues. Figure 22 shows the 15.08 MHz ^{13}C spectrum of 0.02 M ribonuclease A at 45° along with that of the denatured form. The spectrum can be decomposed into a region from the 151 carbonyl carbons; a small group

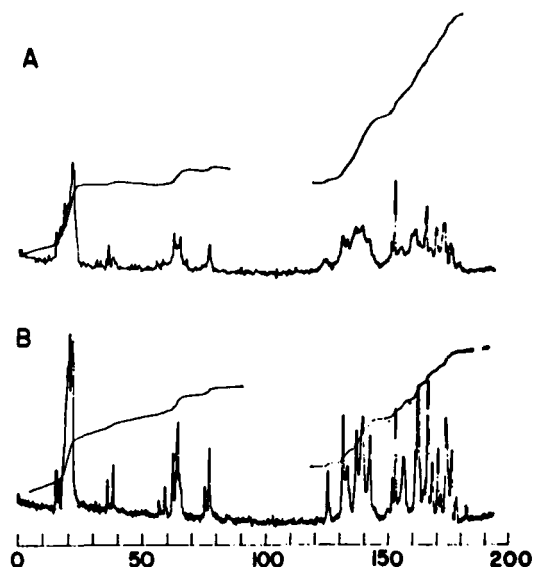


FIGURE 22. Natural abundance ^{13}C spectrum of ribonuclease A at 45° and 15.08 MHz (in ppm upfield from $^{13}\text{CS}_2$); A, native protein at pH 4.12, 0.017 M, 32,768 scans in 6 hr; B, 0.015 M denatured protein at pH 1.46, 31,284 scans in 12 hr. (From Allerhand, A., Doddrell, D., Glushko, V., Cochran, D. W., Wenkert, E., Lawson, P. J., and Gurd, F. R. N., Conformational and segmental motion of native and denatured ribonuclease A in solution. Application of natural abundance carbon-13 partially relaxed Fourier transform nuclear magnetic resonance, *J. Am. Chem. Soc.*, 93, 544, 1971. With permission.)

immediately upfield from the carbonyls containing the aromatic C-6 carbons of the 6 tyrosine residues and the ϵ -carbons of the 4 arginine residues; the 2 small peaks between 55 and 60 ppm above $^{13}\text{CS}_2$ coming from the imidazole C-2 carbons of the 4 histidine residues and the quaternary carbons of the three phenylalanine residues; the band between 60 and 66 ppm above $^{13}\text{CS}_2$ containing the aromatic C-3 carbons of the 6 tyrosines, the imidazole C-5 carbons from the 4 histidines, the 12 aromatic C-4 tyrosine carbons, and the 15 aromatic (C-4, C-5, and C-6) carbons of the 3 phenylalanines; the band between 75 and 80 ppm upfield from $^{13}\text{CS}_2$ arising from the imidazole C-4 carbons of the histidines and the aromatic C-5 of the tyrosines; the band at 126 ppm upfield down $^{13}\text{CS}_2$ reflecting the 10 β -carbons of the threonine residues; and the band between 130 and 150 ppm coming from the β -carbons of serine and all the α -carbons except these of glycine. Figure 23 shows a spectrum of the native enzyme at 25 MHz. The prospect for study of biopolymers is definitely

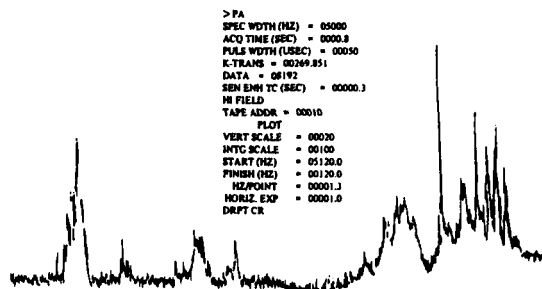


FIGURE 23. Natural abundance ^{13}C spectrum of ribonuclease A at 25.2 MHz and 0.019 M. Reprinted through the courtesy of Varian Associates.

enhanced by the realization that large molecules can be examined in a reasonable length of time.

Further details on the ^{13}C nmr spectra of ribonuclease A were provided recently by Glushko, Lawson, and Gurd,¹⁰⁸ particularly as a function of pH. ^{13}C spectra of ribonuclease A at pH 1.46, 3.23, 4.14, and 6.55 were recorded. Acid denaturation was evident below pH 4 reflecting the loss of chemical shift nonequivalence and a narrowing of individual lines. The narrowing at pH 1.46 allowed a more detailed set of assignments based on previously published assignments for peptides and amino acids. Sixty-nine different carbons were assigned chemical shift values or ranges. The lowest field signals were assigned to the carboxyl carbons of glutamic and aspartic acid. Although many resonances were assigned, there remains uncertainty concerning many other resonances. At higher pH most of the peaks, but not all, broaden and some shift, reflecting deprotonation in some cases. There is a richness in behavior of the pH dependence of shift and linewidth that reveals a true sensitivity to microenvironment and promises the hope of future understanding of these complex processes. The oxidized ribonuclease A spectra at pH 6.72, 4.34, and 1.40 are very similar to those of the acid-denatured protein. The cleavage of the disulfide bonds allows much more chemical shift equivalence and longer T_2 values (smaller linewidth).

Freedman, Cohen, and Chaiken⁹¹ demonstrated what is likely to be a very useful technique in the study of proteins, that of specific enrichment. They used 15%-enriched ^{13}C amino acids obtained from algae grown on $^{13}\text{CO}_2$ to prepare ^{13}C -enriched phenylalanine in the 1 to 15 polypeptide corresponding to the first 15 residues found for ribonuclease A, $\text{NH}_2\text{-Lys-Glu-Thr-Ala-}$

Ala-Ala-Lys-Phe*-Glu-Arg-Gln-His-Met-Asp-Ser-COOH. Use of this polypeptide as part of the ribonuclease S complex allows a "reporter" group to be present due to its highly enhanced intensity. In a more recent communication, Freedman et al.¹⁰⁹ analyzed the amino terminal 1 to 13, 1 to 15, and 1 to 20 peptides of bovine pancreatic ribonuclease A. In Figures 24 and 25 are shown the aliphatic and aromatic/carbonyl regions of the 1 to 13, 1 to 15, and 1 to 20 amino-terminal peptides of ribonuclease A. Amino acid parameters, characteristic peptide formation shifts, differences within the three polypeptides, and the primary structure of the peptides all were used to give the peptide resonance assignments shown. The ¹³C-enriched phenylalanine number 8 residue spectrum aided in the assignment because of its overlap with the C-2 and C-4 carbons of the histidyl imidazole ring. Chaiken et al.¹¹⁰ substantially extended the synthetic approach in their recent studies of ¹⁹F and ¹³C-labeled semi-

synthetic ribonuclease-S' analogs. This semi-synthetic ribonuclease-S' contains the polypeptide fragments synthetic-(1 to 15) and RNase-S-(21 to 124). Again phenylalanine 8 was used as the labeled residue. The ^{13}C chemical shift of the labeled phenylalanine changed significantly on going from the 1 to 15 polypeptide to the complex: e.g., C_O , 1.3 ppm; C_α , +0.7 ppm; and C_β , -0.5 ppm. These shifts and T_1 data on the Phe 8 carbons were interpreted as arising from the formation of an α -helical conformation involving residues 2 to 12 and the concomitant burial of the Phe 8 side-chain into a sterically restricted orientation in a largely nonpolar region. The C_O , C_α , and C_β shift perturbations are very similar to the pattern found in coil-helix transitions for other homopolypeptides.^{102,103} Steric restriction of the phenyl group in the Phe 8 was indicated since the ortho and meta phenyl carbon T_1 's dropped from ~ 220 msec to ~ 82 msec upon complex formation (longer τ_C).

FIGURE 24. (A) The aliphatic region of the ^{13}C spectrum of the amino-terminal 1-20 peptide of RNase A, (B,C) the respective aliphatic regions of the 1-15 and 1-13 amino-terminal peptides of RNase A and, (D) the stick diagram for the three peptides based on the ^{13}C shifts of individual amino acids: (A), 0.045 M at pH 5.5, 20.6 h; (B), 0.035 M at pH 2.0, 15.4 h; and (C), 0.048 M at pH 5.5, 15.4 h. Chemical shifts downfield from external $^{13}\text{CH}_3\text{I}$. (From Freedman, M. H., Lyerla, J. R., Jr., Chaiken, I. M., and Cohen, J. S., Carbon-13 nuclear magnetic resonance studies on selected amino acids, peptides, and proteins, *Eur. J. Biochem*, 32, 215, 1973. With permission.)

An alternate form of labeling of ribonuclease A was tried by Nigen et al.,¹¹¹ who treated the protein with 60%-enriched (2-¹³C) bromoacetate.

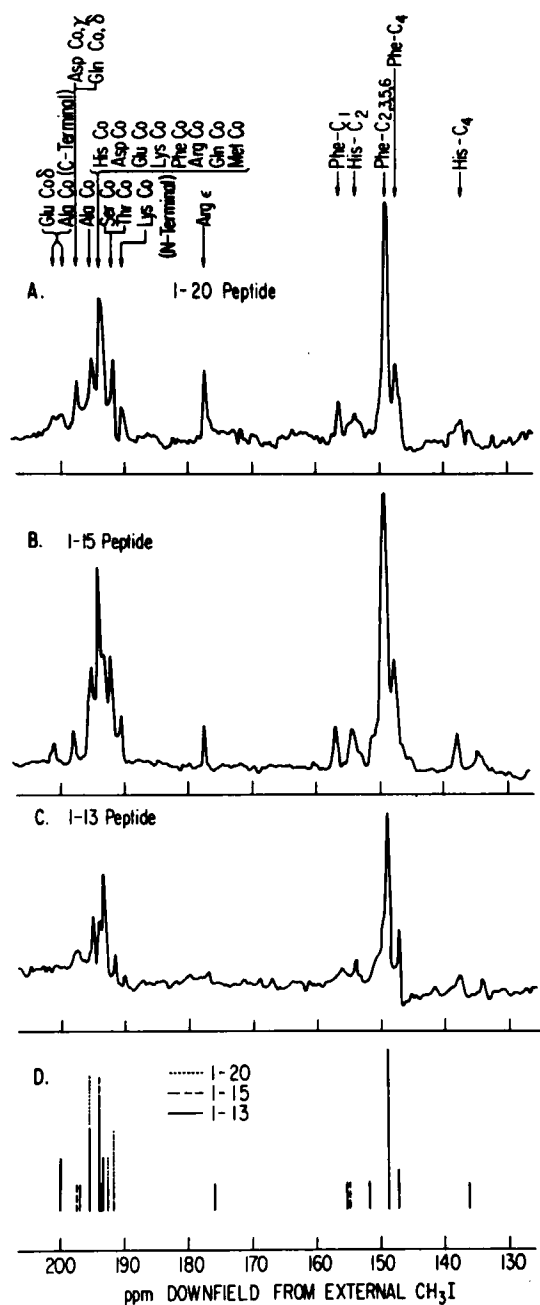


FIGURE 25. (A-C) The aromatic/carbonyl region of the ¹³C spectra of the 1-20, 1-15, 1-13 amino-terminal peptides of RNase A and (D) the respective stick diagram based on amino acid shifts. Chemical shifts downfield from ¹³CH₃I. (From Freedman, M. H., Lyster, J. R., Jr., Chaiken, I. M., and Cohen, J. S., Carbon-13 nuclear magnetic resonance studies on selected amino acids, peptides, and proteins, *Eur. J. Biochem.*, 32, 215, 1973. With permission.)

This carboxymethylation resulted in high selective enrichment (0.85 residue of Nδ-Cm histidine 119 per molecule) and made possible a chemical shift assignment and T₁ value determination. The α-carbon of histidine 119 was found to have a shift 49.1 ppm downfield from TMS and a T₁ (in the adduct) of 29 msec.

Lysozyme seems to be popular as a subject for ¹³C nmr studies. Following Lauterbur's cw study,¹⁰⁶ Chien and Brandts¹¹² published a ¹³C FT spectrum and Freedman et al.¹⁰⁹ repeated the work recently (Figures 26 and 27). Although the ¹³C data are much better resolved than ¹H spectra, it is quite apparent that assignments are difficult to make. It does seem that there are distinguishable threonyl β-carbons and tyrosyl C-4 ring carbons. Upon reduction, the threonyl resonances shift and become equivalent. The sharpening of the resonances in the denatured lysozyme probably reflects the additional mobility gained from cleavage of the disulfide bonds in the native protein and/or elimination of chemical shift nonequivalence. The enhancement in T₁ values in going to denatured forms in other biopolymers (see below) suggests that correlation time effects (independent of chemical shift nonequivalence) are responsible for much of the broadness of the native species resonance in lysozyme.

As with ribonuclease A, Nigen et al.¹¹¹ also used (2-¹³C) bromoacetate to carboxymethylate cyanoferrimyoglobins of sperm whale and harbor seal. The treatment yielded adducts with several histidines, lysines, and glycines in each case. The spectra showed clear enhancements, which were identified as the derivatives at the Nδ and Ne of the dicarboxymethylated histidine residues, the modified NH₂ terminus, and a glycolate ester. Also, several monocarboxymethyl histidine derivatives were in evidence. The high enrichment allowed T₁ measurements of the dicarboxymethylated histidine derivatives. The two peaks so identified had T₁'s of 38 and 39 msec, respectively, in harbor seal myoglobin, and 32 and 34 msec in sperm whale myoglobin.

Conti and Paci¹¹³ presented the first spectra of the heme globins, those of carboxy-myoglobin and hemoglobin (Figures 28 and 29). Some general agreement with composite amino-acid shifts is seen. ¹³CO shifts dramatically in going from free ¹³CO in water to bound ¹³CO, changes of +24 and +29 ppm for myoglobin and hemoglobin, respectively. The resultant shift is similar to that

for $\text{Fe}(\text{CO})_5$. Myoglobin exhibits a sharp ^{13}C signal, while in hemoglobin the resonance seems to be split or severely broadened. This observation was also reported by Moon and Richards¹¹⁴ although the shifts differ in the two reports. The latter authors report a single sharp resonance for

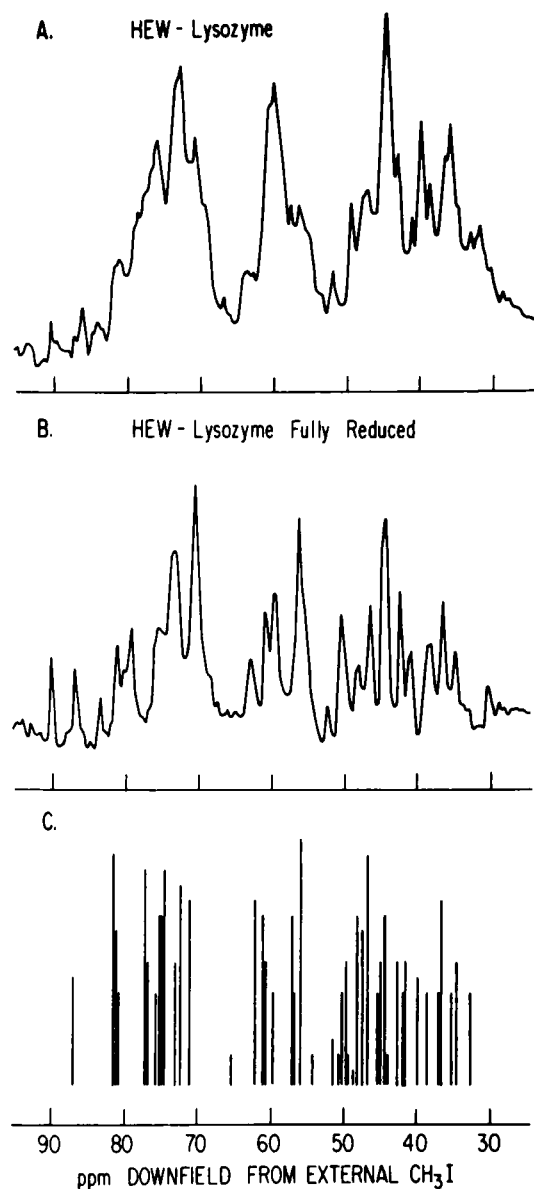


FIGURE 26. (A) The aliphatic region of the ^{13}C spectrum of native hens' egg white lysozyme, (B) the aliphatic region of fully reduced hens' egg white lysozyme, and (C) the respective stick diagram based on the amino-acid shifts. 0.007 M at pH 5.5, 15.4 h. (From Freedman, M. H., Lyerla, J. R., Jr., Chaiken, I. M., and Cohen, J. S., Carbon-13 nuclear magnetic resonance studies on selected amino acids, peptides, and proteins, *Eur. J. Biochem.*, 32, 215, 1973, With permission.)

the carbon monoxide bound in sperm whale carboxymyoglobin at 207.7 ppm for pH 6.79 to 7.29. Adult human hemoglobin showed two partially overlapping resonances at 206.5 and 206.1 ppm for pH 6.35 to 7.90, while virtually identical shifts were noted for fetal human hemoglobin despite the different amino-acid contents. At pH 6.21 mouse hemoglobin gives ^{13}C resonances at 206.4 and 205.9 ppm. Rabbit carboxyhemoglobin has well-separated resonances at 208.0 and 206.0 ppm for pH 6.94 to 7.38. The shifts clearly indicate significant differences between the magnetic environments experienced

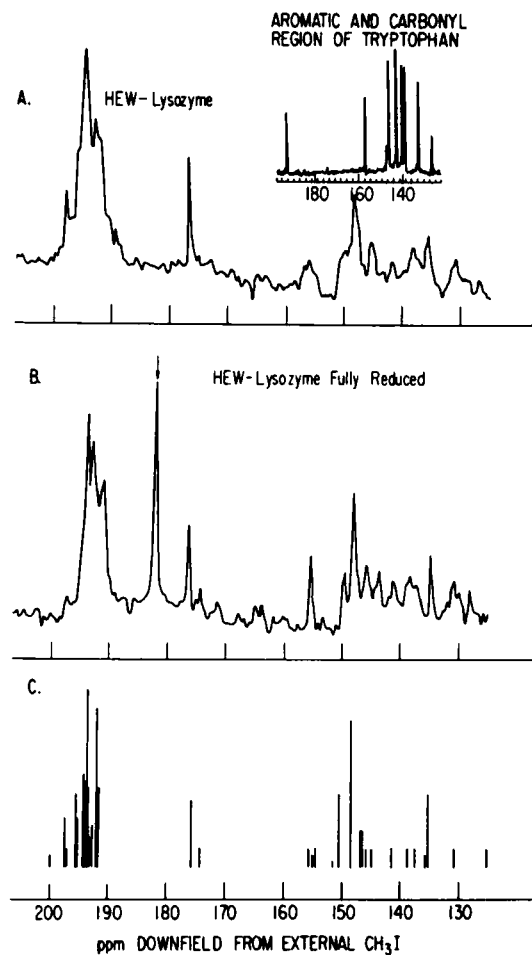


FIGURE 27. (A) The aromatic/carbonyl region of the ^{13}C spectrum of native hens' egg white lysozyme, (B) the aromatic/carbonyl region of fully reduced hens' egg white lysozyme, and (C) the associated stick diagram based on amino-acid shifts. The insert in (A) is the spectrum of tryptophan (pH 5.5), that of the lysozyme pH 5.5. (From Freedman, M. H., Lyerla, J. R., Jr., Chaiken, I. M., and Cohen, J. S., Carbon-13 nuclear magnetic resonance studies on selected amino acids, peptides and proteins, *Eur. J. Biochem.*, 32, 215, 1973. With permission.)

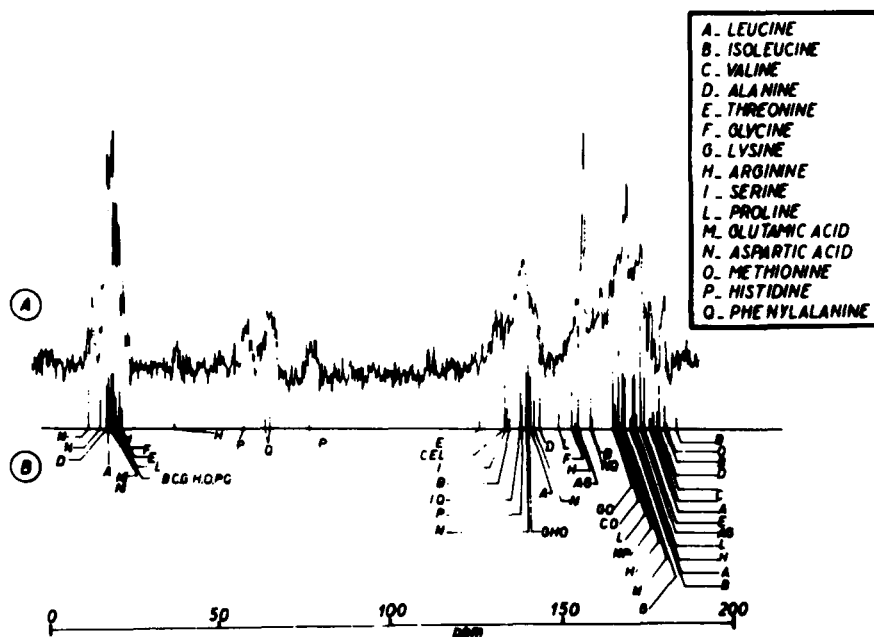


FIGURE 28. ^{13}C spectrum on sperm whale myoglobin. (B) Composite spectrum based on predicted shifts of amino acids. (From Conti, F. and Paci, M., Natural abundance ^{13}C spectra of proteins: carboxy-myoglobin and hemoglobin, *FEBS (Fed. Eur. Biochem. Soc.) Lett.*, 17, 149, 171. With permission.)



FIGURE 29. ^{13}C spectrum of horse hemoglobin. (From Conti, F. and Paci, M., Natural abundance ^{13}C spectra of proteins: carboxy-myoglobin and hemoglobin, *FEBS (Fed. Eur. Biochem. Soc.) Lett.*, 17, 149, 1971. With permission.)

by carbon monoxide bound to α or β subunits. T_1 values were determined to be ~ 0.3 sec for both resonances in rabbit HbCO at pH 7.0 and 3 mM concentration. Exposure of rabbit HbCO to oxygen significantly diminishes the low field resonance faster than the high field signal, indicating a difference in the α and β subunit oxygen affinity. Other data indicate that the β subunit has a higher carbon monoxide affinity, and thus the lower field resonance probably represents ^{13}CO bound to α subunits of rabbit hemoglobin.

Moon and Richards considered various liganded hemoglobins in more detail in a later publica-

tion.¹¹⁵ They examined human and rabbit methemoglobin (Hi), cyanomethemoglobin (HiCN), oxy- (HbO₂), carboxy- (HbCO), and deoxyhemoglobins (Hb), and hemoglobin plus 2,3-diphosphoglycerate. Rather than detailed analysis of each spectrum, differences between spectra were interpreted mainly in terms of differences in relative mobility of amino acid side-chains as reflected in the linewidths and intensities of their respective carbons. (It should be noted that the possibility of chemical shift nonequivalence addition or removal was not considered as a contributing factor in their analysis.) The main changes in progressing from human HbO₂ to Hi, Hb, and Hb + 2,3-P₂Glr were a steady decrease in the ϵ -carbon intensity of the lysine residues, a smaller decrease in the δ and γ carbons of lysine, and an up to 2-fold increase in the intensity of the alanyl methyl carbons. Moon and Richards¹¹⁵ explained this as a progressive immobilization of the side-chain lysine residues through formation of salt-bridges. The increase in the alanyl methyl intensities was explained as resulting from a decreased T_1 value that then permitted a less saturating condition in view of the short (0.2 sec) acquisition times. (No T_1 values were determined, however, for the alanyl methyls to test this hypothesis.) The

analogous series for rabbit hemoglobin doesn't show quite the same behavior for the ϵ -lysines. Little change occurs between HbO₂ and HbCO, but the greatest effects are seen in going to Hi or Hb. The γ and δ carbons of some glutamic acid residues are visible to the low field of the carbonyls in rabbit hemoglobin but barely visible, if indeed present, in the human hemoglobin spectrum. Moon and Richards¹¹⁵ interpreted this as resulting from a looser structure for rabbit hemoglobin and a very immobilized human hemoglobin rather than from differences in chemical shift for the glutamic acid residues in the two proteins. The β -alanine methyls in the rabbit hemoglobin were felt to be relatively freer to rotate since they have the same relative intensity throughout the rabbit hemoglobin derivatives and even the acid-denatured form. The human hemoglobin studies led to estimates that 25% of those residues free in human HbO₂ are immobilized upon deoxygenation vs. 33% for rabbit HbO₂. This difference was then interpreted as suggesting that deoxygenation of rabbit HbO₂ causes immobilization of one or two more lysine residues than in the human case. The proposed higher flexibility of rabbit vs. human Hb was explained in terms of the rabbit Hb having more amino acids with larger side-chains and fewer proline groups. The data on rabbit hemoglobins show much more similarity within HbO₂, HbCO, and HiCN and Hi or Hb although the conformation of HiCN was stated to be different from the largely indistinguishable conformations of HbCO and HbO₂. Moon and Richards also contend that HbO₂ and Hi differ appreciably in solution.

Packer, Sternlicht, and Rabinowitz¹¹⁶ recently used ¹³C nmr to probe the electron transport mechanism in *Clostridium acidii urici* ferredoxin.

The ¹³C resonances of the 2',6'-ring carbons of both tyrosyl residues of the ferredoxin are shifted ~ 2.7 ppm downfield in the oxidized protein and ~ 7.3 ppm downfield in the methyl viologen-reduced protein from the corresponding signals in free tyrosine. The corresponding 2',6' protons are unchanged, however, in both oxidized and reduced forms. The results are consistent with magnetically equivalent tyrosine residues, close to the two iron-sulfur clusters. The shifts can be explained by a pseudocontact (dipole-dipole) interaction if each tyrosyl residue is specially oriented and 4 to 5 Å from a Fe-S cluster, or a Fermi-contact interaction operating through electron delocalization. No special orientation with respect to the Fe-S cluster is needed in the latter mechanism.

SPIN-LATTICE RELAXATION IN BIOPOLYMERS

Several references have been made above to ¹³C T₁ measurements. In this section the basic mechanisms of spin-lattice relaxation as applied to large molecules will be examined and some concrete examples will be considered. A thorough understanding of T₁ mechanisms is critical for proper interpretation, especially for very large molecules.

A good deal of work has gone into investigating the mechanisms of ¹³C spin-lattice relaxation in the last few years. Representative treatments are those of Kuhlmann, Grant, and Harris,¹¹⁷ Kuhlmann and Grant,¹¹⁸ Sternlicht et al.,⁸⁸ and Doddrell, Glushko, and Allerhand.¹¹⁹

If molecular reorientation can be described by a single rotational correlation time τ_c , the T₁ of a carbon-13 bound to one proton can be expressed in the dipole-dipole mechanism as¹¹⁹

$$\frac{1}{T_1} = \frac{\hbar^2 \gamma_C^2 \gamma_H^2}{10 r_{CH}^6} \left(\frac{\tau_c}{1 + (\omega_H - \omega_C)^2 \tau_c^2} + \frac{3\tau_c}{1 + \omega_C^2 \tau_c^2} + \frac{6\tau_c}{1 + (\omega_H + \omega_C)^2 \tau_c^2} \right) \quad (4)$$

and the nuclear Overhauser effect (max 2.988) as¹¹⁹

$$NOE = 1 + \frac{\gamma_H}{\gamma_C} \left(\frac{\frac{6\tau_c}{1 + (\omega_H + \omega_C)^2 \tau_c^2} - \frac{\tau_c}{1 + (\omega_H - \omega_C)^2 \tau_c^2}}{\frac{\tau_c}{1 + (\omega_H - \omega_C)^2 \tau_c^2} + \frac{3\tau_c}{1 + \omega_C^2 \tau_c^2} + \frac{6\tau_c}{1 + (\omega_H + \omega_C)^2 \tau_c^2}} \right) \quad (5)$$

Note that r_{CH} does not appear in the NOE expression so that nonprotonated as well as

protonated carbons can have the full Overhauser effect, although T₁ may be very long.

For very fast molecular tumbling, $\tau_c < 10^{-10}$ sec; therefore, $\omega_C^2 \tau_c^2 \ll 1$ and the above reduce to

$$\frac{1}{T_1} = \frac{\hbar^2 \gamma_H^2 \gamma_C^2}{r_{CH}^6} \tau_c; \quad \text{NOE} = 1 + \frac{\gamma_H}{2\gamma_C} = 2.988 \quad (6) (7)$$

If $\tau_c \gtrsim 10^{-8}$ sec, the larger expression for T_1 must be used and, furthermore, the NOE drops to 1.153,^{117,119} only 15% greater than the intensity expected from just collapsing the ^{13}C - ^1H multiplets. As τ_c increases, T_1 decreases to a minimum when $\omega_C \tau_c \sim 0.8$ and then increases with longer τ_c . The minimum in T_1 occurs at $\tau_c \sim 7 \times 10^{-9}$ sec at 14 kg but occurs earlier for 23.5 Kg (5×10^{-9} sec) and 52 kg (2×10^{-9} sec). Moreover, the value of T_1 at the minimum increases as the resonance frequency increases, from ~ 0.02 sec at 14 Kg to ~ 0.1 sec at 52 kg. As related above, the NOE drops off from the maximum 2.988 at short correlation times to 1.153 at long τ_c . This is also a function of field (or resonance frequency). The Overhauser enhancement is half gone at $\tau_c = 5 \times 10^{-10}$ sec at 52 kg, $\tau_c = 2 \times 10^{-9}$ sec at 23.5 kg, and $\tau_c = 3 \times 10^{-9}$ sec at 14 kg.¹¹⁹ Thus the signal-to-noise ratio in proton-decoupled ^{13}C Fourier transform spectra of biopolymers will not always improve significantly by going to very high magnetic fields; indeed even allowing the greater magnetization possible, the S/N could be worse. There will, however, be an improvement in chemical shift dispersion and in narrower linewidths¹¹⁹ (for $10^{-10} < \tau_c < 10^{-7}$). The onset of internal rotation, such as methyl rotation, produces interesting effects, even if the rotation is too slow to contribute any spin-rotation relaxation. If a methyl has an internal rotation that is slower than overall molecular rotation, it should, by virtue of having three protons, have a T_1 one third of a methine carbon undergoing the same molecular overall rotation. As the methyl is allowed to spin faster than the overall molecular rotation, the dipole-dipole mechanism becomes less effective. As the methyl approaches being a free rotor, it has a T_1 up to three times longer than the methine carbon.^{118,119} For small molecules this relationship allows a probe for rotational freedom in isotropic tumblers. That is, if a reference carbon embedded in a molecular framework is used, the ratio of a methyl T_1 to the T_1 of the methine

reference carbon gives a direct probe for the methyl freedom of rotation. Now, as the molecule becomes very large and $\omega_C \tau_c \geq 1$, this relationship breaks down, and internal rotation can actually give shorter T_1 's than in restricted situations.¹¹⁹ Thus, observation of longer T_1 's in a biopolymer spectrum, upon treatment of some sort, can lead to a prediction of less restriction to internal rotation. This can be true for cases when $\omega_C \tau_c < 1$ but can be the reverse, as shown above, for a biopolymer where $\omega_C \tau_c > 1$. The NOE increases also as internal rotation commences, goes through a maximum, and decreases as the internal rotation further accelerates, for values of τ_c longer than 10^{-9} sec. Again, however, its value drops off between internal rotation correlation times of 10^{-10} sec and 10^{-8} sec (for long τ_c) and drops faster (from 2.988 to 1.153) with increasing field. The important conclusions to be drawn from these analyses are that it is very important to know which side of the T_1 vs. τ_c minimum at which one is operating (whether "extreme narrowing" conditions are satisfied) and thus whether it is appropriate to interpret linewidth changes (T_2) as reflecting T_1 changes. (In the extreme narrowing region $T_1 = T_2$ in normal cases.) It is critical, for as has been seen, T_1 observations can have diametrically opposed interpretation depending on τ_c .

At this point it might be appropriate to spend some time considering how the T_1 values are determined. Virtually all the T_1 values mentioned previously have been determined using the inversion-recovery FT method. Although the 180° -t- 90° sequence has its origin in the early days of nmr, Vold et al.¹²⁰ were the first to use the FT experiment to determine *all* the T_1 relaxation times within a spectrum. The technique basically consists of using a 180° pulse that nutates the net magnetization along the field direction, M_z , to an orientation exactly along the negative field direction, $-M_z$. If a 90° pulse is immediately applied, the magnetization will be flipped into the xy plane, and its precession will induce a time-dependent signal in the receiver coil. If the field is homogeneous, the signal will die away slowly; if inhomogeneous, it will die away quickly. This time-dependent signal is the free-induction decay that, when Fourier transformed, gives the high resolution spectrum. Since the 180° pulse put the magnetization in the negative field direction, the signals in the FT spectrum will appear inverted. For a series of experiments with varying t, a

different degree of reestablishment of the magnetization M will occur at a rate governed by the spin-lattice relaxation times of the individual lines in the spectrum. Thus, as t becomes longer, the lines will grow more positive, null, and return to their full, positive intensities. The function $\ln(S_\infty - S_t)$ vs. t has a slope of $-T_1$, where S_∞ is the normal positive intensity and S_t is the intensity at time t . Figures 30 and 31 show the ordinary FT spectrum and a series of these 180° - t - 90° spectra at 15 MHz for cholesteryl chloride,¹²¹ and Figure 32 shows the plotted data for several of the carbons. The computed T_1 's are listed in Figure 33. Note that these are very short relaxation times relative to what was felt concerning ^{13}C T_1 's for many years. Even nonprotonated carbons have T_1 's of only a few sec and full NOE. Analogous data for cortisone acetate taken at 25 MHz are presented in Figure 34.¹²² Allerhand et al.¹²¹ also determined the T_1 's in sucrose as a function of concentration in water. Even in going from 0.5 M to 2 M most of the T_1 's dropped by a factor of 3 to 4 (longer τ_c in the more viscous solution). Using the above equations for $\omega_C^2 \tau_c^2 \ll 1$, Allerhand et al.¹²¹ calculated τ_c 's of $\sim 10^{-10}$ sec for 1 M cholesterol chloride in CCl_4 at 15 MHz and 42°C , 7×10^{-11} sec, and 3×10^{-10} sec for 0.5

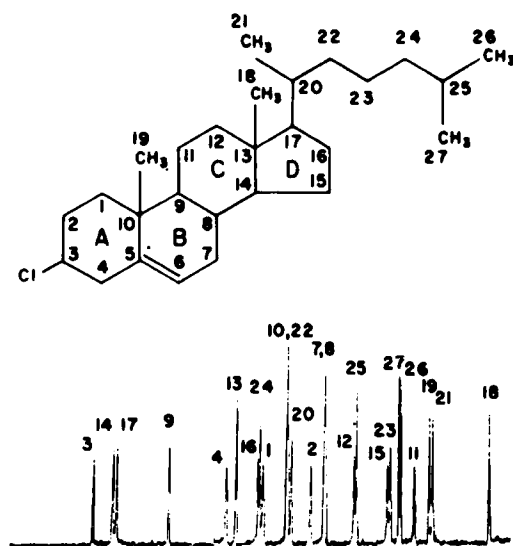


FIGURE 30. Structure and ^{13}C spectrum of cholesterol chloride, 1 M in CCl_4 at 15.08 MHz and 42°C . (From Allerhand, A., Doddrell, D., and Komoroski, R. A., Natural abundance carbon-13 partially relaxed fourier transform nuclear magnetic resonance spectra of complex molecules, *J. Chem. Phys.*, 55, 189, 1971. With permission of the American Institute of Physics.)

M and 2 M sucrose in water at 42°C . Estimates¹²¹ of methyl group internal rotation times in cholesterol and CH_2OH side-chain internal rotations in sucrose were $\leq 5 \times 10^{-12}$ sec and 9×10^{-10} to 3×10^{-10} sec, respectively.

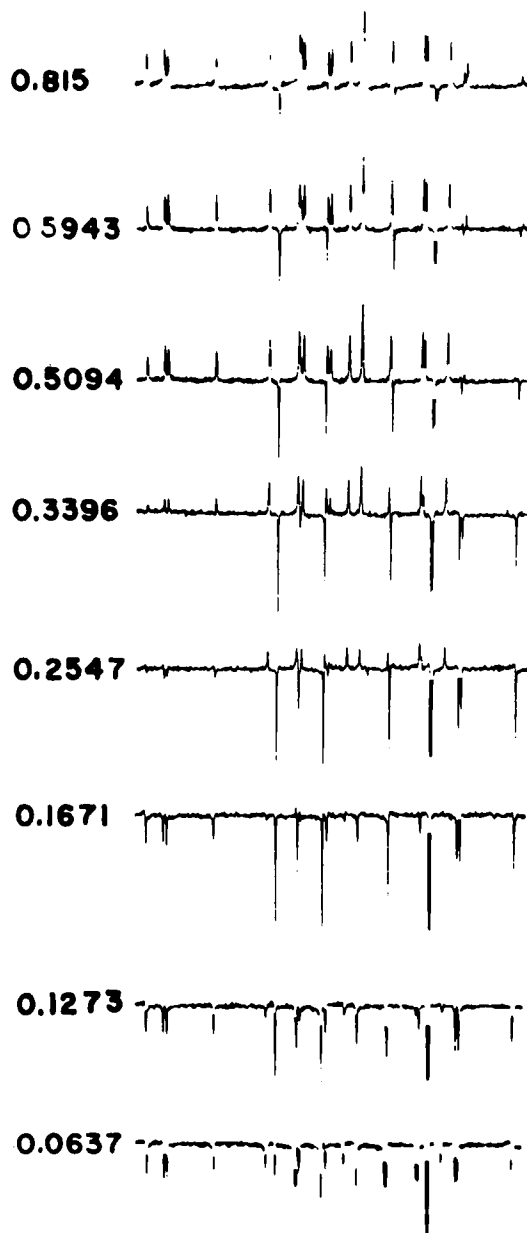


FIGURE 31. Carbon-13 partially relaxed spectra using the 180° - τ - 90° pulse sequence for 1 M cholesterol chloride in CCl_4 at 15.08 MHz and 42°C . The numbers represent τ in the pulse sequence. Recycle time = 21.7 sec. (From Allerhand, A., Doddrell, D., and Komoroski, R. A., Natural abundance carbon-13 partially relaxed fourier transform nuclear magnetic resonance spectra of complex molecules, *J. Chem. Phys.*, 55, 189, 1971. With permission of the American Institute of Physics.)

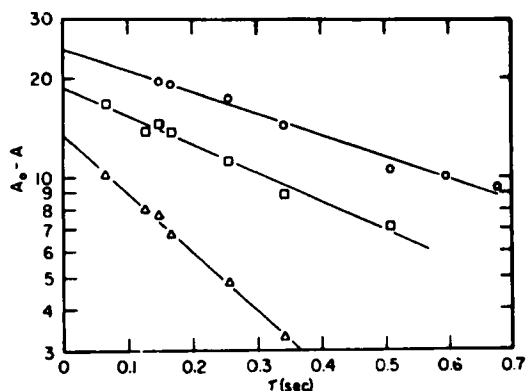


FIGURE 32. Semilogarithmic plots of the difference between the intensity of a line in a completely relaxed spectrum and that line's intensity after a delay of τ sec in the 180° - τ - 90° pulse sequence vs. the delay time τ for C-24 (circles), C-17 (squares), and C-11 (triangles) of 1 M cholesterol chloride in CCl_4 , at 15.08 MHz and 42°C . (From Allerhand, A., Doddrell, D., and Komoroski, R. A., Natural abundance carbon-13 partially relaxed fourier transform nuclear magnetic resonance spectra of complex molecules, *J. Chem. Phys.*, 55, 189, 1971. With permission of the American Institute of Physics.)

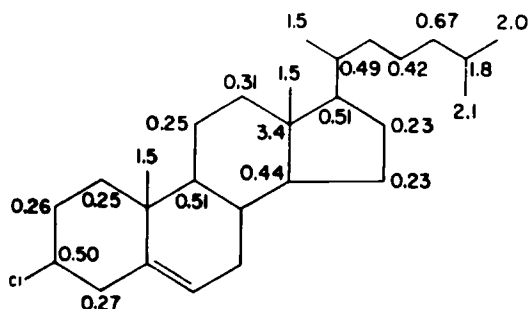


FIGURE 33. ^{13}C spin-lattice relaxation times, in sec, of 1 M cholesterol chloride in CCl_4 at 15.08 MHz and 42°C . (From Allerhand, A., Doddrell, D., and Komoroski, R. A., Natural abundance carbon-13 partially relaxed fourier transform nuclear magnetic resonance spectra of complex molecules, *J. Chem. Phys.*, 55, 189, 1971. With permission of the American Institute of Physics.)

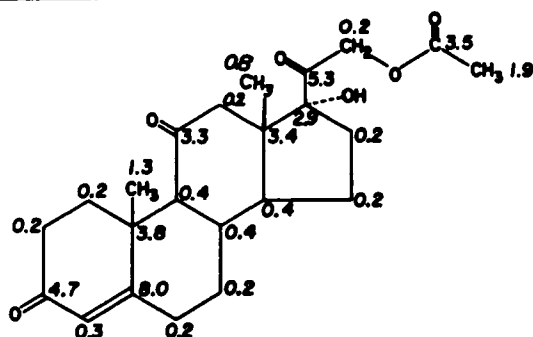


FIGURE 34. ^{13}C spin-lattice relaxation times, in seconds of cortisone acetate at 25.2 MHz.¹²² (From Freeman, R., private communication. With permission of Varian Associates.)

Similar studies¹²¹ on 1 M aqueous AMP again showed protonated carbon relaxation times from 0.11 to 0.19 sec at 15 MHz and 42°C , while the nonprotonated carbons had T_1 's 2.4 to 5.3 sec. As the molecular size is increased, τ_c becomes longer and comes into a region where the "extreme narrowing" conditions do not hold. Thus T_1 's might be expected to start increasing with increasing molecular weight. This is correct, but before that happens other mechanisms can contribute fluctuating magnetic fields to induce relaxation. If a large molecule is not rigid but has considerable flexibility, particularly with regard to segmental motion, the appropriate τ_c effective for spin-lattice relaxation is that of segmental motion, not overall molecular rotation. This was nicely demonstrated for polystyrene by Allerhand and Hailstone.¹²³ For molecular weights lower than 2,000, τ_c is determined by the overall molecular rotation time. As the molecular weight becomes $>2,000$ the segmental motion and overall rotation are comparable in time. The T_1 's at mol wt = 2,100 range from 71 to 180 msec. In going to 10,300 mol wt the T_1 's shorten to 50 to 99 msec and stay essentially constant up to mol wt = 860,000. The linewidths (and therefore T_2 's) also remain constant. This constancy in T_1 and T_2 results from the domination of τ_c by segmental motion having $\tau = 6 \times 10^{-10}$ sec at 44°C . The phenyl ring in polystyrene is capable of internal rotation so that the *ortho* and *meta* carbons could, in principle, have longer T_1 's than the *para* carbons. However, the *ortho*, *meta*, and *para* carbon T_1 's were all essentially equal, and thus the internal rotations must be appreciably longer than 6×10^{-10} sec.

Ribonuclease A was the first biopolymer for which ^{13}C relaxation times were reported.¹²⁴ In the native protein (0.019 M at 45° , pH 6.51, and 15 MHz) the carbonyls have T_1 's in the range of 400 msec, α -carbons ~ 40 msec, β -carbons ~ 40 msec, rigid side-chains ~ 30 msec, and ϵ -carbons in lysine ~ 30 msec. The corresponding values in the acid-denatured protein are ~ 540 msec, ~ 120 msec, ~ 100 msec, not obtained, and ~ 300 msec. The 180° - t - 90° spectra are shown in Figure 35. Glushko, Lawson, and Gurd¹⁰⁸ extended the analysis to include pH dependence for native and denatured forms of ribonuclease A. They presented data for T_1 and calculated effective rotational correlation times (based on the above full equation) at pH 6.55, 4.14, and 2.12. They also

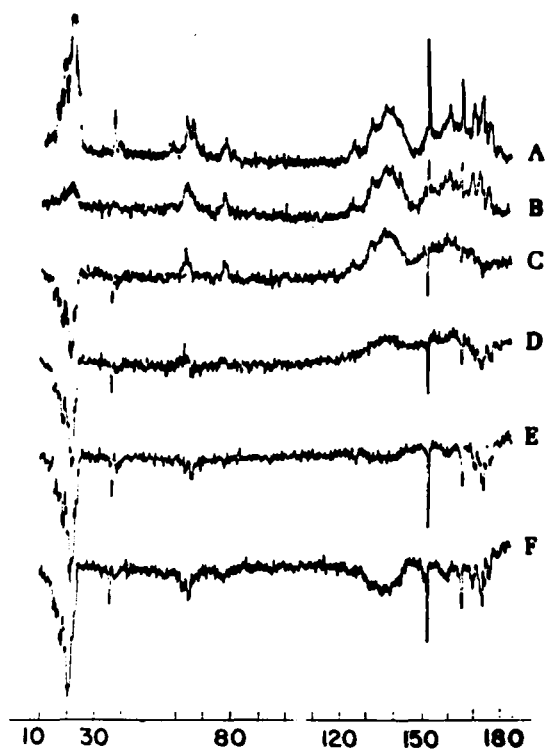


FIGURE 35. ^{13}C spectra of 0.019 *M* ribonuclease A at 45°, pH 6.53, and 15.08 MHz. Each spectrum is the result of 16,384 scans with a 1.36 sec recycle (6 h/spectrum). Chemical shifts are in ppm upfield from external $^{13}\text{CS}_2$. (A) normal FT spectrum, (B to F) partially relaxed spectra in the $180^\circ\text{-}\tau\text{-}90^\circ$ sequence with delay times of 336.9, 82.2, 39.8, 18.6, and 7.96 msec, respectively. (From Allerhand, A., Doddrell, D., Glushko, V., Cochran, D. W., Wenkert, E., Lawson, P. J., and Gurd, F. R. N., Conformational and segmental motion of native and denatured ribonuclease A in solution. Application of natural abundance carbon-13 partially relaxed fourier transform nuclear magnetic resonance, *J. Am. Chem. Soc.*, 93, 544, 1971. With permission of American Chemical Society.)

examined oxidized ribonuclease at pH 4.34 and 1.40. Selective results were tabulated for identifiable residues such as carbons in tyrosine, phenylalanine, histidine, tyrosine, threonine, lysine, and valine. T_1 's from 30 to 295 msec were observed with values longer at the low pH. The oxidized ribonuclease had T_1 's similar to those of the acid-denatured form. The lysine side-chain carbons show interesting behavior, reflecting their relatively free environment. In progressing through the β , γ , δ , and ϵ carbons of lysine, at pH 6.55 the T_1 's are 66, 100, 188, and 278 msec, respectively. At pH 2.12 these change to 93, 121, 151, and 295 msec. The progressive mobility in the lysine side-chain is clear as is the greater flexibility at low

pH. The α -carbons at pH 6.55 produce a broad envelope, the maximum of which has a T_1 of 30 msec. However, at pH 2.12 it splits, and the four most prominent peaks have T_1 values of 61, 59, 55, and 67 msec, respectively. In using the above full equation to calculate τ_c from an observed T_1 , two solutions are possible, one on each side of the minimum of the T_1 vs. τ_c curve. Glushko et al. reproduced each of these solutions for τ_c from their T_1 data. In most cases these were different by at least an order of magnitude in τ_c . For example, for the carbon of threonine at pH 2.12, values of τ_c of 8.7×10^{-10} and 4.5×10^{-8} are possible for a T_1 of 59 msec. For the more mobile lysine side-chain, the comparison is even more disparate, giving τ_c values of 1.6×10^{-7} and 2.3×10^{-10} from the 100 msec T_1 of the γ lysine carbon at pH 6.55. Other measurements of fluorescence depolarization give an overall molecular rotational correlation time of a few tenths of a nanosecond. Since this value determines an upper bound on τ_c , values greater than 10^{-8} are unreasonable. The τ_c must then be in the "extreme narrowing" region, and thus $T_1 = T_2$ for most cases. The observed linewidths are consistent with the calculated τ_c 's of 6×10^{-11} to 2.7×10^{-9} sec. Some of the T_1 's give τ_c 's too close to separate on the basis of the above discussion, e.g., a T_1 of 35 msec gives τ_c solutions of 1.9×10^{-9} and 2.4×10^{-8} sec. It is interesting to note that the crowded valine and threonine side-chain methyl groups show τ_c values the same as that of the relatively free alanine methyl, suggesting that methyl rotation controls the T_1 . The T_1 's for the alanine methyls and backbone methine carbons are in the ratio of 3:1, a value expected for a methyl rotating fast compared to the isotropic rotation of the backbone carbons.

Komoroski and Allerhand¹²⁵ have recently determined T_1 's and ^{13}C chemical shifts in unfractionated yeast transfer-RNA in the presence of Mg^{2+} over a temperature range of 27 to 82°C. Using mononucleotides as guides, chemical shifts were assigned based on the denatured form at 82°C. Only the 4' carbon of the ribose rings was shifted appreciably (1.5 ppm) from that in the mononucleotides. Figure 36 shows spectra of polyadenylic acid, transfer RNA (unfolded) at 80°C and transfer RNA (folded) at 52°C. The data in Figure 37 show that the line broadening in going to the folded form is not due to shorter T_2 , since dilution has the same effect, but possibly to

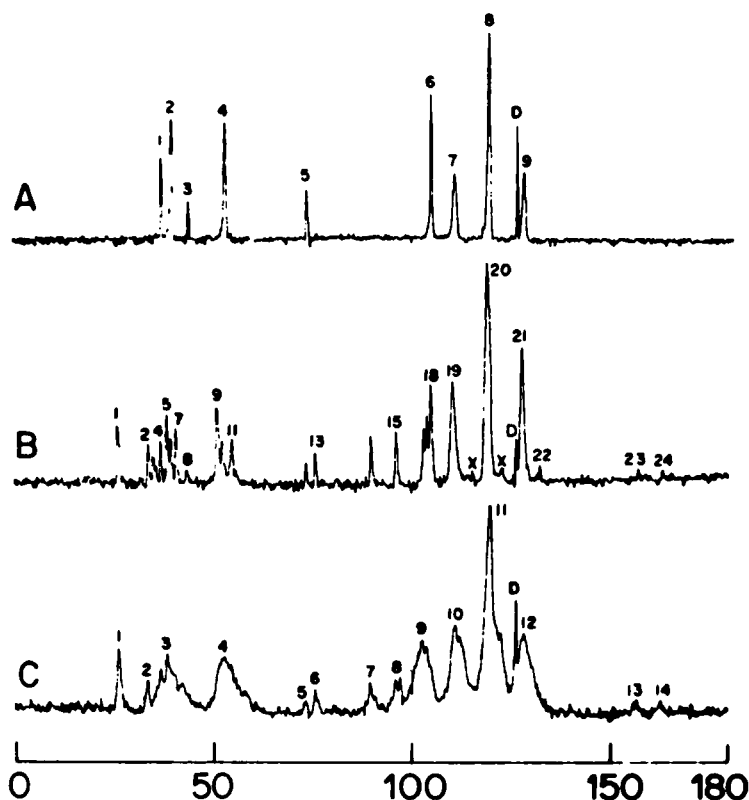


FIGURE 36. ^{13}C spectra of aqueous nucleic acids at 15.18 MHz (in ppm upfield from $^{13}\text{CS}_2$): (A) polyadenylic acid, pH 6.92, 59°; (B) unfractionated tRNA, 80°C; (C) unfractionated tRNA, 52°. (From Komoroski, R. A. and Allerhand, A., Natural-abundance carbon-13 fourier transform nuclear magnetic resonance spectra and spin-lattice relaxation times of unfractionated yeast transfer-RNA, *Proc. Natl. Acad. Sci. USA*, 69, 1804, 1972. With permission.)

tRNA aggregation. In contrast to the gradual linewidth behavior, the ribose carbon T_1 's were essentially independent of temperature up to 60° beyond which they rose rapidly.

Figure 38 illustrates the partially relaxed spectra at 54°C and 15 MHz. The T_1 values allowed calculation of a value of 3×10^{-8} sec for the effective rotational correlation time of the folded tRNA backbone, while at 80° the unfolded form has a value of 2.5×10^{-10} sec, a value indicating very rapid segmental motion. The lack of change in T_1 in going to 35°C and the severe broadening can be interpreted as chemical-shift nonequivalence caused by aggregation. However, how this is actually accomplished is still unknown. No internal motion of the bases was indicated.

Specific labeling of a macromolecule was utilized recently by Browne et al.^{126,127} where they specifically enriched the C_2 (ring) carbon of

the four histidine residues of tryptophan synthetase α subunit. In addition to the normal ^{13}C enrichment, they also specifically labeled the ^{13}C with deuterium. Since the magnetogyric ratios γ_{C} and $\gamma_{\text{D,H}}$ enter quadratically into the dipole-dipole contributions to T_1 and T_2 , going from γ_{H} to γ_{D} should result in a much longer T_2 and hence, narrower lines. Tryptophan synthetase α subunit has four histidines, one or more of which appear to be located at or near the active site. The protein has a molecular weight of 29,000. The enriched histidine carbons show up clearly in the ^{13}C spectrum and have a linewidth of 50 ± 5 Hz and a measured T_1 of 0.5 sec. In the absence of proton decoupling the line remained unsplit, showing essentially complete deuterium substitution, and with proton decoupling no NOE was observed, indicating that probably relaxation via the deuterium was the only important pathway.

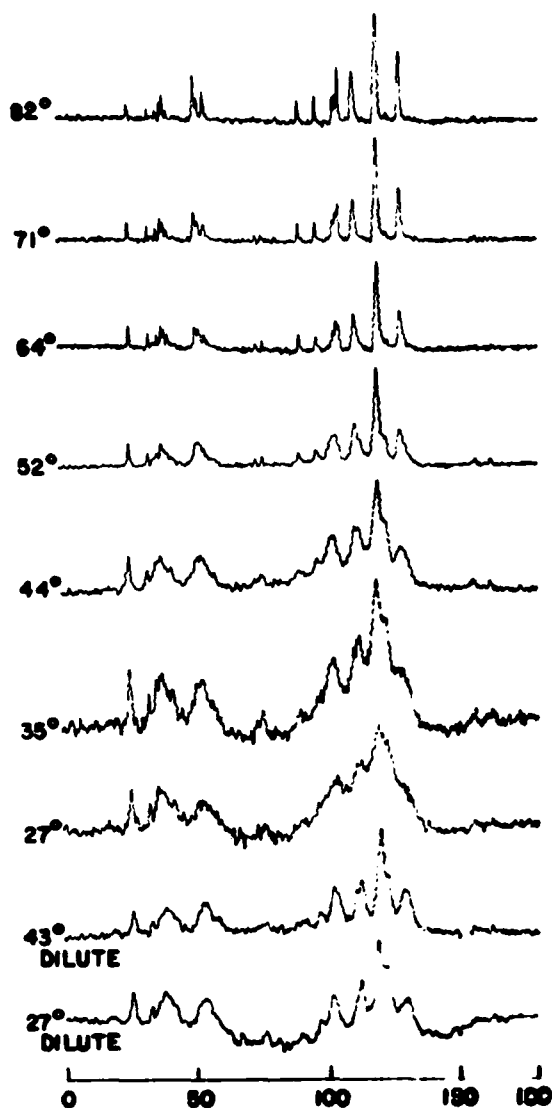


FIGURE 37. Temperature and concentration dependence of the ^{13}C spectrum of unfractionated tRNA (pH 7.0) at 15.18 MHz. 200 mg/ml of tRNA were used for all spectra except those marked "dilute" which were 80 mg/ml. (From Komoroski, R. A. and Allerhand, A., Natural-abundance carbon-13 fourier transform nuclear magnetic resonance spectra and spin-lattice relaxation times of unfractionated yeast transfer-RNA, *Proc. Natl. Acad. Sci. USA*, 69, 1804, 1972. With permission.)

However, other protonated carbons also gave no NOE, suggesting very long τ_c value for these carbons. Assuming that the labeled histidine carbon is only relaxed via dipole-dipole relaxation with deuterium, an expression for $1/T_1$ similar to the full equation above predicts a τ_c (using $T_1 = 0.5$ sec) of 2.7×10^{-8} sec. This value is reasonable for overall rotational reorientation of a globular

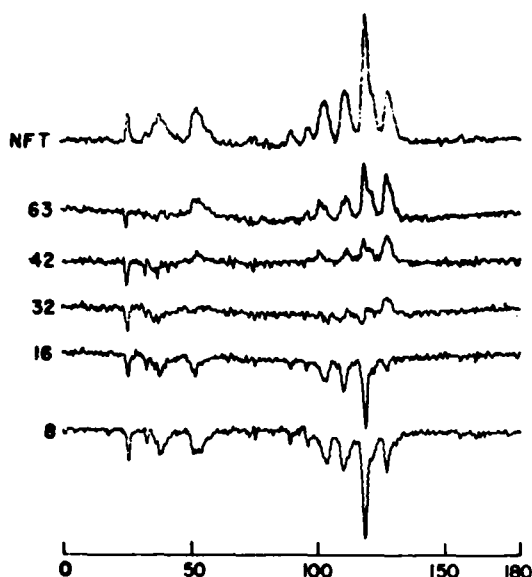


FIGURE 38. Partially relaxed ^{13}C spectra of unfractionated tRNA, pH 7.0, at 54°, and 15.18 MHz. NFT signifies normal fourier transform spectrum. Delay times (in msec.) are listed adjacent to the partially relaxed spectra. (From Komoroski, R. A. and Allerhand, A., Natural-abundance carbon-13 fourier transform nuclear magnetic resonance spectra and spin-lattice relaxation times of unfractionated yeast transfer-RNA, *Proc. Natl. Acad. Sci. USA*, 69, 1804, 1972. With permission.)

protein and suggests that the four histidines are rather restricted in their rotation. In an analysis of the linewidth of the deuterated carbon-13 resonance, estimates of contributions to $1/\pi T_2$ of 5 Hz (dipole-dipole) and 15 Hz (scalar coupling) were made. No other mechanisms were estimated to have important contributions. Thus the observed resonance likely consisted of four resonances each approximately 20 Hz in width and spread over 1 ppm.

CORRINOIDS AND PORPHYRINS

The great importance of metalloporphyrins such as vitamin B_{12} and chlorophyll in biochemistry has prompted a number of ^{13}C nmr studies in the last two years. Doddrell and Allerhand¹²⁸ have reported ^{13}C FT spectra at 15 MHz of cobinamide dicyanide, vitamin B_{12} , dicyanocobalamin, and coenzyme B_{12} . In addition to chemical shift comparisons and off-resonance coherent decoupling, partially relaxed spectra such as shown in Figure 39 were of aid in assignments. Figures 40 and 41 show the structure and 25 MHz FT spectra of vitamin B_{12} . Almost all the lines

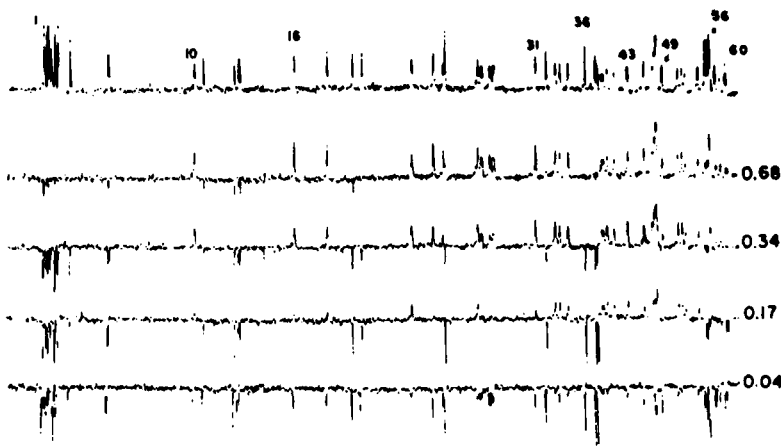


FIGURE 39. Partially relaxed ^{13}C spectra of 0.14 *M* aqueous dicyanocobalamin (56°C and pH 9.8) at 15.08 MHz (3.1 h/spectrum). The top spectrum is the normal FT spectrum; the others are partially relaxed spectra with delay times indicated (in seconds). (From Doddrell, D. and Allerhand, A., Assignments in the carbon-13 nuclear magnetic resonance spectra of vitamin B_{12} , coenzyme B_{12} , and other corrinoids: application of partially relaxed fourier transform spectroscopy, *Proc. Natl. Acad. Sci. USA*, 68, 1083, 1971. With permission.)

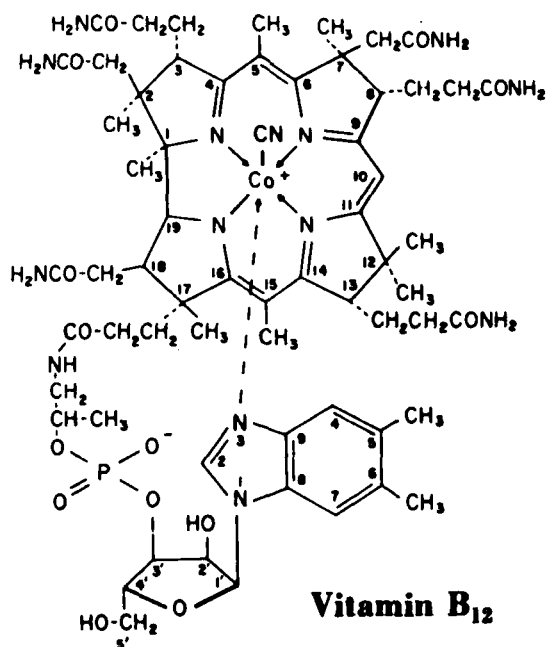


FIGURE 40. Structure of vitamin B_{12} .

were assigned in the 15 MHz spectrum with some uncertainties. ^{13}C - ^{31}P couplings were also observed and used as assignment aids. The partially

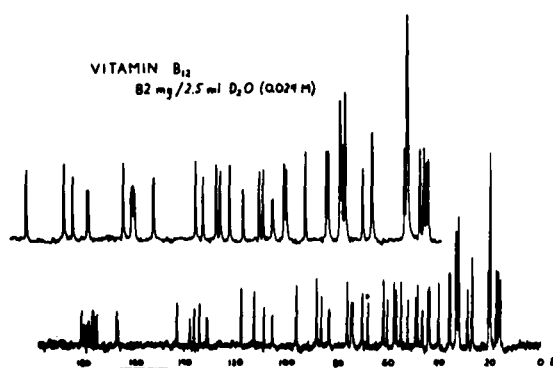


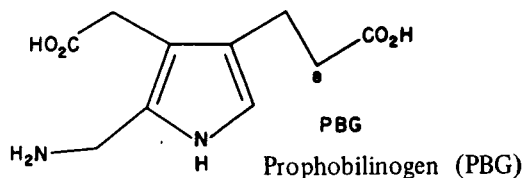
FIGURE 41. ^{13}C spectrum of vitamin B_{12} (82 mg/2.5 ml) at 25.2 MHz (9 hr). (With permission of Varian Associates.)

relaxed spectra were of considerable use in complex regions of the spectra.

If the amide function on C-17 is simply replaced by -OH and the cobalt ligand other than CN replaced by water, there results the subject of a subsequent study by Doddrell and Allerhand,¹²⁹ aquocyanocobryic acid. This can exist in two forms by switching the cyano and H_2O ligands on the cobalt and, in fact, shows 60 resolved resonances (composition $\text{C}_{46}\text{H}_{67}\text{CoN}_{11}\text{O}_9$) while

the dicyano analog only has 38 resolved lines. Isomer shifts of up to 1.3 ppm were observed, suggesting not only electronic differences but conformational changes in the corrin ring.

Brown, Katz, and Shemin¹³⁰ investigated the biosynthetic origin of the methyl group on C-1 in vitamin B₁₂ using (5-¹³C)-aminolevulinic acid (H₂NCH₂COCH₂CH₂COOH). This acid had been previously thought to contribute eight carbons to the product B₁₂. The authors observed also seven resonances in the enriched B₁₂ spectrum and none corresponding to the C-1 methyl. The carbons derived from the (5-¹³C)-aminolevulinic acid were C-4, -5, -9, -10, -14, -15, and -16. Their results allowed unambiguous identifications of these resonances, something not possible in the earlier work of Doddrell and Allerhand.¹²⁸ In a pair of closely related studies Scott et al.^{131,132} used (2-¹³C)- and (5-¹³C)-aminolevulinic acid and also showed that no C-1 methyl resonance enhancement occurred. The (2-¹³C)-aminolevulinic acid resulted in eight high-field signals, seven ¹³CH₂CONH₂, and a C-12 methyl, in agreement with earlier ¹⁴C studies. Use of (¹³CH₃) methionine did enhance the C-1 methyl resonance (and thus prove its origin) as well as 6 others (the C-2, -5, -7, -12 (one), -15, and -17 methyls). The role of porphobilinogen (PBG)



in the biosynthesis of vitamin B₁₂ led Scott et al.¹³² to use C-8 labeled PBG and the correspondingly labeled cyclic tetramer, of PBG, uroporphyrinogen. When used biosynthetically as precursors these gave identical enhancements in the product B₁₂ spectrum for the 4 methylenes on C-3, C-8, C-13 and C-17. The data gave strong support for the biosynthetic sequence PBG → uroporphyrinogen → vitamin B₁₂.

Doddrell and Caughey¹³³ used ¹³C FT nmr to probe electron delocalization in the inner 16-membered porphyrin skeleton. Several model porphyrins were studied: deuterioporphyrin IX dimethyl ester, deuterioporphyrin diethyl ester, 2,4 diacetyl deuterioporphyrin IX dimethyl ester, 2,4 dipropionyldeuterioporphyrin IX dimethyl ester, mesoporphyrin IX dimethyl ester, and proto-

porphyrin IX diethyl ester. The large ~30 ppm upfield shift of the meso carbons relative to the outer ring sp² carbons was interpreted as resulting from strong resonance effects on the meso carbons via the inner 16-membered ring with the outer sp² carbons nearly pure double bonds.

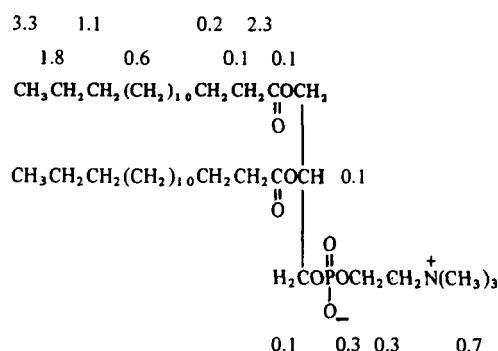
Placing a magnesium ion in the porphyrin ring leads naturally to chlorophyll on which a few ¹³C nmr investigations have been carried out.^{134,135} Katz et al.¹³⁴ have studied chlorophyll's aggregation behavior in nonpolar solvents where the keto carbonyl function in ring V serves as an axial donor for the magnesium ion in another chlorophyll molecule. By studying the chemical shift of this keto carbon as a function of the position of the equilibrium Chl·Chl + 2THF ⇌ 2Chl·THF, they observed an upfield shift with added THF, progressing from a broad resonance in Chl·Chl, sharpening, and finally moving to a point 2.42 ppm upfield for the free keto group. They decomposed the keto carbon shift as having components due to ring currents (upfield) and C=O-Mg coordination (downfield). Removal of aggregation removes the latter effect.

The entire ¹³C spectrum of chlorophyll has been reported by Strouse, Kollman, and Matwiyoff.¹³⁵ The availability of 90%-enriched ¹³C enabled the workers to prepare 90% ¹³C chlorophyll in two forms (A and B) differing only in replacing a methyl by a formyl group. ¹³C-¹³C couplings were manifest in the spectra and aided in assignments. Interestingly, an olefinic carbon on the phytol side-chain is most affected by aggregation, strongly shifted, and broadened. Further work on this may reflect valuable stereochemical information on the structure of aggregated chlorophyll.

LIPIDS, LECITHINS, AND MEMBRANES

The hope for direct probing of biological structures by ¹³C nmr is now starting to have some concrete fruition. Cell membranes still are poorly understood, particularly with regard to their transport properties. During the last two years two groups in England have used ¹³C nmr to investigate the structure and mobility of membranes and membrane models. Oldfield and Chapman¹³⁶ and Metcalfe et al.¹³⁷ first considered lecithins, both synthetic dipalmitoyl lecithins,^{136,137} and egg yolk lecithin. The latter gave broad signals assignable to olefinic,

methylenic, methyl, and $-N^+Me_3$ bands. Dipalmitoyl lecithin gave sharp lines, however.^{136,137} The $-N^+Me_3$ signals in egg lecithin were much narrower than those of the other bands. This was interpreted as reflecting a greater relative mobility. Metcalfe et al.¹³⁷ also considered sonicated and unsonicated lecithin. The former gave a spectrum very similar to dipalmitoyl lecithin, but the latter was severely broadened (except for the $-N^+Me_3$ signal). They suggested that the broadening was due primarily to chemical shift nonequivalence rather than shorter T_2 values. Some preliminary T_1 data were also given and expanded upon in a later paper (see below). In view of the success with the lecithins, Metcalfe et al.¹³⁷ examined human erythrocyte membranes. The ^{13}C spectrum showed several broad bands with a few relatively sharp signals, one of which was assigned to the $-N^+(CH_3)_3$ carbons of the lecithin in the membrane. Subsequently, Levine, Birdsall, Lee, and Metcalfe¹³⁸ published full details concerning relaxation and temperature dependence measurements on dipalmitoyl lecithin (sonicated) as well as ^{13}C T_1 measurements on di-7-fluoropalmitoyl lecithin and dioleoyl lecithin. Below 40°C, sonicated dipalmitoyl lecithin shows only the $-N^+Me_3$ signal with very broad resonances from the fatty acid chains. Above 40°C, resolved resonances are observed from the fatty acid chains for the carbonyl carbons (C_1), the terminal methyls (C_{16}), and for carbons -2, -3, -14, and -15, in addition to the main methylene envelope of carbons -4 to -13. T_1 values were determined for sonicated dipalmitoyl lecithin at 52°C in D_2O (in seconds) as



The T_1 values for all the chain carbons are the average for the two chains, and the T_1 for C_4 - C_{13} (the methylene envelope) is a composite value calculated from unresolved resonances. The T_1 's decrease with temperature down to the thermal

transition point, below which they could not be measured. Introduction of an ^{19}F label does not appear to significantly affect the bilayer structure since, aside from the fluorinated carbon, the carbons have similar shifts and T_1 values. Placing a double bond in the C_{18} chains of dioleoyl lecithin not only shifts some of the methylene resonances but also causes consistent increases in chain carbon T_1 values and increases the $-N^+Me_3$ T_1 from 0.70 sec to 1.06 sec. The solvent dependence of T_1 was determined for dipalmitoyl lecithin in D_2O and $CDCl_3$ and compared with the heterogeneous egg lecithin in CD_3OD at 52°C. In $CDCl_3$ lecithin exists as spherical micelles containing 60 to 70 molecules. In general, the T_1 's for egg lecithin were longer than those of dipalmitoyl lecithin in $CDCl_3$, which were in turn longer than the T_1 's in D_2O .

In an effort to make more specific observations, Metcalfe et al.¹³⁹ studied membranes of *Acholeplasma laidlawii* grown in media supplemented by 60%-enriched ($1-^{13}C$) palmitic acid. Specific enrichment, it was felt, should allow direct comparison of the relaxation times of the enriched nuclei in the intact membranes and in vesicles of the extracted lipids in bilayers. Specific carbon observation allowed investigation of the extent to which the proteins in the membrane structure influence the mobility of the lipids and thus provided information concerning these interactions via the lipid T_1 data. The enriched membrane gave high enhancement of the carboxyl resonance relative to the $(CH_2)_n$ resonance at natural abundance, an overall incorporation of 24% of the enriched palmitic acid. Two non-equivalent side-chain carboxyls were observed as well as an unassigned, additional, partially resolved resonance to high-field of the doublet. Again no resonances were observable below 40°C. The carboxyl resonance had a linewidth of 130 Hz at 55% for the intact membrane vs. 40 Hz in the sonicated vesicles of the membrane lipid. The experiments clearly point out the feasibility of making relaxation measurements on defined lipid resonances in intact membranes.

Keough, Oldfield, Chapman, and Beryon¹⁴⁰ have very recently reported ^{13}C nmr studies of unsonicated egg lecithin, egg lecithin-cholesterol (1:1), and ox-brain sphingomyelin, together with spectra of chloroplast and mitochondrial membranes and erythrocyte ghosts. Addition of cholesterol severely broadens most of the egg

lecithin resonances, interpreted as resulting from restricted motion and less efficient time-averaging of the ^{13}C - ^1H dipole interactions. The olefinic oleoyl residues' linewidths changed from 71 ± 15 Hz to 161 ± 25 Hz upon addition of equimolar cholesterol. The cholesterol is apparently so immobilized that it gives no resolved resonances. The sphingomyelin gave a significantly more resolved spectrum than the egg lecithin or egg lecithin-cholesterol, except for the olefinic carbon (relative to egg lecithin), which was broader. This was expected since the double bonds in sphingomyelin are predominantly located in the sphingosine residue, near the polar/apolar interface, whereas in the egg lecithin they are ~ 9 carbons along the acyl chain in the bilayer and are hence more mobile. Very good resolution was obtained on rat liver mitochondrial membranes while the erythrocyte ghosts gave much broader resonances. A mitochondrial membrane spectrum was calculated from known amino acid and lipid composition. The comparison with the experimental spectrum was good in regard to the lipids, but the protein resonances did not appear in the expected relative intensity. This was interpreted as reflecting fairly immobilized proteins, embedded in the more mobile lipid bilayer. These pioneering investigations are sure to prod significant future activity in the study of intact biomembranes. There are inherent dangers, however, which must be considered, particularly in the interpretation of linewidths. Relaxation measurements must be performed, preferably on specifically enriched molecules, to unambiguously separate changes in T_2 from changes in linewidth resulting from a different pattern of chemical shift nonequivalence.

THE FUTURE

The foregoing details the remarkable progress made in the use of ^{13}C nmr in biochemistry and

biology in the last few years. The rate of growth is sure to be exponential in the near future as instrumentation becomes available to a wider circle of users. Technical improvements will lower the sensitivity boundaries so that milligram and submilligram quantities of compounds are analyzable. Improved design and larger sample tubes will make possible the study of slightly soluble compounds and macromolecules. Figure 42 shows spectra obtained in 20-mm tubes where a single carbon in a macromolecule containing 613 carbons is observable. The numbered carbons 1 to 22 are nonprotonated carbons only, out of 28 nonprotonated aromatic carbons in lysozyme. Of course, 40 hr was necessary to achieve this signal-to-noise. Future improvements will undoubtedly reduce this time to a more manageable period. For small to intermediate size molecules or very large molecules capable of segmental motion, superconducting fields will gain at least a factor of two in signal-to-noise ratio. The ready availability and dropping costs of ^{13}C , ^2H , and ^{15}N are making specific enrichment or "tagging" more practical. As data systems drop in cost and rise in capability, entirely automated disk systems will become more widely available, allowing the accumulation of, for example, 32,000 word transforms, adaptive T_1 and T_2 programs for automatic relaxation time determination, "stringing together" of T_1 , off-resonance, selective, and gated decoupling experiments, and Overhauser effect determinations. We are indeed only beginning.

Addendum

Since the completion of this review, several additional papers have appeared and others, previously missed, have been noted. In the interest of completeness these have been included in the reference list beginning with Reference 142 and are grouped according to area.

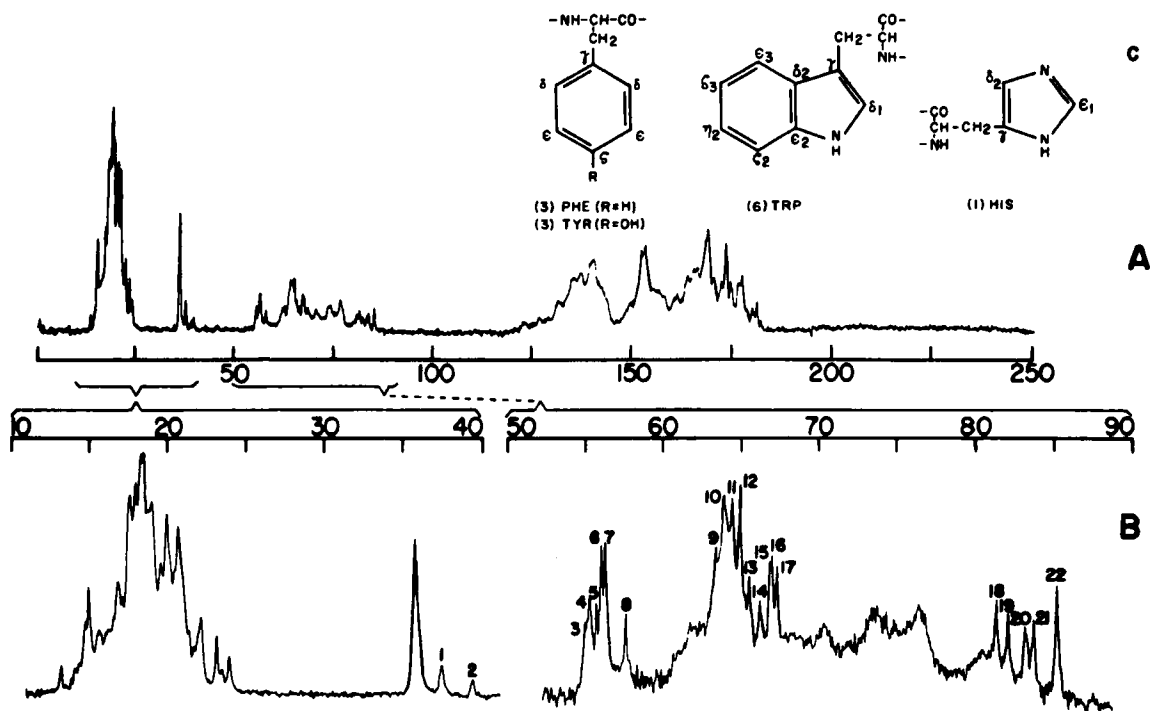


FIGURE 42. ^{13}C spectrum of native hens' egg white lysozyme: (A) Full spectrum (ppm upfield from $^{13}\text{CS}_2$) at 15.18 MHz in a 20-mm tube, 12 hr accumulation time; (B) 40 hr accumulation of the unsaturated carbon region; (C) structure of amino-acid residues with quantity represented in lysozyme shown in parentheses. (From Allerhand, A., Childers, R. F., Goodman, R. A., Oldfield, E., and Ysern, X., Increased sensitivity in ^{13}C FT using 20-mm sample tubes, *Am. Lab.*, 4, 19, 1972. With permission.)

REFERENCES

1. Lauterbur, P. C., ^{13}C Nuclear magnetic resonance spectra, *J. Chem. Phys.*, 26, 217, 1957.
2. Holm, C. H., Observation of chemical shielding and spin coupling of ^{13}C nuclei in various chemical compounds by nuclear magnetic resonance, *J. Chem. Phys.*, 26, 707, 1959.
3. For reviews of ^{13}C NMR see (a) Stothers, J. B., *Carbon-13 NMR Spectroscopy*, Academic Press, New York, 1972; and (b) Levy, G. C. and Nelson, G. L., *Carbon-13 Nuclear Magnetic Resonance for Organic Chemists*, Wiley Interscience, New York, 1972.
4. Ernst, R. R., Nuclear magnetic double resonance with an incoherent radio-frequency field, *J. Chem. Phys.*, 45, 3845, 1966.
5. Ernst, R. R. and Anderson, W. A., Application of fourier transform spectroscopy to magnetic resonance, *Rev. Sci. Instrum.*, 37, 93, 1966.
6. Becker, E. D. and Farrar, T. C., *Pulse and Fourier Transform NMR*, Academic Press, New York, 1971.
7. Buchanan, G. W., Ross, D. A., and Stothers, J. B., A new approach to conformational analysis. Carbon-13 nuclear magnetic resonance, *J. Am. Chem. Soc.*, 88, 4301, 1966.
8. Hall, L. D. and Johnson, L. F., Chemical studies by ^{13}C nuclear magnetic resonance spectroscopy: Some chemical shift dependencies of oxygenated derivatives, *Chem. Commun.*, 509, 1969.
9. Perlin, A. S. and Casu, B., Carbon-13 and proton magnetic resonance spectra of D-glucose- ^{13}C , *Tetrahedron Lett.*, 2921, 1969.
10. Dorman, D. E., Angyal, S. J., and Roberts, J. D., Nuclear magnetic resonance spectroscopy. Carbon-13 spectra of some inositols and their O-methylated derivatives, *J. Am. Chem. Soc.*, 92, 1351, 1970.
11. Dorman, D. E. and Roberts, J. D., Nuclear magnetic resonance spectroscopy. Carbon-13 spectra of some pentose and hexose aldopyranoses, *J. Am. Chem. Soc.*, 92, 1355, 1970.
12. Perlin, A. S., Casu, B., and Koch, H. J., Configurational and conformational influences on the carbon-13 chemical shifts of some carbohydrates, *Can. J. Chem.*, 48, 2596, 1970.
13. Breitmaier, E., Voelter, W., Jung, G., and Tänzler, C., Influences of configuration, conformation, and substituent on the ^{13}C chemical shifts in glycosides, *Chem. Ber.*, 104, 1147, 1971.
14. Voelter, W., Breitmaier, E., Price, R., and Jung, G., Conformational analysis of pyranoses using ^{13}C resonances, *Chimia*, 25, 168, 1971.
15. Voelter, W., Breitmaier, E., and Jung, G., Pulse fourier transform ^{13}C -NMR spectroscopy of mutarotating sugars, *Angew. Chem. Int. Ed.*, 10, 935, 1971.

16. Coxin, B. and Johnson, L. F., The NMR spectroscopy of derivatives of 6-amino-6-deoxy-D-glucose-6-¹⁵N. ¹³C fourier transform and internuclear, double- and triple-resonance studies, *Carbohydr. Res.*, 20, 105, 1971.
17. Doddrell, D. and Allerhand, A., Study of anomeric equilibria of ketoses in water by natural abundance carbon-13 fourier transform nuclear magnetic resonance, D-fructose and D-turanose, *J. Am. Chem. Soc.*, 93, 2779, 1971.
18. Allerhand, A. and Doddrell, D., Strategies in the application of partially relaxed fourier transform nuclear magnetic resonance spectroscopy in assignments of carbon-13 resonances in complex molecules. Stachyose, *J. Am. Chem. Soc.*, 93, 2777, 1971.
19. Yamaoka, N., Usui, T., Matsuda, K., and Tuzimura, K., ¹³C nuclear magnetic resonance spectra of glucobioses, *Tetrahedron Lett.*, 2047, 1971.
20. Perlin, A. S., Casu, B., Sanderson, G. R., and Tse, J., Methyl α and β -D-idopyranosiduronic acids synthesis and conformational analysis, *Carbohydr. Res.*, 21, 123, 1972.
21. Perlin, A. S., Ng Ying Kin, N. M. K., Bhattacharjee, S. S., and Johnson, L. F., The ¹³C fourier transform spectrum of heparin. Evidence for a biose repeating sequence of residues, *Can. J. Chem.*, 50, 2437, 1972.
22. Binkley, W. W., Horton, D., Bhacca, N. S., and Wander, J. D., Physical studies on oligosaccharides related to sucrose. Part III. Cmr studies on 1-kestose and nystose, *Carbohydr. Res.*, 23, 301, 1972.
23. Reich, H. J., Jautelat, M., Messe, M. T., Weigert, F. J., and Roberts, J. D., Nuclear magnetic resonance spectroscopy. Carbon-13 spectra of steroids, *J. Am. Chem. Soc.*, 91, 7445, 1969.
24. Lukacs, G., Picot, A., Lusinchi, X., Koch, H. J., and Perlin, A. S., Steroidol alkaloids CXXV. ¹³C nuclear magnetic resonance of connessine and derivatives, *C. R. Acad. Sci. Ser. C*, 272, 2171, 1971.
25. Lukacs, G., Khuong-Lum, Q., Bennett, C. R., Buckwalter, B. L., and Wenkert, E., Carbon-13 nuclear magnetic resonance spectroscopy of naturally occurring substances. Lanosterol and dihydrolanosterol, *Tetrahedron Lett.*, 3515, 1972.
26. Khuong-Lum, Q., Lukacs, G., Pancrazi, A., and Gontarel, R., Steroidal alkaloids CXLV. ¹³C nuclear magnetic resonance of natural products and related compounds VII. New method of preparation of azido- and amino-steroid epimers at C-5, *Tetrahedron Lett.*, 3579, 1972.
27. Baloch, B., Wilson, D. M., and Burlingame, A. L., Carbon-13 NMR study of the stereochemistry of steranes from oil shale of the Green River Formation (Eocene), *Nature*, 233, 261, 1971.
28. Gough, J. L., Guthrie, J. P., and Stothers, J. B., Stereochemical assignments in steroids by ¹³C nuclear magnetic resonance spectroscopy: configuration of the A/B ring junction, *J. Chem. Soc. D Chem. Commun.*, 979, 1972.
29. Lukacs, G., Lusinger, X., Hagaman, E. W., Buckwalter, B. L., Schell, F. M., and Wenkert, E., ¹³C nuclear magnetic resonance of natural products and related compounds XII. Fluorosteroids, *C. R. Acad. Sci. Ser. C*, 274, 1458, 1972.
30. Wenkert, E., Cochran, D. W., Schell, F. M., Archer, R. A., and Matsumoto, K., CMR spectral analysis of tetrahydrocannabinol and its isomers, *Experientia*, 28, 250, 1972.
31. Wenkert, E., Clouse, A. O., Cochran, D. W., and Doddrell, D., ¹³C nuclear magnetic resonance spectroscopy of naturally occurring substances. Camphor and related compounds, *Chem. Commun.*, 1433, 1969.
32. Wenkert, E., Chang, C., Clouse, A. O., and Cochran, D. W., Carbon-13 nuclear magnetic resonance spectroscopy of naturally occurring substances. Gelsamine, *Chem. Commun.*, 961, 1970.
33. Archer, R. A., Cooper, R. D. G., Demarco, P. V., and Johnson, L. F., Structural studies of some penicillins and related sulfoxides, *Chem. Commun.*, 1291, 1970.
34. Moore, R. E., Ghatak, U. R., Chakravarty, J., Dasgupta, R., and Johnson, L. F., Mass spectrometry and proton and carbon-13 nuclear magnetic resonance spectroscopy in assigning stereochemistry to derivatives of des-N-morphinan and des-N-isomorphinan, *Chem. Commun.*, 1136, 1970.
35. Joseph-Nathan, P., Gonzalez, P., Johnson, L. F., and Shoolery, J. N., Natural abundance ¹³C NMR studies of perezone and derivatives, *Organic Mag. Resonance*, 3, 23, 1971.
36. Zetta, L., Gotti, G., and Fuganti, G., ¹³C NMR spectrum of narciclasine tetraacetate, *Tetrahedron Lett.*, 4447, 1971.
37. Crain, W. O., Jr., Wildman, W. C., and Roberts, J. D., Nuclear magnetic resonance spectroscopy. Carbon-13 spectra of nicotine, quinine, and some *amaryllidaceae* alkaloids, *J. Am. Chem. Soc.*, 93, 990, 1971.
38. Sprague, P. W., Doddrell, D., and Roberts, J. D., Nuclear magnetic resonance spectroscopy. ¹³C spectra of the veratrum alkaloids, jervine and veratramine, *Tetrahedron*, 27, 4857, 1971.
39. Gribble, G. W., Nelson, R. B., Levy, G. C., and Nelson, G. L., Carbon-13 fourier transform nuclear magnetic resonance spectroscopy of the alkaloid 1, 2, 3, 4, 7, 12, 12b-octahydroindolo (2, 3-a) quinolizine, *J. Chem. Soc., Chem. Commun.*, 703, 1972.
40. Rabaron, A., Koch, M., Plot, M., Peyroux, J., Wenkert, E., and Cochran, D. W., Structural analysis by carbon-13 nuclear magnetic resonance spectroscopy. Arenaine, *J. Am. Chem. Soc.*, 93, 6270, 1971.
41. Jones, A. J. and Benn, M. H., The application of carbon-13 magnetic resonance to structural problems: two new diterpenoid alkaloids from *Delphinium Bi-color* nut, *Tetrahedron Lett.*, 4351, 1972.
42. Briggs, J., Hart, F. A., Moss, G. P., and Randall, E. W., A ready method of assignment for ¹³C nuclear magnetic resonance spectra: The complete assignment of the ¹³C spectrum of borneol, *Chem. Commun.*, 364, 1971.
43. Wenkert, E., Cochran, D. W., Hagaman, E. W., Lewis, R. B., and Schell, F. M., Carbon-13 nuclear magnetic resonance spectroscopy with the aid of a paramagnetic shift reagent, *J. Am. Chem. Soc.*, 93, 6271, 1971.

44. Wenkert, E. and Buckwalter, B. L., Carbon-13 nuclear magnetic resonance spectroscopy of naturally occurring substances X. Pimaradienes, *J. Am. Chem. Soc.*, 94, 4367, 1972.
45. Pregosin, P. S., Randall, E. W., and McMurry, T. B. H., ^{13}C fourier studies. The configurational dependence of the carbon-13 chemical shifts in santonin derivatives, *J. Chem. Soc., Perkin Trans. I*, 299, 1972.
46. Weidenmuller, H. L., Cavagna, F., Fehlihaber, H. W., and Präve, P., 2-Carboxymethyl-3-N-hexyl-maleic acid anhydride, *Tetrahedron Lett.*, 3519, 1972.
47. Hikino, H., Koriyama, S., and Takemoto, T., Stereostructure of leucothol B and D, diterpenoids of *Leucothoe grayana*, *Tetrahedron Lett.*, 3831, 1972.
48. Gansow, O. A., Beckenbaugh, W. M., and Sass, R. L., Carbon-13 nuclear magnetic resonance of pharmaceutical agents: benzocaine hydrochloride anesthetics, *Tetrahedron. Lett.*, 28, 2691, 1972.
49. Tanabe, M. and Seto, H., Biosynthetic studies with carbon-13: mollisin, *Biochemistry*, 9, 4851, 1970, and references therein.
50. Tanabe, M., Hamasaki, T., Seto, H., and Johnson, L., Biosynthetic studies with carbon-13: ^{13}C nuclear magnetic resonance spectra of the metabolite sterigmatocystin, *J. Chem. Soc. D Chem. Commun.*, 1539, 1970.
51. Tanabe, M., Seto, H., and Johnson, L., Biosynthetic studies with carbon-13. Carbon-13 nuclear magnetic resonance spectra of radicinin, *J. Am. Chem. Soc.*, 92, 2157, 1970.
52. Tanabe, M., Hamosaki, T., Thomas, D., and Johnson, L., Biosynthetic studies with carbon-13. Asperlin, *J. Am. Chem. Soc.*, 93, 273, 1971.
53. McInnes, A. G., Smith, D. G., Vining, L. C., and Johnson, L., Use of ^{13}C in biosynthetic studies. Location of isotope from labelled acetate and formate in the fungal tropolone, sepedonin, by ^{13}C nuclear magnetic resonance spectroscopy, *Chem. Commun.*, 325, 1971.
54. Neuss, N., Nash, C. H., Lemke, P. A., and Grutzner, J. B., The use of carbon-13 nuclear magnetic resonance (CMR) spectroscopy in biosynthetic studies. Incorporation of carboxyl and methyl carbon-13 labeled acetates into cephalosporin C, *J. Am. Chem. Soc.*, 93, 2337, 1971.
55. Neuss, N., Nash, C. H., Lemke, P. A., and Grutzner, J. B., The use of ^{13}C NMR (C.M.R.) spectroscopy in biosynthetic studies of β -lactam antibiotics, *Proc. R. Soc. Lond.*, B179, 335, 1971.
56. Cushley, R. J., Anderson, D. R., Lipsky, S. R., Sykes, R. J., and Wasserman, H. H., Carbon-13 fourier transform nuclear magnetic resonance spectroscopy II. The pattern of biosynthetic incorporation of (1- ^{13}C)- and (2- ^{13}C) acetate into prodigiosin, *J. Am. Chem. Soc.*, 93, 6284, 1971.
57. Yamazaki, M., Maebayashi, Y., and Miyaki, K., Biosynthesis of ochratoxin A, *Tetrahedron Lett.*, 2301, 1971.
58. Wat, C-K., McInnes, A. G., Smith, D. G., and Vining, L. C., Use of ^{13}C in biosynthetic studies. Location of isotope from labeled acetate and formate in shanorellin by ^{13}C nuclear magnetic resonance spectroscopy, *Can. J. Biochem.*, 50, 620, 1972.
59. Polonsky, J., Boskevitch, Z., Cagnoli-Bellavita, N., Ceccherelli, P., Buckwalter, B. L., and Wenkert, E., Carbon-13 nuclear magnetic resonance spectroscopy of naturally occurring substances XI. Biosynthesis of the virescenosides, *J. Am. Chem. Soc.*, 94, 4369, 1972.
60. Yamazaki, M., Katoh, F., Ohishi, J., and Koyana, Y., Study on biosynthesis of aureothin, a nitro-containing metabolite from *Streptomyces luteoreticuli* using ^{13}C -NMR spectrometry, *Tetrahedron Lett.*, 2701, 1972.
61. Westley, J. W., Pruess, D. L., and Pitcher, R. G., Incorporation of (1- ^{13}C) butyrate into antibiotic X-537A: ^{13}C nuclear magnetic resonance study, *J. Chem. Soc. D Chem. Commun.*, 161, 1972.
62. Battersby, A. R., Moron, J., McDonald, E., and Feeney, J., Studies of porphyrin biosynthesis by ^{13}C -nuclear magnetic resonance; synthesis of (^{13}C) porphobilinogen and its incorporation into protoporphyrin-IX, *J. Chem. Soc. D Chem. Commun.*, 920, 1972.
63. Lukacs, G., Use of ^{13}C enriched precursors in the study of biosynthetic problems by nuclear magnetic resonance, *Bull. Soc. Chim. Fr.*, 351, 1972.
64. Stothers, J. B., *Carbon-13 NMR Spectroscopy*, Academic Press, New York, 1972, Chapt. 7.
65. Tarpley, A. R., Jr. and Goldstein, J. H., Carbon-13 nuclear magnetic resonance spectra of uracil, thymine, and the 5-halouracils, *J. Am. Chem. Soc.*, 93, 3573, 1971.
66. Ellis, G. and Jones, R. G., Carbon-13 nuclear magnetic resonance studies of piperidine and piperazine compounds. Part I. Empirical substituent parameters for C-methyl and N-methyl groups, *J. Chem. Soc., Perkin Trans. II*, 437, 1972.
67. Malinowski, E. R., Substituent effects. IX. Correlation of carbon-13, proton-1, and fluorine-19 nuclear magnetic resonance chemical shifts of some aromatic compounds by pair-wise additivity, *J. Phys. Chem.*, 76, 1593, 1972.
68. Lippmaa, E. and Mägi, M., ^{13}C , ^{14}N , ^{15}N , and ^{17}O NMR spectra of nitropyrroles and nitroimidazoles, *Org. Mag. Resonance*, 4, 153, 1972.
69. Lippman, E. and Mägi, M., ^{13}C , ^{14}N , ^{15}N , and ^{17}O NMR spectra of the charged species of nitropyrroles and nitroimidazoles, *Org. Mag. Resonance*, 4, 197, 1972.
70. Jones, A. J., Casy, A. F., and McErlane, K. M. J., A carbon-13 magnetic resonance study of the stereochemistry in isomeric 1, 2, 5-trimethyl-4-phenylpiperidine-4-ols, *Tetrahedron Lett.*, 1727, 1972.
71. Jones, A. J. and Hassan, M. M. A., Carbon-13 magnetic resonance. Chemical shift additivity relationships in N-methyl-4-piperidones, *J. Org. Chem.*, 37, 2332, 1972.

72. Long, K. R., Long, R. C., Jr., and Goldstein, J. H., Carbon-13 nuclear magnetic resonance investigation of pyridine nicotinamide, their cations and related compounds, *J. Mag. Resonance*, 8, 207, 1972.
73. Jones, A. J., Winkley, M. W., Grant, D. M., and Robins, R. K., Carbon-13 nuclear magnetic resonance: naturally occurring nucleosides, *Proc. Natl. Acad. Sci. USA*, 65, 27, 1970.
74. Spiesscke, H. and Schneider, W. G., The determination of electron densities in azulene from ^{13}C and ^1H nuclear resonance shifts, *Tetrahedron Lett.*, 468, 1961.
75. Jones, A. J., Grant, D. M., Winkley, M. W., and Robins, R. K., Carbon-13 magnetic resonance XVII. Pyrimidine and purine nucleosides, *J. Am. Chem. Soc.*, 92, 4079, 1970.
76. Jones, A. J., Grant, D. M., Winkley, M. W., and Robins, R. K., Carbon-13 magnetic resonance XVIII. Selected nucleosides, *J. Phys. Chem.*, 74, 2684, 1970.
77. Dorman, D. E. and Roberts, J. D., Nuclear magnetic resonance spectroscopy: ^{13}C spectra of some common nucleotides, *Proc. Natl. Acad. Sci. USA*, 65, 19, 1970.
78. Mantsch, H. H. and Smith, I. C. P., Fourier-transformed ^{13}C NMR spectra of polyuridylic acid, uridine, and related nucleotides – the use of ^{31}P ^{13}C couplings for conformation analysis, *Biochem. Biophys. Res. Commun.*, 46, 808, 1972.
79. Lapper, R. D., Mantsch, H. H., and Smith, I. C. P., A carbon-13 and hydrogen-1 nuclear magnetic resonance study of the conformations of 3', 5' and 2', 3'-cyclic nucleotides. A demonstration of the angular dependence of three-bond spin-spin coupling between carbon and phosphorous, *J. Am. Chem. Soc.*, 94, 6243, 1972.
80. Lapper, R. D., Mantsch, H. H., and Smith, I. C. P., A carbon-13 nuclear magnetic resonance study of the conformation of 3', 5' cyclic nucleotides, *J. Am. Chem. Soc.*, in press.
81. Lapper, R. D. and Smith, I. C. P., A ^{13}C and ^1H nuclear magnetic resonance study of the conformations of 2', 3'-cyclic nucleotides, *J. Am. Chem. Soc.*, in press.
82. Lemieux, R. N., Nagabhushan, T. L., and Paul, B., Relationship of ^{13}C to vicinal ^1H coupling to the torsional angle in uridine and related structures, *Can. J. Chem.*, 50, 773, 1972.
83. Kreishman, G. P., Witkowski, J. T., Robins, R. K., and Schweizer, M. P., The use of proton and carbon-13 nuclear magnetic resonance for assignment of the glycosylation site in 3- and 5-substituted 1- β -D-ribofuranosyl-1, 2, 4-triazoles, *J. Am. Chem. Soc.*, 94, 5894, 1972.
84. Blumenstein, M. and Raftery, M. A., ^{31}P and ^{13}C nuclear magnetic resonance studies of nicotinamide-adenine dinucleotide and related compounds, *Biochemistry*, 11, 1643, 1972.
85. Horsley, W. J. and Sternlicht, H., Carbon-13 magnetic resonance studies of amino acids and peptides, *J. Am. Chem. Soc.*, 90, 3738, 1968.
86. Horsley, W., Sternlicht, H., and Cohen, J. S., Carbon-13 magnetic resonance studies of carbon-13 enriched amino acids, *Biochem. Biophys. Res. Commun.*, 37, 47, 1969.
87. Horsley, W., Sternlicht, H., and Cohen, J. S., Carbon-13 magnetic resonance studies of amino acid and peptides II., *J. Am. Chem. Soc.*, 92, 680, 1970.
88. Sternlicht, H., Kenyon, G. L., Packer, E. L., and Sinclair, J., Carbon-13 nuclear magnetic resonance studies of heterogeneous system. Amino acids bound to cationic exchange resin, *J. Am. Chem. Soc.*, 93, 199, 1971.
89. Hagen, R. and Roberts, J. D., Nuclear magnetic resonance spectroscopy, ^{13}C spectra of aliphatic carboxylic acids and carboxylate anions, *J. Am. Chem. Soc.*, 91, 4504, 1969.
90. Voelter, W., Jung, G., Breitmaier, E., and Bayer, E., ^{13}C chemical shifts of amino acids and peptides, *Z. Naturforsch.*, 26B, 213, 1971.
91. Freedman, M. H., Cohen, J. S., and Chaiken, I. M., Carbon-13 fourier transform nuclear magnetic resonance studies of peptides, *Biochem. Biophys. Res. Commun.*, 42, 1148, 1971.
92. Gurd, F. R. N., Lawson, P. J., Cochran, D. W., and Wenkert, E., Carbon-13 nuclear magnetic resonance of peptides in the amino-terminal sequence of sperm whale myoglobin, *J. Biol. Chem.*, 246, 3725, 1971.
93. Christl, M. and Roberts, J. D., Nuclear magnetic resonance spectroscopy. Carbon-13 chemical shifts of small peptides as a function of pH, *J. Am. Chem. Soc.*, 94, 4565, 1972.
94. Thomas, W. A. and Williams, M. K., ^{13}C nuclear magnetic resonance spectroscopy and *cis/trans* isomerism in dipeptides containing proline, *J. Chem. Soc. D Chem. Commun.*, 994, 1972.
95. Jung, G., Breitmaier, E., Voelter, W., Keller, T., and Tänzler, C., Fourier transform ^{13}C NMR spectroscopy of biologically active cysteine peptides, *Angew. Chem. Int. Ed.*, 9, 894, 1970.
96. Gibbons, W. A., Sogn, J. A., Stern, A., Craig, L. C., and Johnson, L. F., ^{13}C nuclear magnetic resonance spectrum of gramicidin S-A, a deca peptide antibiotic, *Nature*, 227, 840, 1970.
97. Ohnishi, M., Fedarko, M. C., Baldeschwieler, J. D., and Johnson, L. F., Fourier transform C-13 NMR analysis of some free and potassium-ion complexed antibiotics, *Biochem. Biophys. Res. Commun.*, 46, 312, 1972.
98. Pretsch, E., Vasak, M., and Simon, W., ^{13}C nuclear magnetic resonance study of the complexation of macrocyclic antibiotics with Na^+ , K^+ , Rb^+ , Cs^+ , NH_4^+ and Ba^{2+} , *Helv. Chim. Acta*, 55, 1098, 1972.
99. Deslauriers, R., Walter, R., and Smith, I. C. P., A carbon-13 nuclear magnetic resonance study of oxytocin and its oligo-peptides, *Biochem. Biophys. Res. Commun.*, 48, 854, 1972.
100. Deslauriers, R., Walter, R., Prasad, K. V. M., and Smith, I.C.P., Conformational studies of oxytocin, lysine vasopressin, arginine vasopressin, and arginine vasotocin by carbon-13 nuclear magnetic resonance spectroscopy, *Proc. Natl. Acad. Sci. USA*, in press.

101. Lyerla, Jr., J. R. and Freedman, M. H., Spectral assignment and conformational analysis of cyclic peptides by carbon-13 nuclear magnetic resonance, *J. Biol. Chem.*, 247, 8183, 1972.
102. Paolillo, L., Tancredi, T., Temussi, P. A., Trivellone, E., Bradbury, E. M., and Crane-Robinson, C., The helix-coil transition of poly (α -benzyl L-glutamate) using ^{13}C resonance spectroscopy, *J. Chem. Soc. D Chem. Commun.*, 335, 1972.
103. Boccalon, G., Verdini, A. S., and Giacometti, G., Helix-coil transition of a synthetic polypeptide monitored by fourier transform carbon-13 nuclear magnetic resonance, *J. Am. Chem. Soc.*, 94, 3639, 1972.
104. Lyerla, Jr., J. R., Barber, B. H., and Freedman, M. H., ^{13}C chemical shifts accompanying helix formation, *Can. J. Biochem.*, in press.
105. Reynolds, W. F., Peat, I. R., Freedman, M. H., and Lyerla, Jr., J. R., Determination of tautomeric form of the imidazole ring of L-histidine in basic solution by ^{13}C magnetic resonance spectroscopy, *J. Am. Chem. Soc.*, 95, 328, 1973.
106. Lauterbur, P. C., ^{13}C nuclear magnetic resonance spectra of proteins, *Appl. Spectrosc.*, 24, 450, 1970.
107. Allerhand, A., Cochran, D. W., and Doddrell, D., Carbon-13 fourier transform nuclear magnetic resonance, II. Ribonuclease, *Proc. Natl. Acad. Sci. USA*, 67, 1093, 1970.
108. Glushko, V., Lawson, P. J., and Gurd, F. R. N., Conformational states of bovine pancreatic ribonuclease A observed by normal and partially relaxed carbon 13 nuclear magnetic resonance, *J. Biol. Chem.*, 247, 3176, 1972.
109. Freedman, M. H., Lyerla, Jr., J. R., Chaiken, I. M., and Cohen, J. S., Carbon-13 nuclear magnetic resonance studies on selected amino acids, peptides and proteins, *Eur. J. Biochem.*, 32, 215, 1973.
110. Chaiken, I. M., Freedman, M. H., Lyerla, Jr., J. R., and Cohen, J. S., Preparation and studies of ^{19}F - and enriched ^{13}C -labeled semisynthetic ribonuclease-S' analogs, *J. Biol. Chem.*, 248, 884, 1973.
111. Nigen, A. M., Keim, P., Marshall, R. C., Morrow, J. S., and Gurd, F. R. N., Carbon-13 nuclear magnetic resonance spectroscopy of myoglobins and ribonuclease A carboxymethylated with enriched (2^{-13}C) bromoacetate, *J. Biol. Chem.*, 247, 4100, 1972.
112. Chien, J. C. W. and Brandts, J. F., Natural abundance fourier transform of carbon-13 nuclear magnetic resonance spectra of lysozyme, *Nat. New Biol.*, 230, 209, 1971.
113. Conti, F. and Paci, M., Natural abundance ^{13}C spectra of proteins: carboxy-myoglobin and hemoglobin, *FEBS (Fed. Eur. Biochem. Soc.) Lett.*, 17, 149, 1971.
114. Moon, R. B. and Richards, J. H., Nuclear magnetic resonance studies of ^{13}CO binding to various hemoglobins, *J. Am. Chem. Soc.*, 94, 5093, 1972.
115. Moon, R. B. and Richards, J. H., Conformational studies of various hemoglobins by natural-abundance ^{13}C NMR spectroscopy, *Proc. Natl. Acad. Sci. USA*, 69, 2193, 1972.
116. Packer, E. L., Sternlicht, H. and Rabinowitz, J. C., ^{13}C NMR of oxidized and methyl viologen-reduced *clostridium acidu urici* ferredoxin: tyrosine and its possible role in electron transport, *Proc. Natl. Acad. Sci. USA*, 69, 3278, 1972.
117. Kuhlmann, K. F., Grant, D. M., and Harris, R. K., Nuclear Overhauser effects and ^{13}C relaxation times in ^{13}C -[H] double resonance spectra, *J. Chem. Phys.*, 52, 3439, 1970.
118. Kuhlmann, K. F. and Grant, D. M., Carbon-13 relaxation and internal rotation in mesitylene and o-xylene, *J. Chem. Phys.*, 55, 2998, 1971.
119. Doddrell, D., Glushko, V., and Allerhand, A., Theory of nuclear Overhauser enhancement and ^{13}C - ^1H dipolar relaxation in proton-decoupled carbon-13 NMR spectra of macromolecules, *J. Chem. Phys.*, 56, 3683, 1972.
120. Vold, R. L., Waugh, J. S., Klein, M. P., and Phelps, D. E., Measurement of spin-lattice relaxation in complex systems, *J. Chem. Phys.*, 48, 3831, 1968.
121. Allerhand, A., Doddrell, D., and Komoroski, R. A., Natural abundance carbon-13 partially relaxed fourier transform nuclear magnetic resonance spectra of complex molecules, *J. Chem. Phys.*, 55, 189, 1971.
122. Freeman, R., Private Communication.
123. Allerhand, A. and Hailstone, R. K., Carbon-13 fourier transform nuclear magnetic resonance X. Effect of molecular weight on ^{13}C spin lattice relaxation times of polystyrene in solution, *J. Chem. Phys.*, 56, 3718, 1972.
124. Allerhand, A., Doddrell, D., Glushko, V., Cochran, D. W., Wenkert, E., Lawson, P. J., and Gurd, F. R. N., Conformational and segmental motion of native and denatured ribonuclease A in solution. Application of natural abundance carbon-13 partially relaxed fourier transform nuclear magnetic resonance, *J. Am. Chem. Soc.*, 93, 544, 1971.
125. Komoroski, R. A. and Allerhand, A., Natural-abundance carbon-13 fourier transform nuclear magnetic resonance spectra and spin lattice relaxation times of unfractionated yeast transfer-RNA, *Proc. Natl. Acad. Sci. USA*, 69, 1804, 1972.
126. Browne, D. T., Kenyon, G. L., Packer, E. L., Wilson, D. M., and Sternlicht, H., Studies of macromolecular structure by ^{13}C nuclear magnetic resonance. I. The dynamic state of the histidine residues in tryptophan synthetase and subunit, *Biochem. Biophys. Res. Commun.*, 50, 42, 1973.
127. Browne, D. T., Kenyon, G. L., Packer, E. L., Sternlicht, H., and Wilson, D. M., Studies of macromolecular structure by ^{13}C nuclear magnetic resonance. II. A specific labeling approach to the study of histidine residues in proteins, *J. Am. Chem. Soc.*, 95, 1316, 1973.

128. Doddrell, D. and Allerhand, A., Assignments in the carbon-13 nuclear magnetic resonance spectra of vitamin B₁₂, coenzyme B₁₂, and other corrinoids: application of partially relaxed fourier transform spectroscopy, *Proc. Natl. Acad. Sci. USA*, 68, 1083, 1971.
129. Doddrell, D. and Allerhand, A., Direct observation of two forms of aquocyanocobyrinic acid in water by carbon-13 fourier transform nuclear magnetic resonance, *Chem. Commun.*, 728, 1971.
130. Brown, C. E., Katz, J. J., and Shemin, D., The biosynthesis of vitamin B₁₂: A study by ¹³C magnetic resonance spectroscopy, *Proc. Natl. Acad. Sci. USA*, 69, 2585, 1972.
131. Scott, A. I., Townsend, C. A., Okada, K., Kajiwar, M., Whitman, P. J., and Cushley, R. J., Biosynthesis of corrinoids. Concerning the origin of the methyl groups in vitamin B₁₂, *J. Am. Chem. Soc.*, 94, 8267, 1972.
132. Scott, A. I., Townsend, C. A., Okada, K., Kajiwar, M., and Cushley, R. J., Biosynthesis of corrinoids. Uroporphyrinogen III as a precursor of vitamin B₁₂, *J. Am. Chem. Soc.*, 94, 8269, 1972.
133. Doddrell, D. and Caughey, W. S., Carbon-13 fourier transform nuclear magnetic resonance study of some porphyrins. Evidence for a preferred delocalization pathway, *J. Am. Chem. Soc.*, 94, 2510, 1972.
134. Katz, J. J., Janson, T. R., Kostka, A. G., Uphaus, R. A., and Closs, G. L., Chlorophyll-Chlorophyll interactions. Ring V keto carbonyl donor properties from carbon-13 nuclear magnetic resonance, *J. Am. Chem. Soc.*, 94, 2883, 1972.
135. Strouse, C. E., Kollman, V. H., and Matwiyoff, N. A., *Biochem. Biophys. Res. Commun.*, 46, 328, 1972.
136. Oldfield, E. and Chapman, D., Carbon-13 pulse fourier transform NMR of lecithins, *Biochem. Biophys. Res. Commun.*, 43, 949, 1971.
137. Metcalfe, J. C., Birdsall, N. J. M., Feeney, J., Lee, A. G., Levine, Y. K., and Partington, P., ¹³C NMR spectra of lecithin vesicles and erythrocyte membranes, *Nature*, 233, 199, 1971.
138. Levine, Y. K., Birdsall, N. J. M., Lee, A. G., and Metcalfe, J. C., ¹³C nuclear magnetic resonance relaxation measurements of synthetic lecithins and the effect of spin-labeled lipids, *Biochemistry*, 11, 1416, 1972.
139. Metcalfe, J. C., Birdsall, N. J. M., and Lee, A. G., ¹³C NMR spectra of *Acholeplasma* membranes containing ¹³C labeled phospholipids, *FEBS (Fed. Eur. Biochem. Soc.) Lett.*, 21, 335, 1972.
140. Keough, K. M., Oldfield, E., Chapman, D., and Benyon, P., Carbon-13 and proton nuclear magnetic resonance of unsonicated model and mitochondrial membranes, *Chem. Phys. Lipids*, 10, 37, 1973.
141. Allerhand, A., Childers, R. F., Goodman, R. A., Oldfield, E., and Ysern, X., Increased sensitivity in ¹³C FT using 20-mm sample tubes, *Am. Lab.*, 4, 19, 1972.

Supplementary References

Carbohydrates

142. Schwarcz, J. A. and Perlin, A. S., Orientational dependence of vicinal and geminal ¹³C-¹H coupling, *Can. J. Chem.*, 50, 3667, 1972.
143. Conway, E., Guthrie, R. D., Gero, S. D., Lukacs, G., Sepulchre, A. M., Hagaman, E. W., and Wenkert, E. A., ¹³C NMR chemical shift study of *trans*-fused bicyclic hexopyranoside derivatives, *Tetrahedron Lett.*, 4879, 1972.
144. Breitmaier, E., Jung, G., and Voelter, W., ¹³C resonance of disaccharides with galactose residues, *Chimia*, 362, 1971.
145. Sepulchre, A. M., Lukacs, G., Vass, G., and Gero, S. D., Synthesis and pulse fourier transform ¹³C-nmr spectra of branched-chain carbohydrates, *Angew. Chem. Int. Ed.*, 11, 148, 1972.
146. Lukacs, G., Sepulchre, A. M., Gateau-Olesker, A., Vass, G., Gero, S. D., Guthrie, R. D., Voelter, W., and Breitmaier E., Configurational assignment of quaternary centres containing C-1, 3 dithianyl branched chain in alicyclic and carbohydrate chemistry by ¹³C N.M.R. spectroscopy, *Tetrahedron Lett.*, 5163, 1972.
147. Sepulchre, A. M., Lukacs, G., Vass, G. and Gero, S. D., Synthesis of long-chain or ramified carbohydrates by nucleophilic acetylation. Structure determination by ¹H and ¹³C NMR, *Bull. Soc. Chim. Fr.*, 4000, 1972.
148. Jennings, H. J. and Smith, I. C. P., Determination of the composition and sequence of a glucan containing mixed linkages by carbon-13 nuclear magnetic resonance, *J. Am. Chem. Soc.*, 95, 606, 1973.

Natural Products

149. Voelter, W., Jung, G., Breitmaier, E., and Price, R., Structure and carbon-13 chemical shift of natural substances. Pulse-fourier transform carbon-13 NMR spectroscopy of riboflavin, *Hoppe-Seyler's Z. Physiol. Chem.*, 352, 1034, 1971.
150. Lukacs, G. and Smith, R. M., ¹³C NMR studies on natural products and related compounds. VI. Structural application: vancosamine, a new amino-sugar containing a branched side-chain, isolated from vancomycin, *Bull. Soc. Chim. Fr.*, 3995, 1972.
151. Lukacs, G. and Bennett, C. R., ¹³C NMR studies on natural products and related compounds. VII. α -Ecdysone, *Bull. Soc. Chim. Fr.*, 3996, 1972.
152. Knight, S. A., The carbon-13 NMR spectra of lanosterol, euphadienol and euphenol, *Tetrahedron Lett.*, 83, 1973.
153. Lukacs, G., Pirou, F., Gero, S. D., Van Dorp, D. A., Hagaman, E. W., and Wenkert, E. W., Carbon-13 nuclear magnetic resonance spectroscopy of naturally occurring substances. Prostaglandins, *Tetrahedron Lett.*, 515, 1973.
154. Mantsch, H. H. and Smith, I. C. P., A study of solvent effects on the ¹³C nuclear magnetic resonance spectra of cholesterol, pyridine and uridine, *Can. J. Chem.*, in press.

Biosynthesis

155. Maebayashi, Y., Miyaki, K., and Yamazaki, M., Application of ^{13}C nmr to the biosynthetic investigations. I. Biosynthesis of ochratoxin A., *Chem. Pharm. Bull.* (Tokyo), 20, 2172, 1972.

Nucleotides

152. Breitmaier, E. and Voelter, W., A ^{13}C nuclear magnetic resonance study of the enzyme cofactor flavin-adenine dinucleotide, *Eur. J. Biochem.*, 31, 234, 1972.
157. Birdsall, B. and Feeney, J., The ^{13}C and ^1H nuclear magnetic resonance spectra and methods of their assignment for nucleotides related to dihydronicotinamide adenine dinucleotide phosphate (NADPH), *J. Chem. Soc., Perk. Trans. II*, 1643, 1972.
158. Breitmaier, E. and Voelter, W., Structures and conformations of adenosine analogs established by ^{13}C resonance, *Tetrahedron*, 29, 227, 1973.
159. Kotowycz, G. and Hayamitsu, K., A carbon-13 nuclear magnetic resonance study of nucleotide – metal interactions. Binding of manganese (II) with adenine nucleotides, *Biochemistry*, 12, 517, 1973.

Amino Acids and Peptides

160. Pease, L. G., Deber, C. M., and Blout, E. R., Cyclic peptides. V. ^1H and ^{13}C nuclear magnetic resonance determination of the preferred β conformation for proline-containing cyclic hexapeptides, *J. Am. Chem. Soc.*, 95, 258, 1973.
161. Jung, G., Breitmaier, E., and Voelter, W., Carbon-13 nuclear magnetic resonance spectroscopic investigation of the pH dependence of charge distribution, *Eur. J. Biochem.*, 24, 438, 1972.
162. Voelter, W., Zech, K., Grimminger, W., Breitmaier, E., and Jung, G., Application of the ^{13}C NMR spectroscopy to the control of peptide synthesis, *Chem. Ber.*, 105, 3650, 1972.
163. Jung, G., Ottmad, M., Voelter, W., and Breitmaier, E., Circular-dichroism and ^{13}C NMR investigations of the dissociation of amino acids, *Fresenius' Z. Anal. Chem.*, 261, 328, 1972.
164. Smith, I. C. P., Deslauriers, R., Saito, H., Walter, R. W., Garrigou-Lagrange, C., McGregor, H., and Sarantakis, D., Carbon-13 nmr studies of peptide hormones and their components, *Ann. N. Y. Acad. Sci.*, in press.
165. Brewster, A. I. R., Hruby, V. J., Spatola, A. F., and Bovey, F. A., Carbon-13 nmr spectra of oxytocin-related oligopeptides, and related analogs, *Biochemistry*, in press.
166. Smith, I. C. P., Deslauriers, R., and Walter, R., A carbon-13 nuclear magnetic resonance study of neurohypophyseal hormones and related oligopeptides, in *Chemistry and Biology of Peptides*, Meienhofer, J., Ed., Ann Arbor Science Publishers, Ann Arbor, Mich., 1972, 29.
167. Deslauriers, R., Garrigou-Lagrange, C., Bellocq, A.-M., and Smith, I. C. P., Carbon-13 nuclear magnetic resonance studies on thyrotropin-releasing factor and related peptides, *FEBS Lett.*, in press.
168. Bovey, F. A., NMR in the conformational analysis of polypeptides, especially cyclic polypeptides, *Chemistry and Biology of Peptides*, Meienhofer, J., Ed., Ann Arbor Science Publishers, Ann Arbor, Mich., 1972, 3.
169. Zimmer, S., Haar, W., Maurer, W., Ruterjans, H., Fermandjian, S., and Fromageot, P., Investigation of the structure of angiotensin using ^{13}C nuclear magnetic resonance spectra, *Eur. J. Biochem.*, 29, 80, 1972.
170. Wuthrich, K., Tun-Kyi, A., and Schwyzer, R., Manifestations in the ^{13}C -nmr spectra of two different conformations of a cyclic pentapeptide, *FEBS Lett.*, 25, 104, 1972.

Cells

171. Eakin, R. T., Morgan, L. O., Gregg, C. T., and Matwiyoff, N. A., Carbon-13 nuclear magnetic resonance spectroscopy of living cells and their metabolism of a specifically labeled ^{13}C substrate, *FEBS Lett.*, 28, 259, 1972.
172. Matwiyoff, N. A. and Needham, T. E., Carbon-13 NMR spectroscopy of red blood cell suspensions, *Biochem. Biophys. Res. Commun.*, 49, 1158, 1972.

Lipids

173. Lee, A. G., Birdsall, N. J. M., Levine, Y. K., and Metcalfe, J. C., High resolution proton relaxation studies of lecithins, *Biochim. Biophys. Acta*, 255, 43, 1972.
174. Stoffel, W., Zierenburg, O., and Tungel, B. D., ^{13}C nuclear magnetic resonance spectroscopic studies on saturated, mono-, di- and polyunsaturated fatty acids, phospho- and sphingolipids, *Hoppe-Seyler's Z. Physiol. Chem.*, 353, 1962, 1972.
175. Birdsall, N. J. M., Feeney, J., Lee, A. G., Levine, Y. K., and Metcalfe, J. C., Dipalmitoyl-lecithin: Assignment of the ^1H and ^{13}C nuclear magnetic resonance spectra and conformational studies, *J. Chem. Soc., Perk. Trans. II*, 1441, 1972.